SATBAYEV
UNIVERSITY

ISSN 2959-2348 (Online)

ENGINEERING JOURNAL of Satbayev University

Volume 148 (Issue 3)
June 2026

eISSN 2959-2348

eISSN 2959-2348

eISSN 2959-2348

SATBAYEV UNIVERSITY

Engineering Journal of Satbayev University

Volume 148 (2026), Issue 3, 1-8

https://doi.org/10.51301/ejsu.2026.i3.01

Kinetics of reduction of lead chloride and oxychloride with sodium carbonate

G.Zh. Moldabayeva[1], B.S. Baimbetov[1], Ye.B. Tazhiyev[1*], A.A. Dauletbakova[1], G.M. Koishina[1], S.K. Jumankulova[1], M.D. Turan[2], A.A. Iskendirov[1]

[1]*Satbayev University, Almaty, Kazakhstan*

[2]*Firat University, Elazig, Turkey*

**Corresponding author: y.tazhiyev@satbayev.university*

Abstract. This study investigates the kinetic behaviour of the reduction reaction between lead chloride ($PbCl_2$) and lead oxychloride ($PbO \cdot PbCl_2$) with sodium carbonate in the presence of carbon in a reducing atmosphere. The relevance of this research stems from the need to develop effective technologies for processing lead-containing secondary production dusts and to optimise the composition of sodium-containing fluxes. Thermodynamic evaluation of the reactions using the Outotec HSC Chemistry software package demonstrated that, within the temperature range of 500-1000°C, both reactions exhibit negative ΔG values and high equilibrium constants, indicating their thermodynamic feasibility. Kinetic studies were carried out using thermogravimetric analysis under isothermal conditions in the temperature range of 800-1100°C for the $PbCl_2$–Na_2CO_3–C system and 500-800°C for the $PbO \cdot PbCl_2$–Na_2CO_3–C system. It was established that the reductive interaction proceeds via a multistage mechanism with a change in the rate-controlling step as the degree of conversion increases. For the $PbO \cdot PbCl_2$–Na_2CO_3–C system, the initial stage of the process is satisfactorily described by the first-order reaction equation, indicating the predominance of chemical control; the apparent activation energy at this stage is 33.5 kJ/mol. As the degree of conversion increases, the activation energy rises to 62-80 kJ/mol, which indicates a transition to a regime complicated by diffusion and structural limitations. The $PbO \cdot PbCl_2$–Na_2CO_3–C system is characterized by higher reactivity and rapid attainment of significant conversion degrees. At moderate conversion levels, the process proceeds predominantly under chemical control ($E_a \approx$ 43-44 kJ/mol); however, at $\alpha \geq 55\%$, an increase in activation energy up to 74 kJ/mol is observed, indicating an increasing influence of mass transfer. It is shown that the presence of oxygen in the structure of lead oxychloride significantly affects the kinetic characteristics of the reductive process in sodium-containing flux systems. The obtained results can be used in optimizing technological schemes for processing lead-containing dusts in order to enhance metal recovery and improve the energy efficiency of the process.

Keywords: *lead-containing dust, lead chloride, lead oxychloride, sodium carbonate, reductive electric smelting, solid-state reaction kinetics, activation energy, thermogravimetric analysis.*

Received: 10 March 2026
Received in revised form: 04 June 2026
Accepted: 15 June 2026
Available online: 30 June 2026

1. Introduction

Secondary lead accounts for a significant share of the global market, with approximately half of the world's lead consumption being met through the recycling of lead-containing waste [1-4]. According to analytical data [5], the global secondary lead market is estimated at approximately USD 18.7 billion in 2025 and is projected to grow to about USD 26.3 billion by 2035, with an average annual growth rate of around 3.5% (Figure 1). The high recycling rate is driven by both economic and environmental factors, including the relative ease of scrap collection and a reduction in energy consumption by up to 35-40% compared to the production of primary lead from ore [5].

The main contribution to the secondary lead market comes from the recycling of battery production waste, including lead-containing dusts generated during the manufacture and recycling of lead-acid batteries [6-7]. These materials contain lead, antimony, chlorine, and a number of associated elements which, under rational processing conditions, can serve as sources of additional raw materials [8, 9]. However, a significant portion of such fine dust waste accumulates at industrial sites, creating environmental burdens while simultaneously representing an underutilized resource [10]. This highlights the need to develop efficient processing technologies that ensure both minimization of environmental impact and recovery of valuable components.

Dust waste from battery recycling represents complex multicomponent materials. Their composition includes various lead compounds – sulfates ($PbSO_4$), sulfides (PbS), oxides (PbO), oxysulfates ($PbO \cdot PbSO_4$), and chloride compounds ($PbCl_2$, $PbO \cdot PbCl_2$) – as well as impurities of Zn, Sb, Cd, and As [8, 11].

gulnara.moldabayeva@satbayev.university; b.baimbetov@satbayev.university; y.tazhiyev@satbayev.university; a.dauletbakova@satbayev.university; g.koishina@satbayev.university; s.jumankulova@satbayev.university; mdturan@firat.edu.tr; a.iskendirov@satbayev.university

Engineering Journal of Satbayev University. eISSN 2959-2348. Published by Satbayev University

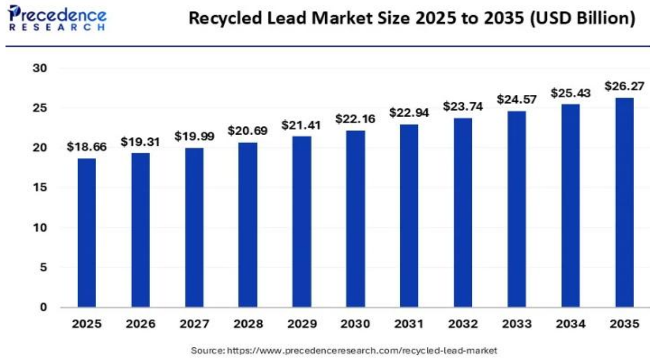

Figure 1. Forecast of the secondary lead market growth (2025-2035)

Differences in chemical reactivity and thermochemical behavior of these compounds necessitate a differentiated approach to their processing.

Electrothermal methods, particularly reductive electric smelting using sodium salts, demonstrate significant potential for the comprehensive recovery of lead and associated elements [12-14]. Sodium salts used as fluxes can be partially replaced by calcium compounds (carbonate or oxide), which are capable of binding chlorine from lead chloride compounds and transferring it into the slag phase. This contributes to improved process selectivity, reduced metal losses, and expansion of the raw material base for fluxing agents. In the present work, primary attention is focused on studying the kinetic regularities of the reductive interaction of lead chloride compounds ($PbCl_2$ and $PbO{\cdot}PbCl_2$) with sodium carbonate in a carbon-containing medium. Lead compounds of other classes, as well as systems involving calcium-containing fluxes ($CaCO_3$, CaO), were not considered in this series of experiments and will be the subject of further investigation.

2. Materials and methods

2.1. Raw materials

Chemically pure substances were used for the kinetic studies to model the main chloride compounds of lead present in battery production dust wastes: lead chloride ($PbCl_2$, analytical grade, ≥99%) and lead oxychloride ($PbO{\cdot}PbCl_2$, ≥99%). Sodium carbonate (Na_2CO_3, ≥99%) was used as a fluxing additive, and carbon powder (≥99%) served as the reducing agent. The particle size of all components did not exceed 0.074 mm. The sample masses were selected in accordance with the stoichiometry of the reactions under consideration. The use of chemically pure reagents made it possible to eliminate the influence of extraneous impurities and to obtain reproducible data on the kinetic characteristics of the studied systems, thereby providing a basis for the subsequent extrapolation of the results to real industrial materials.

2.2 Experimental procedure

Thermodynamic analysis of the reductive reactions of $PbCl_2$ and $PbO{\cdot}PbCl_2$ with sodium carbonate in the presence of carbon was carried out using the licensed software package Outotec HSC Chemistry v. 8.1.5 (Reaction Equations module). Calculations were performed in the temperature range of 500-1000°C for stoichiometric reagent compositions with determination of the Gibbs free energy change (ΔG), enthalpy change (ΔH), entropy change (ΔS), and equilibrium constant.

Kinetic studies of the interfacial interaction of lead chloride and oxychloride compounds with fluxing additives and a reducing agent were carried out using thermogravimetric analysis under isothermal conditions. The experiments were performed on a laboratory thermogravimetric setup consisting of a vertical tubular electric furnace with an adjustable working zone, a quartz reaction retort, a continuous mass recording system, and a temperature control unit (Figure 2).

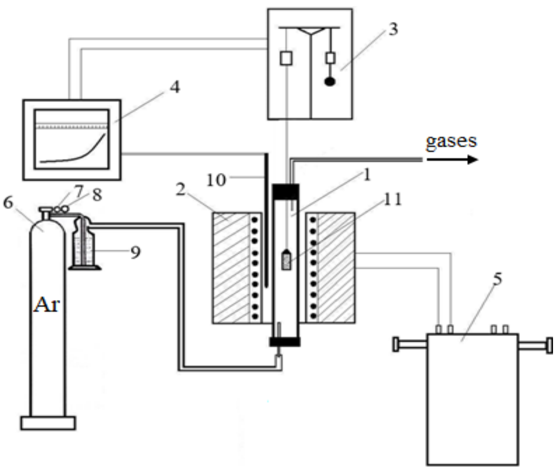

Figure 2. Schematic diagram of the thermogravimetric setup for studying reaction kinetics: 1 – quartz retort; 2 – electric furnace; 3 – ADV-200 analytical balance; 4 – KSP-4 potentiometer; 5 – voltage regulator; 6 – argon cylinder; 7 – rotameter; 8 – manometer; 9 – gas purification system; 10 – tungsten–rhenium thermocouple; 11 – alumina crucible with sample

The samples were heated to the required temperature within the range of 500-1000°C. Isothermal kinetic experiments were conducted primarily in the temperature interval of 800-1100°C, corresponding to the conditions of reductive electric smelting of lead-containing dusts. Temperature control was maintained within ±5°C using a tungsten–rhenium thermocouple and an automatic regulation system. The reactions were carried out in an inert gas atmosphere (argon), supplied to the lower part of the reaction chamber. The argon flow ensured the removal of gaseous reaction products and prevented oxidation of the sample. The sample was placed in an alumina crucible, which was positioned in the isothermal zone of the retort and suspended from analytical balances with a measurement accuracy of 10^{-4} g. The sample was introduced into the working zone after stabilization of the furnace temperature; the time required to reach isothermal conditions did not exceed 1-5 s. The mass change of the sample was recorded continuously throughout the experiment.

Kinetic parameters were determined from the dependencies of the degree of conversion on time at fixed temperatures. The approach to the analysis of kinetic data and the interpretation of temperature dependences was based on classical principles of extractive metallurgy kinetics [15]. The degree of conversion was calculated from the change in sample mass associated with the release of gaseous reaction products. Experimental data were processed using the Arrhenius equation to determine the apparent activation energy and the pre-exponential factor. All experiments were performed in at least three replicates; the deviation of results did not exceed 5%. After completion of the experiment, the samples were cooled to room temperature in an argon atmosphere, followed by control weighing and phase analysis of the reaction products.

3. Results and discussion

3.1. Thermodynamic assessment of the reductive reactions of $PbCl_2$ and $PbO \cdot PbCl_2$ with Na_2CO_3 in a reducing tmosphere

To investigate the reductive interaction of lead chloride and lead oxychloride with sodium carbonate in a reducing atmosphere, two model systems were examined. System I represent the interaction of $PbCl_2$ with sodium carbonate and carbon, while system II represents the reduction of $PbO \cdot PbCl_2$ in the presence of sodium carbonate.

For convenience, these systems are hereafter referred to as systems (1) and (2). The overall reactions are expressed as follows:

$$PbCl_2+Na_2CO_3+C \rightarrow Pb+2NaCl+CO_2(g)+CO(g); \quad (1)$$

$$PbO \cdot PbCl_2+Na_2CO_3+C \rightarrow 2Pb+2NaCl+2CO_2(g); \quad (2)$$

To preliminarily evaluate the thermodynamic feasibility of the reactions, the Gibbs free energy change (ΔG) and equilibrium constant (K) were calculated over the temperature range of 500-1000°C. It was found that, for both reactions, the ΔG values remain negative over the entire investigated temperature range and become more negative with increasing temperature (Table 1). Specifically, for reaction (I), ΔG decreases from −97.9 kJ/mol at 500°C to −244.3 kJ/mol at 1000°C, while for reaction (II) it decreases from −171.5 to −321.0 kJ/mol.

Table 1. Values of the Gibbs free energy change (ΔG) and the logarithm of the equilibrium constant (log K) in the temperature range of 500-1000°C

T, °C	500	600	700	800	900	1000
Reaction I						
ΔG, kJ	-97.947	-127.217	-155.821	-183.780	-214.968	-244.298
Log K	6.618	7.611	8.365	8.946	9.572	10.024
Reaction II						
ΔG, kJ	-171.472	-202.021	-231.836	-260.936	-292.879	-320.974
Log K	11.586	12.087	12.445	12.702	13.042	13.170

The log K values for reaction (I) lie within 6.6-10.0, while for reaction (II) they fall within 11.6-13.2, reflecting a substantial thermodynamic driving force and a pronounced shift of equilibrium toward the reaction products. The more negative ΔG values and higher equilibrium constants associated with reaction (II) indicate enhanced thermodynamic stability of the products and agree with the experimentally observed higher reactivity of the $PbO \cdot PbCl_2$-Na_2CO_3-C system.

Therefore, both reactions are thermodynamically feasible throughout the studied temperature range, and the observed differences in reaction rate and changes in the kinetic regime are mainly attributable to kinetic factors rather than thermodynamic constraints.

3.2. Kinetics of the reductive interaction of $PbCl_2$ and $PbO \cdot PbCl_2$ with sodium carbonate in a reducing atmosphere

Although both reactions are thermodynamically feasible throughout the studied temperature range, they exhibit markedly different kinetic behaviors, requiring a detailed examination of the reaction mechanism and rate-controlling stages.

3.2.1. Kinetics of the interaction of $PbCl_2$ with Na_2CO_3 and C (system I)

Analysis of the kinetic data obtained under isothermal conditions in the temperature range of 800-1100°C showed that the interaction of lead chloride with sodium carbonate and carbon proceeds with a change in the kinetic regime as the reaction progresses. At the initial stage of the reaction, at degrees of conversion $\alpha \leq 0.2$, the experimental dependences are satisfactorily described by the first-order reaction equation, indicating the predominance of chemical control. As the interaction time and the degree of conversion increase, deviations from first-order kinetics are observed, associated with a change in the rate-limiting step. At higher degrees of conversion, the process shifts to a transitional regime, indicating a more complex interaction mechanism and the involvement of mass transfer factors and structural changes in the solid phase, which are characteristic of topochemical reactions in the solid state [16].

Figure 3 presents the dependences of the degree of conversion on time for system I at various temperatures. An increase in temperature leads to process acceleration and the attainment of high conversion degrees within a shorter time, which served as the basis for the subsequent calculation of reaction rates and kinetic parameters.

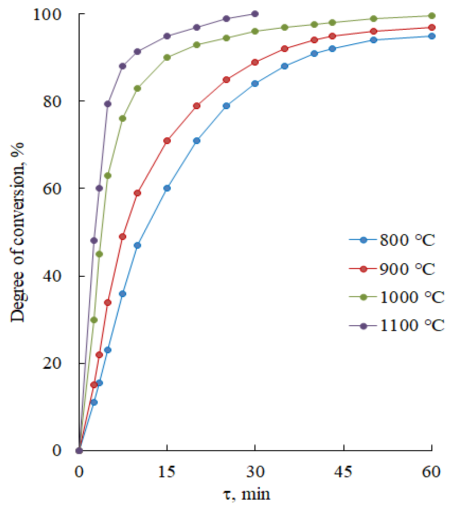

Figure 3. Dependence of the degree of conversion on time for system I ($PbCl_2$–Na_2CO_3–C)

Based on the experimental $\alpha(\tau)$ dependences, the reaction rate was calculated as $v = d\alpha/d\tau$. The dependences of the reaction rate on the degree of conversion for system I are presented in Figure 4.

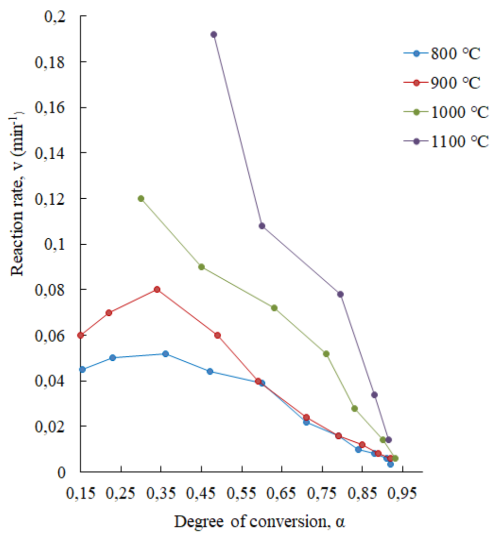

Figure 4. Dependence of the reaction rate on the degree of conversion (α) for system I ($PbCl_2$–Na_2CO_3–C)

Analysis of the obtained data shows that, at identical degrees of conversion, the reaction rate increases with increasing temperature, particularly at the early stages of the process ($\alpha \approx 0.2$-0.4). As the degree of conversion increases, a decrease in the reaction rate and a convergence of the curves obtained at different temperatures are observed, indicating a change in the rate-limiting step and a transition from chemical control to a mixed kinetic regime. At 900°C, a pronounced maximum is observed in the rate versus conversion dependence in the region of $\alpha \approx 0.3$-0.35, which is associated with the intensification of the chemically controlled stage at the initial stage of interaction. At a lower temperature (800°C), this effect is less pronounced due to the slower activation of the reaction, whereas at higher temperatures (1000-1100°C), the rate maximum shifts toward lower degrees of conversion and is partially not detected experimentally because of the high reaction rate.

For the initial stage of the process, described by the first-order reaction equation ($\alpha \approx 0.2$), the apparent activation energy determined from the analysis of the reaction rate constants (K) is 33.5 kJ/mol. The temperature coefficient of the rate constant varies only slightly and lies within the range of 1.4-1.7. The obtained value reflects the kinetics of the chemically controlled stage and corresponds to an idealized description of the initial reaction period.

To evaluate the temperature dependence of the initial reaction rate, the dependence of ln v_0 on $10^3/T$ was analyzed, where v_0 is the reaction rate at the first recorded time point ($\tau = 2.5$ min). The resulting relationship (Figure 5) is linear ($R^2 \approx 0.97$), and the calculated apparent activation energy is about 62 kJ/mol. The higher E_a value compared to that of the chemically controlled stage is attributed to experimental factors and the onset of structural and diffusion limitations at elevated temperatures.

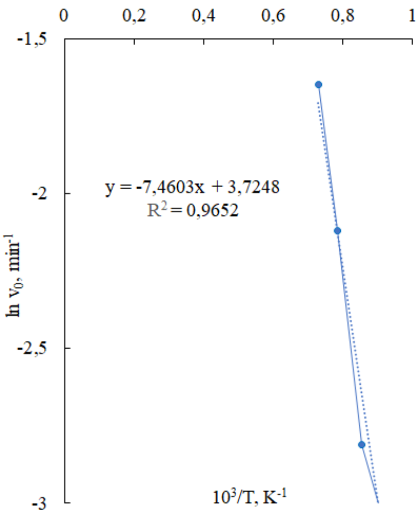

Figure 5. Dependence of ln v_0 on $10^3/T$ for system I ($PbCl_2$–Na_2CO_3–C)

In the region of higher degrees of conversion for system I, temperature dependences of ln k versus $10^3/T$ were constructed (Figure 6). The linear character of the obtained relationship ($R^2 \approx 0.98$) confirms the applicability of the Arrhenius equation. The calculated apparent activation energy is approximately 80 kJ/mol, indicating a significant complication of the interaction mechanism and a transition from chemical control to a regime influenced by mass transfer and the formation of a dense product layer.

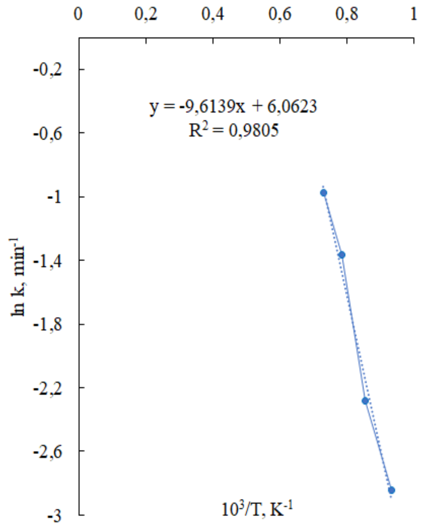

Figure 6. Dependence of ln k on $10^3/T$ for system I ($PbCl_2$–Na_2CO_3–C)

The reductive interaction of $PbCl_2$ with Na_2CO_3 and C proceeds via a multistage mechanism with a change in the kinetic regime as the reaction progresses. At the initial stage, the reaction follows first-order kinetics and is characterized by a relatively low apparent activation energy (33.5 kJ/mol), indicating the predominance of chemical control. As the degree of conversion and temperature increase, the influence of structural and diffusion factors becomes more pronounced, leading to an increase in the apparent activation energy to approximately 62-80 kJ/mol. The obtained results indicate a transition from a chemically controlled stage to a regime influenced by mass transfer and the formation of a dense product layer [16].

3.2.2. Kinetics of the interaction of $PbO \cdot PbCl_2$ with Na_2CO_3 and C (system II).

The kinetics of the reductive interaction of lead oxychloride with sodium carbonate and carbon were investigated under isothermal conditions in the temperature range of 500-800°C. In contrast to system I, this system is characterized by high reactivity, manifested in the rapid attainment of significant degrees of conversion already at the initial stages of the process. Similar acceleration of reductive processes in the presence of sodium fluxes has previously been reported during the processing of lead-containing materials and concentrates [13, 14].

Figure 7 presents the dependences of the degree of conversion on time for system II at various temperatures. An increase in temperature leads to a sharp acceleration of the process: at 700-800°C, the degree of conversion reaches approximately 90-95% within 30-40 min, whereas at 500-600°C it amounts to about 56-65% over the same period. The shape of the curves is characterized by an intensive increase in conversion at the initial stage followed by a gradual slowdown of the process, indicating a change in the rate-limiting step as reaction products accumulate and the structure of the solid phase evolves. Due to the high reaction rate and the rapid attainment of significant degrees of conversion, the identification of a linear region corresponding to first-order kinetics and the accurate determination of the rate constant k for system II are complicated. Therefore, the temperature dependence of the kinetic parameters was analyzed based on the apparent activation energy values determined at fixed degrees of conversion.

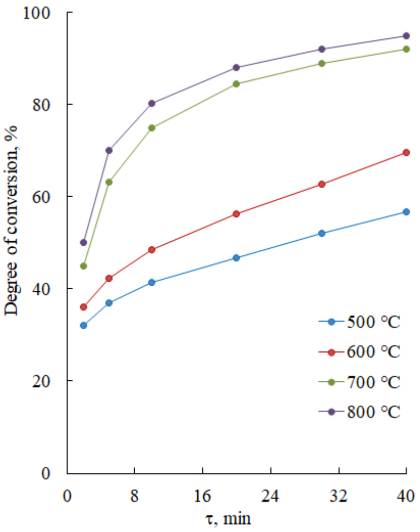

Figure 7. Dependence of the degree of conversion on time for system II ($PbO·PbCl_2$–Na_2CO_3–C) at various temperatures

To evaluate changes in the reaction mechanism, the apparent activation energy was analyzed at degrees of conversion of α = 45% and α = 55%. The obtained values are presented in Table 2 and illustrated in Figure 8.

Table 2. Apparent activation energy values for the interaction of $PbO·PbCl_2$ with Na_2CO_3 and C at different degrees of conversion

Degree of conversion α, %	Temperature range, °C	E_a, kJ/mol
45	500-600	43.5
45	600-700	43.5
45	700-800	44.0
55	500-600	64.5
55	600-700	66.5
55	700-800	74.0

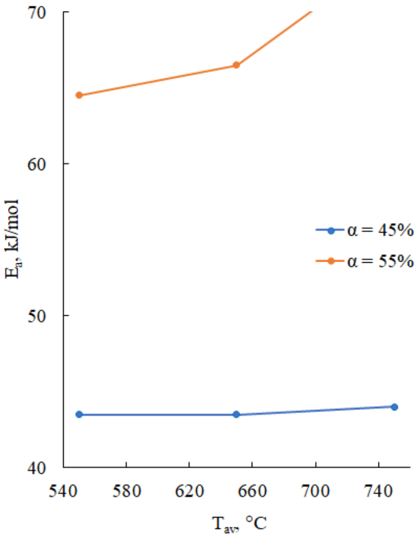

Figure 8. Dependence of the apparent activation energy (E_a) on the average temperature of the temperature interval (T_{av}) for system II ($PbO·PbCl_2$–Na_2CO_3–C) at degrees of conversion α = 45% and α = 55%

It was established that at α = 45%, the apparent activation energy remains nearly constant, amounting to 43.5-44.0 kJ/mol throughout the entire investigated temperature range, which is characteristic of a predominantly chemically controlled reaction regime. As the degree of conversion increases to α = 55%, the apparent activation energy rises from 64.5 to 74.0 kJ/mol with increasing temperature. This indicates a complication of the reaction mechanism and an increasing influence of structural and diffusion limitations typical of multistage topochemical reactions [16].

The increase in activation energy values with increasing degree of conversion confirms the multistage nature of the reductive interaction of lead oxychloride with sodium carbonate and carbon. The initial stage of the reaction proceeds predominantly under chemical control, whereas at later stages mass transfer processes and the formation of a dense product layer begin to play a significant role, hindering the further progression of the reaction.

3.3. Comparative analysis of kinetic behavior in systems I and II

A comparative analysis of the kinetic behavior of systems I ($PbCl_2$-Na_2CO_3-C) and II ($PbO·PbCl_2$-Na_2CO_3-C) reveals significant differences in reaction rate, kinetic regime, and limiting stages of the reduction process, despite the use of the same sodium-based fluxing additive. These differences are primarily associated with the chemical nature of the lead-containing compounds and the presence of oxygen in the structure of lead oxychloride.

In system I, the reduction of lead chloride proceeds relatively slowly and allows a clear identification of the initial stage governed by chemical kinetics. The experimental data demonstrate that at low degrees of conversion the process is satisfactorily described by a first-order kinetic model, enabling the determination of the apparent rate constant and subsequent Arrhenius analysis. The relatively low apparent activation energy at the initial stage indicates that the reaction rate is mainly controlled by chemical interaction between $PbCl_2$, Na_2CO_3, and carbon. As the reaction proceeds, the accumulation of reaction products and changes in the solid-phase structure lead to a transition toward a mixed kinetic regime, accompanied by an increase in the apparent activation energy, which is consistent with general kinetic concepts of extractive metallurgy and solid-state reaction theory [15-18].

In contrast, system II is characterized by a substantially higher reaction rate and rapid attainment of high degrees of conversion, even at moderate temperatures. The presence of oxygen in the $PbO·PbCl_2$ structure facilitates the decomposition of the compound and promotes faster interaction with sodium carbonate and the reducing agent. As a result, the initial chemically controlled stage is significantly shortened, and the reliable determination of the rate constant based on a first-order kinetic model becomes impractical. For this reason, the kinetic analysis of system II was performed using the apparent activation energy determined at fixed degrees of conversion.

The comparison of apparent activation energies further highlights the fundamental differences between the two systems. For system I, the activation energy at the initial stage is relatively low and increases progressively with conversion, reflecting the gradual transition from chemical control to a regime influenced by mass transfer and structural factors. In system II, the activation energy at moderate conversion levels ($\alpha \approx$ 45%) remains nearly constant over the investigated temperature range, indicating a predominantly chemically controlled process. However, at higher degrees of conversion ($\alpha \approx$ 55%), a pronounced increase in the apparent activation energy is observed, which points to the growing influence of diffusion limitations and the formation of a dense product layer.

The thermodynamic analysis confirmed that both reactions are feasible over the studied temperature range and exhibit a significant driving force. Therefore, the observed differences in reaction behavior are primarily associated with kinetic factors rather than thermodynamic limitations.

Overall, the comparative analysis demonstrates that the introduction of an oxygen-containing lead compound substantially alters the kinetic characteristics of the reduction process in sodium fluxing systems. While both systems ultimately exhibit a multistage reaction mechanism, the relative contribution of chemical and diffusion-controlled stages differs markedly. These findings are of practical importance for optimizing flux composition and operating conditions in the processing of lead-containing dusts, particularly with regard to achieving high metal recovery while maintaining process efficiency.

4. Conclusions

Thermodynamic analysis demonstrated that both reduction reactions are feasible in the temperature range 500–1000°C and are characterized by a substantial driving force.

It was established that the reductive interaction of lead chloride and lead oxychloride with sodium carbonate and carbon proceeds via a multistage mechanism accompanied by a change in the kinetic regime as the reaction progresses.

For system I ($PbCl_2$-Na_2CO_3-C), the initial stage of the process is satisfactorily described by first-order kinetics, indicating the predominance of chemical control and allowing reliable determination of the rate constant and apparent activation energy.

System II ($PbO \cdot PbCl_2$-Na_2CO_3-C) exhibits significantly higher reactivity and rapid attainment of high degrees of conversion, which substantially shortens the chemically controlled stage and limits the applicability of first-order kinetic analysis.

Analysis of the apparent activation energy values shows that, for system I, the increase in activation energy with increasing conversion reflects a gradual transition from chemical control to a regime influenced by mass transfer and structural changes of the solid phase, in agreement with kinetic models reported for carbothermic reduction of metallurgical dusts. In contrast, for system II, a predominantly chemically controlled regime is preserved at moderate conversion levels.

The obtained results demonstrate that the presence of oxygen in the structure of lead oxychloride has a pronounced effect on the reduction kinetics in sodium-based fluxing systems and should be considered when developing and optimizing technological schemes for the processing of lead-containing dusts.

Author contributions

Conceptualization: GZM, BSB; Data curation: SKJ, MDT; Formal analysis: YBT, MDT; Funding acquisition: GZM; Investigation: AAD, SKJ; Methodology: YBT, AAD; Project administration: GZM; Resources: AAI, GMK; Software: MDT, SKJ; Supervision: BSB, GZM; Validation: GMK, AAI, YBT; Visualization: MDT, SKJ, GMK; Writing – original draft: GZM, BSB, AAD; Writing – review & editing: YBT, GMK, SKJ. All authors have read and agreed to the published version of the manuscript.

Funding

This research is funded out within the framework of grant funding of the Science Committee of the Ministry of Science and Higher Education of the Republic of Kazakhstan for 2025-2027, Grant No. AP26198395 «Development of energy-saving and import-exempt innovative technology for the integrated processing of lead-containing waste and secondary raw materials with the replacement of scarce reaction-fluxing components with industrial waste».

Acknowledgements

The authors express their sincere gratitude to the editor and anonymous reviewers for their constructive comments and valuable suggestions, which have significantly improved the quality of this manuscript.

Conflicts of interests

The authors declare no conflict of interest.

Data availability statement

The original contributions presented in this study are included in the article. Further inquiries can be directed to the corresponding author.

References

[1] International Lead Association. (2014). Lead recycling: Sustainability in action (Technical report). *Retrieved from:* https://www.ila-lead.org/UserFiles/File/ILA9927%20FS_Recycling_2014.pdf

[2] Ichlas, Z.T., Rustandi, R.A., & Mubarok, M.Z. (2020). Selective nitric acid leaching for recycling of lead-bearing solder dross. *Journal of Cleaner Production, 264,* 121675. https://doi.org/10.1016/j.jclepro.2020.121675

[3] Bača, P., & Vanýsek, P. (2023). Issues concerning manufacture and recycling of lead. *Energies, 16*(11), 4468. https://doi.org/10.3390/en16114468

[4] Vivar, Y., Velásquez-Yévenes, L., & Vargas, C. (2025). Sustainable recovery of lead from secondary waste in chloride medium: A review. *Minerals, 15(3),* 244. https://doi.org/10.3390/min15030244

[5] Precedence Research. (n.d.). Recycled lead market report. *Retrieved from:* https://www.precedenceresearch.com/recycled-lead-market

[6] Díaz, G., & Andrews, D. (1996). Placid: A clean process for recycling lead from batteries. *JOM, 48,* 29-31. https://doi.org/10.1007/BF03221358

[7] Ferracin, L.C., Chácon-Sanhueza, A.E., Davoglio, R.A., Rocha, L.O., Caffeu, D.J., Fontanetti, A.R., Rocha-Filho, R.C., Biaggio, S.R., & Bocchi, N. (2002). Lead recovery from a typical Brazilian sludge of exhausted lead–acid batteries using an electrohydrometallurgical process. *Hydrometallurgy, 65*(2-3), 137-144. https://doi.org/10.1016/S0304-386X(02)00087-7

[8] Barbin, N.M., Kazantsev, G.F., Moiseev, G.K., & Vatolin, N.A. (2002). Lead recovery from PbO, $PbCl_2$, PbS, $PbSO_4$ and their mixtures in carbonate melts. *Inorganic Materials, 38*(12*),* 1216-1223. https://doi.org/10.1023/A:1021363102585

[9] Ignatiev, V.S., & Koroteev, E.S. (2009). Industrial processing of lead chloride dust. *Metallurgy Series, National Metallurgical Academy of Ukraine, 15*, 141-143.

[10] Zhang, X., Yang, L., Li, Y., Li, H., Wang, W., & Ye, B. (2012). Impacts of lead/zinc mining and smelting on the environment and human health in China. *Environmental Monitoring and Assessment, 184,* 2261-2273. https://doi.org/10.1007/s10661-011-2115-6

[11] Toyshybek, A.M., & Moldabayeva, G.Zh. (2018). Study of thermodynamic parameters of reactions during electric smelting of lead battery dusts. *Vestnik KazNRTU, 1(125),* 152-155.

[12] Moldabayeva, G.Zh. (2023). *Technologies for comprehensive processing of lead-containing waste in non-ferrous metallurgy*. Almaty.
[13] Gutiérrez Pérez, V.H., Osorio Hernández, J.D., Sánchez Alvarado, R.G., Cruz Ramírez, A., Olvera Vázquez, S.L., & Rivera Salinas, J.E. (2021). Lead recovery from a lead concentrate throughout direct Smelting reduction process with mixtures of Na2CO3 and SiC to 1000° C. *Metals, 12*(1), *58*. https://doi.org/10.3390/met12010058
[14] Salem, A., Tavakkoli-Osgouei, Y., & Jamshidi, S. (2010). Kinetic study of barite carbothermic reduction in the presence of sodium carbonate as catalyst. *Iranian Journal of Chemical Engineering*, *7,* 58-67.
[15] Vignes, A. (2013). *Extractive metallurgy 1: basic thermodynamics and kinetics*. John Wiley & Sons. https://doi.org/10.1002/9781118618974
[16] Sviridova, T.V. (2011). *Solid-state chemistry: Topochemical kinetics*. Belarusian State University, 23 p.
[17] Pickles, C.A. (2008). Thermodynamic analysis of the selective carbothermic reduction of electric arc furnace dust. *Journal of Hazardous Materials, 150(2),* 265-278. https://doi.org/10.1016/j.jhazmat.2007.04.097
[18] Muvunyi, R.A. (2023). Kinetics of Carbothermal Reduction of Electric Arc Furnace Dust from a Stainless Steel Plant: Muvunyi, Zheng, Li, Ma, Owusu-Acheaw, and Zhang. *JOM*, *75*(4), 1137-1147. https://doi.org/10.1007/s11837-022-05682-6

Қорғасын хлориді мен оксихлоридінің натрий карбонатымен тотықсыздану кинетикасы

Г.Ж. Молдабаева[1], Б.С. Баимбетов[1], Е.Б. Тажиев[1*], А.А. Даулетбакова[1], Г.М. Қойшина[1], С.К. Джуманкулова[1], М.Д. Тұран[2], А.А. Искендиров[1]

[1]*Satbayev University, Алматы, Қазақстан*
[2]*Фырат Университеті, Элязыг, Түркия*

**Корреспонденция үшін автор: y.tazhiyev@satbayev.university*

Аңдатпа. Осы мақалада көміртектің қатысуымен қорғасын хлориді ($PbCl_2$) мен қорғасын оксихлоридінің ($PbO \cdot PbCl_2$) натрий карбонатымен тотықсыздана әрекеттесуінің кинетикалық заңдылықтары зерттелді. Зерттеудің өзектілігі екінші реттік өндірістен алынатын қорғасынқұрамды шаңдарды өңдеудің тиімді технологияларын әзірлеу және натрийқұрамды флюстердің құрамын оңтайландыру қажеттілігімен негізделеді. Кинетикалық зерттеулер $PbCl_2$–Na_2CO_3–C жүйесі үшін 800-1100°C және $PbO \cdot PbCl_2$–Na_2CO_3–C жүйесі үшін 500-800ºC температура аралығында изотермиялық жағдайларда термогравиметриялық әдіспен жүргізілді. Тотықсыздана әрекеттесу процесі түрлену дәрежесінің артуына қарай шектейтін сатының өзгеруімен сипатталатын көпсатылы механизм бойынша жүретіні анықталды. $PbCl_2$–Na_2CO_3–C жүйесі үшін процестің бастапқы бөлігі бірінші реттік реакция теңдеуімен қанағаттанарлық сипатталады, бұл химиялық бақылаудың басым екенін көрсетеді; осы сатыдағы көрінетін энергия активациясы 33.5 кДж/мольді құрайды. Түрлену дәрежесінің артуымен энергия активациясының 62-80 кДж/мольге дейін өсуі байқалады, бұл процестің диффузиялық және құрылымдық шектеулермен күрделенген режимге ауысуын көрсетеді. $PbO \cdot PbCl_2$–Na_2CO_3–C жүйесі жоғары реакциялық қабілетімен және түрленудің едәуір дәрежелеріне жылдам жетуімен сипатталады. Орташа түрлену дәрежелерінде процесс негізінен химиялық бақылау жағдайында жүреді ($E_a \approx 43\text{-}44$ кДж/моль), алайда $\alpha \geq 55\%$ кезінде энергия активациясының 74 кДж/мольге дейін өсуі байқалады, бұл массаалмасу әсерінің күшейетінін көрсетеді. Қорғасын оксихлоридінің құрылымындағы оттегінің болуы натрийқұрамды флюстік жүйелердегі тотықсыздандыру процесінің кинетикалық сипаттамаларына елеулі әсер ететіні көрсетілді. Алынған нәтижелер қорғасынқұрамды шаңдарды өңдеудің технологиялық схемаларын оңтайландыруда, металды шығару дәрежесін арттыру және процестің энергия тиімділігін жоғарылату мақсатында қолданылуы мүмкін.

Негізгі сөздер: *қорғасын құрамды шаң, қорғасын хлориді, натрий карбонаты, тотықсыздандырып электрбалқыту, қатты фазалы реакциялар кинетикасы, энергия активациясы, термогравиметриялық талдау*.

Кинетика восстановления хлорида и оксихлорида свинца карбонатом натрия

Г.Ж. Молдабаева[1], Б.С. Баимбетов[1], Е.Б. Тажиев[1*], А.А. Даулетбакова[1], Г.М. Қойшина[1], С.К. Джуманкулова[1], М.Д. Туран[2], А.А. Искендиров[1]

[1]*Satbayev University, Алматы, Казахстан*
[2]*Фират Университет, Элязыг, Турция*

**Автор для корреспонденции: y.tazhiyev@satbayev.university*

Аннотация. В работе исследованы кинетические закономерности восстановительного взаимодействия хлорида свинца ($PbCl_2$) и оксихлорида свинца ($PbO \cdot PbCl_2$) с карбонатом натрия в присутствии углерода. Актуальность исследования обусловлена необходимостью разработки эффективных технологий переработки свинецсодержащих пылей вторичного производства и оптимизации состава натрийсодержащих флюсов. Кинетические исследования выполнены термогравиметрическим методом в изотермических условиях в диапазоне температур 800-1100°C для системы $PbCl_2$–

Na_2CO_3–C и 500–800°C для системы $PbO·PbCl_2$–Na_2CO_3–C. Установлено, что восстановительное взаимодействие протекает по многостадийному механизму с изменением лимитирующей стадии по мере увеличения степени превращения. Для системы $PbCl_2$–Na_2CO_3–C начальный участок процесса удовлетворительно описывается уравнением реакции первого порядка, что свидетельствует о преобладании химического контроля; кажущаяся энергия активации на этой стадии составляет 33.5 кДж/моль. С увеличением степени превращения наблюдается рост энергии активации до 62-80 кДж/моль, что указывает на переход к режиму, осложнённому диффузионными и структурными ограничениями. Система $PbO·PbCl_2$–Na_2CO_3–C характеризуется более высокой реакционной способностью и быстрым достижением значительных степеней превращения. При умеренных степенях превращения процесс протекает преимущественно в условиях химического контроля ($E_a \approx$ 43-44 кДж/моль), однако при $\alpha \geq 55\%$ наблюдается увеличение энергии активации до 74 кДж/моль, свидетельствующее о возрастании влияния массопереноса. Показано, что присутствие кислорода в структуре оксихлорида свинца существенно влияет на кинетические характеристики восстановительного процесса в натрийсодержащих флюсовых системах. Полученные результаты могут быть использованы при оптимизации технологических схем переработки свинецсодержащих пылей с целью повышения извлечения металла и энергоэффективности процесса.

Ключевые слова: *свинецсодержащая пыль, хлорид свинца, оксихлорид свинца, карбонат натрия, восстановительная электроплавка, кинетика твёрдофазных реакций, энергия активации, термогравиметрический анализ.*

Publisher's note

All claims expressed in this manuscript are solely those of the authors and do not necessarily represent those of their affiliated organizations, or those of the publisher, the editors and the reviewers.

SATBAYEV UNIVERSITY

Engineering Journal of Satbayev University

Volume 148 (2026), Issue 3, 9-15

https://doi.org/10.51301/ejsu.2026.i3.02

Thermodynamic justification of chloride sublimation of nonferrous metals from chalcopyrite-magnetite ore Irisu in the presence of calcium chloride

M.A. Tuleyev[1*], V.M. Shevko[1], D.K. Aitkulov[2], Yu.P. Udalov[3]

[1]*M. Auezov South Kazakhstan University, Shymkent, Kazakhstan*
[2]*National Center on complex processing of mineral raw materials of the Republic of Kazakhstan, Almaty, Kazakhstan*
[3]*Saint-Petersburg State Institute of Technology, Saint-Petersburg, Russia*

**Corresponding author: mustafa19930508@mail.ru*

Abstract. The presence of nonferrous metals, particularly copper, in the chalcopyrite-magnetite ore of the Irisu deposit precludes its use in metallurgical production. This requires preliminary metal extraction. This article presents the results of a study on the extraction of nonferrous metals from Irisu ore by chloride sublimation roasting. The study was conducted using computer thermodynamic modeling and the HSC-10 software package, which is based on the minimum Gibbs free energy principle. Calcium chloride was used as the chlorinating agent. The effects of temperature and pressure on the chloride sublimation of nonferrous metals and the behavior of iron and sulfur during this process were determined. It was established that the interaction of Irisu ore with calcium chloride is accompanied by the formation of gaseous chlorides: $AgCl_{(g)}$, $CoCl_{2(g)}$, $Cu_2Cl_{2(g)}$, $Cu_3Cl_{3(g)}$, $Cu_4Cl_{4(g)}$, $CuCl_{(g)}$, $FeCl_{2(g)}$, $PbCl_{(g)}$, $PbCl_{2(g)}$, $ZnCl_{2(g)}$. A decrease in pressure from 0.1 to 0.001 bar reduces the temperature of complete chloride sublimation of copper to 683°C, zinc – 597°C, lead – 593°C, silver and cobalt to 700°C. The degree of chloride sublimation of iron at 700°C is only 0.24%. In the cinder, it is present to a greater extent in the form of Fe_3O_4 and to a lesser extent in the form of Fe_2O_3 and FeO. Under these conditions, sulfur is almost completely (99.99%) converted into SO_2. Chloride sublimates formed at 700°C and 0.001 bar contain 33.94% copper, 11.57% lead, 5.98% zinc, 2.88% cobalt, 0.2673% silver and 5.49% iron. In this polymetallic concentrate, compared to the ore, the content of copper, zinc and silver increased by 44.6 times, lead – by 44.5 times, cobalt – by 45.3 times.

Keywords: *chalcopyrite-magnetite ore, calcium chloride, thermodynamic modeling, temperature, pressure, chloride sublimation, copper, lead, zinc, cobalt, silver, sulfur.*

Received: 10 February 2026
Received in revised form: 20 May 2026
Accepted: 15 June 2026
Available online: 30 June 2026

1. Introduction

Iron-bearing ores, including those in Kazakhstan, where estimated iron ore reserves are 12.5-16.6 billion tons [1-3], often contain nonferrous metals [4-5]. Therefore, not all ores are suitable for direct metallurgical processing. The Irisu chalcopyrite-magnetite deposit, with reserves of 327.1 million tons, is located in Tyulkubas district of Turkestan region. The deposit's ore field consists of Middle Paleozoic carbonate rocks intruded by alkaline gabbroic intrusions.

The main minerals are magnetite, pyrite, chalcopyrite, pyrrhotite, cobaltite, sphalerite, and galena. The ore contains 30-60% iron, 0.32-0.93% copper, 0.24% lead, 0.09% zinc, and 0.04% cobalt [6-8]. The ore also contains selenium, tellurium, thallium, and 0.56-6.5 g/t silver. In addition to 150 million tons of iron, the ore also contains 2 million tons of copper, which is a valuable resource for ferrous and nonferrous metallurgy. The ore from the Susingen deposit, with reserves of 25 million tons, also falls into this category [9].

Processing iron-bearing ores containing nonferrous metals involves a combination of physical and chemical technologies, such as magnetic separation, flotation, and leaching, including bioleaching. A common drawback of these methods is the multi-stage nature and insufficient recovery of nonferrous metals and often iron as well. Thus, during the processing of sulfide-magnetite ore (35.7% Fe, 0.64% Cu, 1.2 g/t Au), which successively uses X-ray radiometric separation, wet magnetic separation and flotation, 93.6% of copper is extracted into copper concentrate (23.7% Cu, 18.9 g/t Au and 60 g/t Ag), only 76.6% of iron is extracted into magnetite concentrate (66.5% Fe), and only 27% of gold is extracted into gold-bearing concentrate (50 g/t).

During the flotation of copper-magnetite ore (0.3-0.5% Cu) by flotation into copper concentrate (18.5% Cu) only 77.8% of copper was extracted [10]. From the wet magnetic separation tailings of ferrous ores containing 0.29% sulfide copper, no more than 80% of copper was extracted into concentrate (25.3% Cu) by flotation [11], and from similar ore of another Cheremshansky tailings dump only 65.3% of copper was extracted into concentrate [11]. Preliminary (before magnetic separation) magnetic pulse treatment of ore containing 0.14% sulfide copper allowed to increase the copper extraction into sulfide product from 54 to 65% [12]. Using multi-stage wet magnetic separation and flotation of its tailings from iron ore containing copper into magnetic concentrate (65-66% Fe), 79-80% of Fe was extracted, and from tailings into copper concentrate (15.2% Cu) – only 54% of copper [13]. Magnetic separation of the Irisu deposit ore and flotation of its tailings yielded 87-90% iron recovery into magnetic concentrate (69-75% Fe), 75-84% copper recovery into copper concentrate (18.64% Cu), and 67.2-77.3% cobalt recovery into cobalt-pyrite concentrate.

Research [14] presents the results of studies of Fe-Cu-containing ore (1.79% Cu) using a magnetic separation and copper leaching scheme from separation tailings. This method allows for the recovery of only 72% copper.

Gravity enrichment of ore containing 16.5% Fe, 0.13% Cu, and rare earth elements resulted in the conversion of 76.6% iron and 72.6% copper into the heavy fraction, and 77.9% rare earth elements into the light fraction. A combination of magnetic separation and bioleaching of magnetite concentrate yielded 80% of copper and 20% of zinc [15].

The above data demonstrates that existing multi-stage methods do not provide a high level of separation of iron from nonferrous metals in copper-magnetite ores. Currently, they do not meet modern requirements for the integrated use of raw materials. The problem of integrated processing of copper-magnetite ores can be successfully solved by developing a technology that allows for the complete separation of iron from nonferrous metals in a single process step, followed by the production of marketable products from magnetite concentrate. Chloride sublimation is an effective method for the selective extraction of nonferrous metals from iron-containing raw materials. The main advantage of this method is the ability to virtually completely suppress iron chlorination, leaving it in the cinder and extracting the nonferrous metals into chloride sublimes. Based on this, chloride-electrothermal technology may be an effective method for processing Irisu iron-bearing ore. This involves chloride-sublimation roasting in the first stage, with the extraction of copper and other nonferrous metals into a polymetallic concentrate – chloride sublimes and iron-containing magnetite concentrate – from which a ferroalloy is produced in the second stage by electric smelting. The authors of this article have previously conducted studies on the chloride-sublimation of nonferrous metals from various polymetallic natural and technogenic raw materials, with virtually complete iron retention in the cinder [16, 17]. This article presents the results of studies on the equilibrium chloride sublimation of nonferrous metals from chalcopyrite-magnetite ore at the Irisu deposit in the presence of calcium chloride.

2. Materials and methods

The study was conducted using thermodynamic modeling with the HSC-10 software package [18], based on the minimum Gibbs free energy principle, to determine the equilibrium distribution of nonferrous metals and iron (α, %) in the Irisu ore (IO) – $CaCl_2$ – O_2 system. The temperature range for the studies was 300-1700°C, and the pressure range was 0.1-0.001 bar. The ore used in the study was from the Irisu deposit, containing (wt%): 69.4 Fe_3O_4, 10.0 SiO_2, 6 $CaCO_3$, 5.8 $MgCO_3$, 3.3 Al_2O_3, 2.2 $CuFeS_2$, 0.3 PbS, 0.2 ZnS, 0.1 CoS, 0.002 Ag. To improve the efficiency of the research and obtain maximum information from the processes under study, the method of second-order rotatable research design (Box-Hunter plans) was also used in the work, with the resulting regression equations [19] being used to construct volumetric and planar images of the optimization parameters [20, 21]. The temperature and pressure ensuring maximum chloride sublimation of nonferrous metals and minimum chloride sublimation of iron were determined from the image of the overlapping planar images.

3. Results and discussion

The primary material obtained using the HSC-10 complex allowed to establish that in the system under consideration, at a pressure of 0.1 bar, the reaction occurs with the formation of $Ag_{(g)}$, AgCl, $AgCl_{(g)}$, Al_2SiO_5, $CaCl_{2(g)}$, $CaSiO_3$, $CaSO_4$, $Cl_{(g)}$, $CO_{(g)}$, $CO_{2(g)}$, $CoCl_2$, $CoCl_{2(g)}$, $Cu_{(g)}$, $Cu_2Cl_{2(g)}$, $Cu_3Cl_{3(g)}$, $Cu_4Cl_{4(g)}$, CuCl, $CuCl_{(g)}$, $CuCl_{2(g)}$, Fe_2O_3, $FeCl_2$, $FeCl_{2(g)}$, $FeCl_{3(g)}$, FeO, FeS, $FeSiO_3$, MgO, $MgSiO_3$, $O_{2(g)}$, $Pb_{(g)}$, $PbCl_{(g)}$, $PbCl_2$, $PbCl_{2(g)}$, $SO_{2(g)}$, $Zn_{(g)}$, $ZnCl_{(g)}$, $ZnCl_2$, $ZnCl_{2(g)}$.

Figure 1 shows the effect of temperature on the degree of metal distribution in the RI – $CaCl_2$ – O_2 system at 0.1 bar. It is evident that the formation of the target gaseous chlorides: $Cu_4Cl_{4(g)}$, $Cu_3Cl_{3(g)}$, $Cu_2Cl_{2(g)}$ and $CuCl_{(g)}$ ccurs, respectively, in the following temperature ranges: 400-1300°C, 400-1400°C, 900-1500°C, and >800°C.

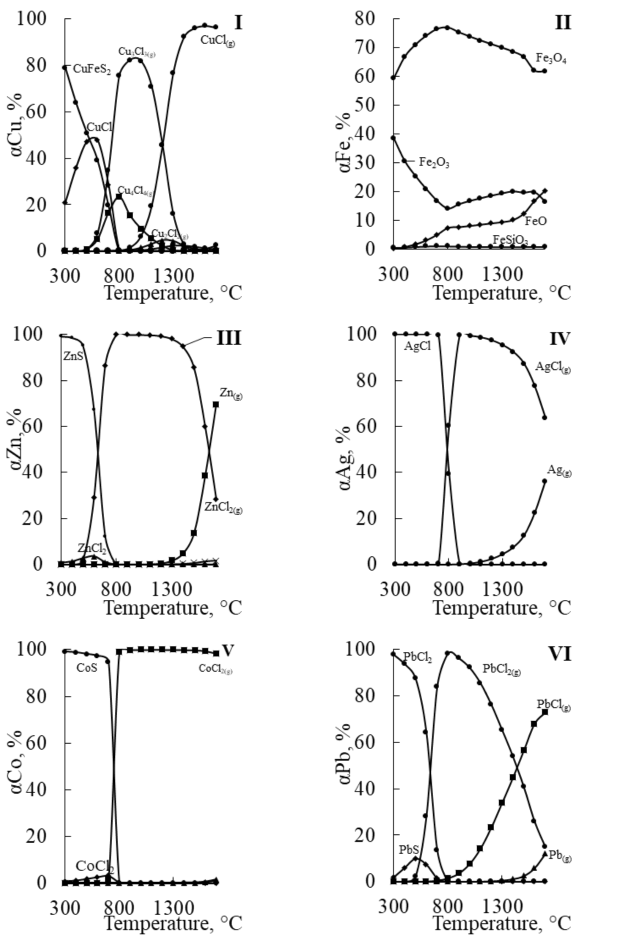

Figure 1. Effect of temperature on the degree of distribution Cu (I), Fe (II), Zn (III), Ag (IV), Co (V), Pb (VI)

Iron is practically not chlorinated in the system, accounting for only 0.23-0.33% at 800-1700°C. Predominantly (59.6-75.3%), iron remains in the form of Fe_3O_4 in the temperature range of 300-1700°C. To a lesser extent, iron is converted into Fe_2O_3 (38-15%), and only 0.32-8.2% into FeO.

The target zinc-containing product, gaseous $ZnCl_{2(g)}$, begins to appear in the system at 400°C. The maximum of this process (99.5-99.9%) occurs at 800-1200°C. Then, as the temperature increases to 1700°C, the decomposition of $ZnCl_{2(g)}$ begins, forming gaseous $ZnCl_{(g)}$ and $Zn_{(g)}$.

Complete chlorination of silver to form AgCl occurs at 300°C. The maximum conversion of silver to gas (99.7%) in the form of AgCl occurs at 900°C. Then, as the temperature increases to 1700°C, the decomposition of $AgCl_{(g)}$ occurs, forming $Ag_{(g)}$ and chlorine (36.2% of gaseous silver is formed at 1700°C). The chlorination of CoS to form $CoCl_2$ begins at 400°C, and gaseous $CoCl_2$ begins at 800°C. In the temperature range of 900-1700°C, all cobalt is present as $CoCl_{2(g)}$.

Chlorination of PbS is virtually complete at 300°C, forming $PbCl_2$, which persists up to 800°C. Formation of gaseous $PbCl_2$ occurs in the range of 400-1700°C, with a maximum (98.4%) at 800°C. At temperatures above 800°C, gaseous $PbCl_2$ forms: $PbCl_2 = PbCl_{(g)} + 0.5Cl_2$. In the temperature range of 1300-1700°C, some elemental lead is in the gaseous state.

Table 1 shows the effect of temperature on the degree of conversion of metals (as the sum of chlorides and elements) into gas (hereinafter $\alpha_{Me(gas)}$) at a pressure of 0.1 bar.

Table 1. Effect of temperature on the degree of distribution of elements in gas

Element	Temperature, °C									
	300	400	500	600	700	800	900	1000	1500	1700
Ag	–	–	–	0.01	0.33	60.52	100	100	100	100
Co	–	–	–	0.05	2.06	99.60	100	100	100	100
Cu	–	0.07	1.81	13.22	51.68	99.46	100	100	100	100
Fe	–	–	–	–	0.03	0.23	0.24	0.24	0.25	0.33
Pb	–	0.05	2.41	28.29	84.77	99.94	100	100	100	100
Zn	–	0.05	2.07	29.21	86.70	99.99	100	100	100	100

Table 1 shows that at 0.1 bar and 900°C, Zn, Cu, Pb, Co, and Ag completely transform into gas. Almost all the iron remains in the cinder. Only 0.24% of the iron transforms into gaseous $FeCl_3$. Figure 2 shows the effect of temperature and pressure on the degree of metal conversion to the gas phase. It is evident that decreasing the pressure from 0.1 to 0.001 bar lowers the temperature for complete gasification of zinc and lead to 600°C, and for Cu, Co, and Ag to 700°C. At 700°C, the degree of iron chloride sublimation is only 0.25%.

When producing cinders, it is important that they contain a minimum amount of sulfur.

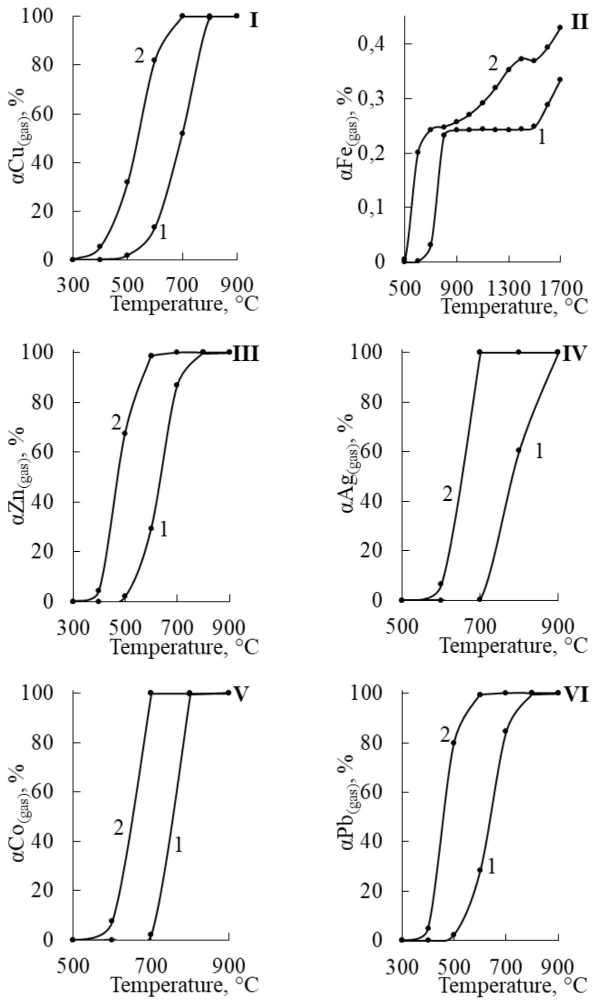

Figure 2. Effect of temperature and pressure on the degree of metal extraction into the gas phase (pressure: 1 – 0.1 bar; 2 – 0.001 bar

Figure 3 shows that the main sulfur-containing substances in the system are $CuFeS_2$, $CaSO_4$, SO_2, ZnS, PbS and CoS. Reducing the pressure from 0.1 to 0.001 bar allows for a reduction in the temperature of virtually complete (99.29%) sulfur conversion to SO_2 from 1300 to 700°C. Only 0.7% sulfur remains in the cinder.

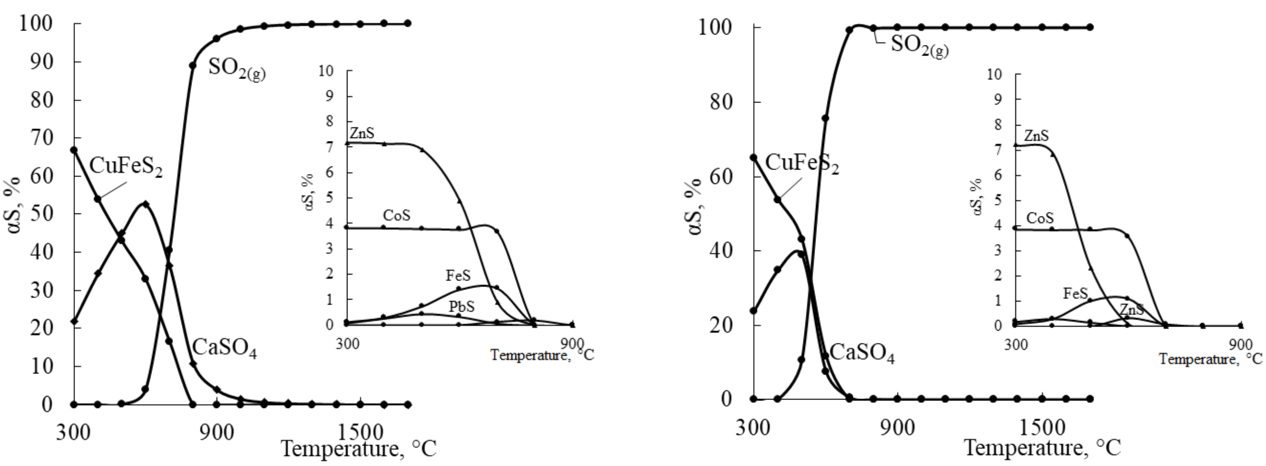

Figure 3. Effect of temperature and pressure on the degree of sulfur distribution (pressure: I – 0.1 bar; II – 0.001 bar)

To determine the temperature and pressure that will maximize the extraction of copper, zinc, lead, silver, and cobalt into gaseous chlorides, further research is being conducted using a second-order rotatable design [19]. Table 2 presents the experimental design matrix and the results of studying the effects of temperature and pressure on the conversion of the main metals from the ore into the gas phase.

Table 2. Effect of temperature and pressure on the degree of conversion of copper, lead, and zinc into the gas phase

No.	Variables				$\alpha Cu_{(gas)}$, %	$\alpha Pb_{(gas)}$, %	$\alpha Zn_{(gas)}$, %
	Coded		Natural				
	X_1	X_2	lgP	T, °C			
1	+	+	-2.7	654	94.3	99.0	99.8
2	–	+	-1.3	654	46.4	75.1	75.3
3	+	–	-2.7	526	37.3	77.3	73.0
4	–	–	-1.3	526	9.0	15.6	16.0
5	1.414	0	-3	590	80.5	96.2	97.2
6	-1.414	0	-1	590	12.7	25.0	27.4
7	0	1.414	-2	680	87.0	98.2	100.0
8	0	-1.414	-2	500	13.4	22.4	18.5
9	0	0	-2	590	40.2	84.7	77.8
10	0	0	-2	590	40.8	85.0	77.6
11	0	0	-2	590	41.0	85.1	77
12	0	0	-2	590	41.6	85.7	76.6
13	0	0	-2	590	41.6	86.0	76.1

Using the data from the table in [20], the following regression equations were obtained:

$$\alpha CU_{(gas)} = 136.09 - 0.56 \cdot T + 63.1 \cdot \lg P + 0.00058 \cdot T^2 + 8.5 \cdot (\lg P)^2 - 0.109 \cdot T \cdot \lg P \quad (1)$$

$$\alpha Pb_{(gas)} = -1450 + 3.89 \cdot T - 247.4 \cdot \lg P - 0.0026 \cdot T^2 - 22.33 \cdot (\lg P)^2 + 0.211 \cdot T \cdot \lg P \quad (2)$$

$$\alpha Zn_{(gas)} = 983.26 + 2.43 \cdot T - 203.95 \cdot \lg P - 0.0015 \cdot T^2 - 15.25 \cdot (\lg P)^2 + 0.18 \cdot T \cdot \lg P \quad (3)$$

Then, according to [21], 3D and planar images of the dependencies $\alpha Cu_{(gas)}$, $\alpha Pb_{(gas)}$, $\alpha Zn_{(gas)} = f$ (lgP, T) were constructed. Table 3 presents the pressure and temperature values at the boundaries of the regions shown in Figure 4, where $\alpha Me_{(gas)}$ ranges from 90 to 100%.

Table 3. Pressure and temperature values at the boundaries of the regions where αMe(gas) ranges from 90 to 100%

Metal	Points of the region	lgP	P, bar	T, °C	$\alpha Me_{(gas)}$, %
Copper	*a*	-2.3	0.005	680	90
	b	-2.5	0.003	680	100
	c	-3.0	0.001	623	100
	d	-3.0	0.001	601	90
Lead	*t*	-1.57	0.027	680	90
	f	-1.95	0.011	680	100
	h	-3.0	0.001	593	100
	u	-3.0	0.001	554	90
Zinc	*o*	-1.67	0.021	680	90
	p	-2.11	0.008	680	100
	l	-3.0	0.001	597	100
	e	-3.0	0.001	551	90

From Table 3 it follows that lead sublimes into chlorides by 90-100% in the temperature range of 554-680°C at 0.011-0.001 bar, zinc – at 551-680°C and 0.021-0.001 bar, and copper – at 601-680°C and 0.005-0.001 bar.

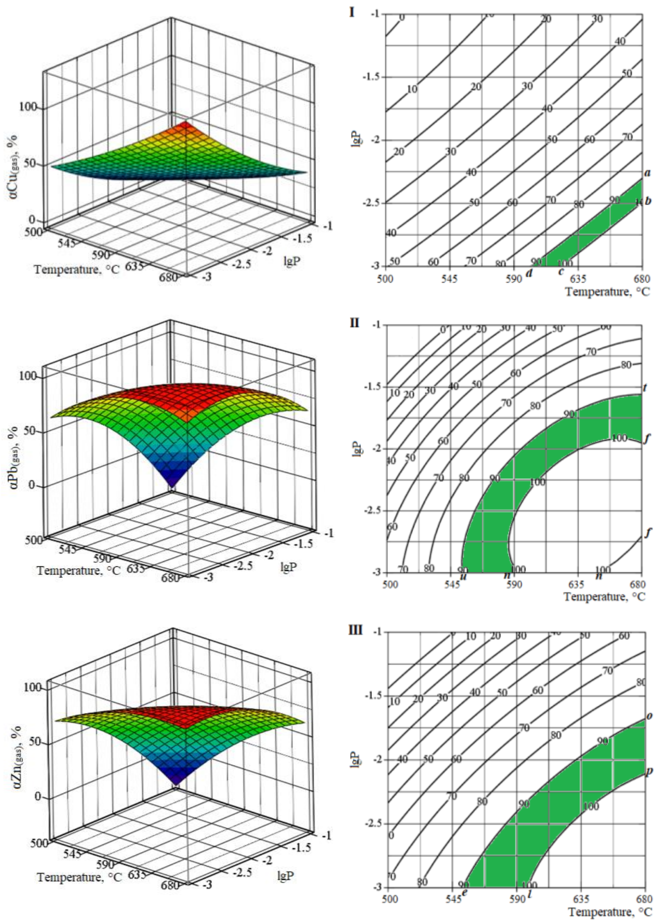

Figure 4. 3D and planar images of the effect of temperature and pressure on the degree of conversion n of metals into gas (metals: I – copper; II – lead; III – zinc)

Figure 5 and Table 3 show that copper undergoes chloride sublimation with greater difficulty than zinc and lead. Therefore, the conditions for copper chloride sublimation determine the optimal parameters for the chloride sublimation of copper, zinc, and lead. These conditions must also be consistent with the conversion of silver and cobalt into gas.

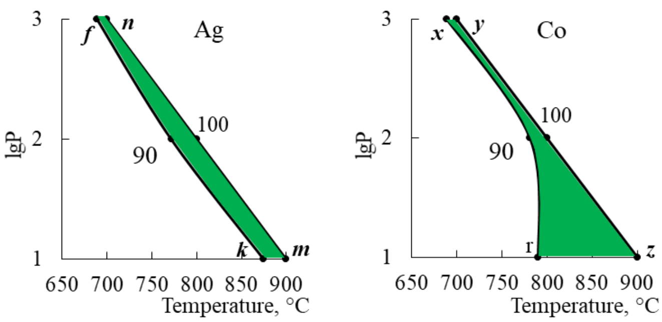

Figure 5. Effect of temperature and pressure on $\alpha Me_{(gas)}$ of silver and cobalt (the numbers near the line indicate the degree of conversion of metal into gas, %)

Figure 5 shows the αMe(gas) regions for silver and cobalt from 90 to 100%, and Table 4 shows the pressure and temperature values for these regions. At a pressure of 0.001-0.01 bar, $\alpha Ag_{(gas)}$ = 90-100% in the temperature range of 698-900°C, while cobalt does so at 689-900°C.

Comparing Tables 3 and 4, it follows that $\alpha Ag_{(gas)}$ and $\alpha Cu_{(gas)}$ decomposition occurs at higher temperatures.

Table 4. lgP and temperature values at the boundaries of the regions where αMe(gas) for Ag and Co ranges from 90 to 100%

Metal	Points of the region	lgP	P, bar	T, °C	$αMe_{(gas)}$, %
Silver	*f*	-3	0.001	698	90
	n	-3	0.001	700	100
	m	-1	0.1	900	100
	k	-1	0.1	875	90
Cobalt	*x*	-3	0.001	689	90
	y	-3	0.001	700	100
	z	-1	0.1	900	100
	r	-1	0.1	790	90

Thus, at 0.001 bar, $αCu_{(gas)}$ = 100% occurs at 623°C, while for cobalt and silver, it occurs only at 700°C. Therefore, the optimal temperature should be determined by the chloride sublimation of silver (698-900°C and 0.01-0.1 bar).

Figure 6 shows the effect of temperature and pressure on the metal concentration in condensed sublimates.

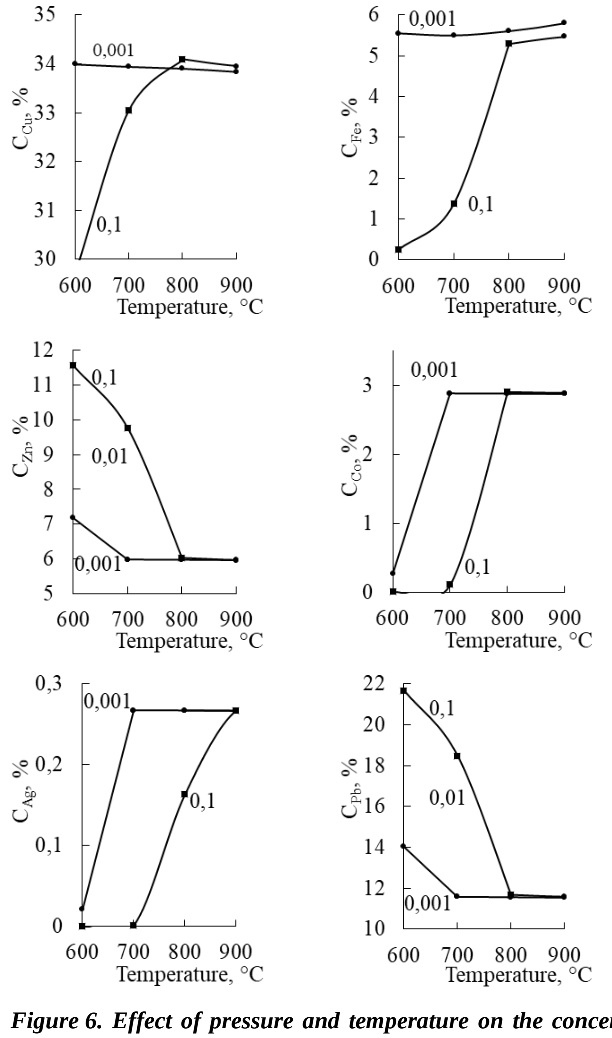

Figure 6. Effect of pressure and temperature on the concentration of metals in condensed sublimates (the numbers near the line indicate pressure in bar)

It is evident that in the region of 800-900°C the change in pressure has virtually no effect on the concentration of copper, lead, zinc, cobalt and silver, amounting to 33.7-34.0%; 11.7-11.6%; 5.97-5.95%, 2.9-2.97%, respectively. The concentration of iron at 600-900°C increases from (5.29 at 800°C) to (5.79 at 900°C). At 700°C and 0.001 bar, when the nonferrous metals had completely converted into gaseous chlorides, the concentration of copper in the condensed sublimes was 33.94%, lead – 11.57%, zinc – 5.98%, cobalt – 2.88%, silver – 0.27%, iron – 5.49%. Chloride sublimates are a polymetallic concentrate in which, in comparison with the ore, the concentration of copper, zinc and silver has increased by 44.6 times, lead – by 44.5 times, cobalt – by 45.3 times. The cinder after roasting the ore at 800°C and 0.001 bar contains by weight %: Fe_3O_4 – 59.81, Fe_2O_3 – 12.03, $CaSiO_3$ – 9.33, $MgSiO_3$ – 6.11, FeO – 5.12, Al_2O_3 – 3.52, SiO_2 – 1.91, $FeSiO_3$ – 1.33, MgO – 0.62, Al_2SiO_5 – 0.21, $CaSO_4$ – 0.01. It can be used in blast furnaces, steelmaking or for the production of ferroalloys.

4. Conclusions

Based on the conducted studies of the equilibrium interaction of Irisu copper-magnetite ore with calcium chloride in the presence of oxygen, the following conclusions can be drawn:

– the chlorination products are chlorides of copper (Cu_4Cl_4, Cu_3Cl_3, Cu_2Cl_2 and CuCl), lead ($PbCl_2$, PbCl), zinc ($ZnCl_2$, ZnCl), iron ($FeCl_3$, $FeCl_2$), silver (AgCl), and cobalt ($CoCl_2$);

– according to the temperature of the beginning of formation of gaseous chlorides, metals form a series: Cu, Zn, Pb, Co, Ag and Fe; this temperature, like the temperature of complete extraction of chlorides into gas, shifts to the region of lower temperatures with decreasing pressure;

– complete chloride sublimation of copper at a pressure of 0.001 bar occurs at 683°C, zinc – 597°C and lead – 593°C, silver and cobalt at 700°C (iron is chlorinated only by 0.24%);

– chloride sublimes formed at 700°C and 0.001 bar contain 33.94% copper, 11.57% lead, 5.98% zinc, 2.88% cobalt, 0.2673% silver and 5.49% iron; chloride sublimes are a polymetallic concentrate in which, compared to the ore, the concentration of copper has increased by 44.6 times, lead – by 44.5 times, zinc and silver – by 44.6 times, cobalt – by 45.3 times;

– sulfur present in the ore at a pressure of 0.001 bar and 700°C is almost completely (99.29%) converted to SO_2.

The cinder after roasting the ore at 800°C and a pressure of 0.001 bar contains the following by weight, %: Fe_3O_4 – 59.381, Fe_2O_3 – 12.03, $CaSiO_3$ – 9.33, $MgSiO_3$ – 6.11, FeO – 5.12, Al_2O_3 – 3.52, SiO_2 – 1.91, $FeSiO_3$ – 1.33, MgO – 0.62, Al_2SiO_5 – 0.21, $CaSO_4$ – 0.01, can be used in the production of cast iron, steel, and ferroalloys.

Author contributions

Conceptualization: V.M.S., M.A.T.; Data curation: V.M.S., M.A.T.; Formal analysis: D.K.A., Yu.P.U.; Funding acquisition: V.M.S., M.A.T.; Investigation: M.A.T., Yu.P.U.; Methodology: V.M.S., D.K.A.; Project administration: V.M.S., D.K.A.; Resources: V.M.S., M.A.T.; Software: M.A.T., Yu.P.U.; Supervision: V.M.S., M.A.T.; Validation: V.M.S., D.K.A.; Visualization: M.A.T., Yu.P.U.; Writing – original draft: V.M.S., M.A.T.; Writing – review & editing: V.M.S., M.A.T. All authors have read and agreed to the published version of the manuscript.

Funding

This research received no external funding.

Acknowledgements

The authors express their sincere gratitude to the editor and anonymous reviewers for their constructive comments and valuable suggestions, which have significantly improved the quality of this manuscript.

Conflicts of interests

The authors declare no conflict of interest.

Data availability statement

The original contributions presented in this study are included in the article. Further inquiries can be directed to the corresponding author.

References

[1] Alshanov, R.A. (2004). *Kazakhstan in the global mineral resource market: problems and solutions: an analytical review*. Almaty.

[2] Mining Sector Diagnostic Report – Kazakhstan. (2023). World Bank Group. *Received from*: http://documents.worldbank.org/curated/en/099081823001539573

[3] Korobkin, V., Nygmanova, A., Tulemissova, Z., & Chaklikov, A. (2025). Geological and Mineralogical Analysis of Zhuantobe Skarns in Central Kazakhstan Considering the Influence of Textural Features on Iron Ore Quality. *Applied Sciences, 15*(17), 9816. https://doi.org/10.3390/app15179816

[4] Krikunova, L.M., Titova, A.P., & Ushakov, V.N. (2006). Geological and genetic types of iron deposits in Uzbekistan. Problems of Ore Deposits and Improving the Efficiency of Geological Exploration. *Proceedings of the International Scientific and Practical Conference*. Tashkent: Institute of Mineral Resources.

[5] Abdrahmanov, K.A., & Sharapatov, A. (2006). Sources of ore components and ore-concentrating factors in the formation of iron ore deposits. Conditions of formation, patterns of placement and forecasting of mineral deposits. *Proceedings of the International Conference*. Tashkent: Tashkent State Technical University

[6] Kazakhstan. National Encyclopedia (2005). *Almaty: Kazakh Encyclopedia*, (2).

[7] Iron-copper-cobalt deposit. (2022). Business Asset. Available at: https://business-asset.com/kz/yuzhnokazaxstanskaya-oblast/kulan/prodazha-nedvizimosti/kzn189550/

[8] Iirsu deposit. (2026). Qazaqstan tarihy. Available at: https://e-history.kz/ru/kazakhstanika/show/11405

[9] Miroshnichenko, L.A., Tilepov, Z.T., Gulyaeva, N.Ya., Zhukov, N.M., & Akylbekov, S.A. (1998). Iron deposits of Kazakhstan: reference book. *Committee for Geology and Subsoil Protection of the Ministry of Ecology and Natural Resources of the Republic of Kazakhstan*. Almaty.

[10] Boriskov, F.F. (2009). Increasing the comprehensive utilization of sulfide-bearing magnetite ores of the Urals. *Development of N.V. Melnikov's Ideas in the Field of Integrated Development of Mineral Resources: Proceedings of the International Meeting Dedicated to the 100th Anniversary of Academician N.V. Melnikov*, 154-156.

[11] Boriskov, F.F., & Antoninova, N.Yu. (2011) Improving the environmental safety of processing sulfide-containing magnetite ores in the Urals. Scientific foundations and practice of processing ores and technogenic raw materials. *Proceedings of the 16th International Scientific and Technical Conference*. Ekaterinburg: Tails KO.

[12] Lavrinenko, A.A., Lucinian, O.G., Kuznetsova, I.N., & Olennikov, V.G. (2023) Obtaining copper concentrate during iron ore processing. *Izvestiya: Non-Ferrous Metallurgy, 1*(1), 5-15. https://doi.org/10.17073/0021-3438-2023-1-5-15

[13] Antoninova, N.Yu., & Boriskov, F.F. (2011). Processing of copper–sulfide magnetite ores. In: *Problems of Subsoil Use: Proceedings of the 5th All-Russian Youth Scientific and Practical Conference*. Yekaterinburg: Institute of Mining, Ural Branch of the Russian Academy of Sciences.

[14] Peng, Z., Fu, X., Pan, Z., Gao, Y., He, D., Fan, X., Yue, T., & Sun, W. (2022). Efficient Recovery of the Combined Copper Resources from Copper Oxide Bearing Limonite Ore by Magnetic Separation and Leaching Technology. *Minerals, 12(10)*, 1258. https://doi.org/10.3390/min12101258

[15] Nekoee Motlagh, M. J., Soltani, F., & Mojeddifar, S. (2023). Iron, copper, and rare earth minerals beneficiation in an IOCG type deposit. *Canadian Metallurgical Quarterly, 63(4)*, 1415-1425. https://doi.org/10.1080/00084433.2023.2285199

[16] Shevko, V.M., Aitkulov, D.K., Aitkulov, B.D., Serzhanov, G.M., & Uteeva, R.A. (2014). *Integrated chloride-electrothermal processing of copper-bearing oxide ores*. Shymkent: South Kazakhstan State University, 235 p.

[17] Shevko, V.M., Aitkulov, D.K., Serzhanov, G.M., Karataeva, G.E., & Badikova, A.D. (2019). *Integrated processing of copper-bearing ore beneficiation tailings*. Shymkent: M. Auezov South Kazakhstan State University, 203 p.

[18] Metso Outotec. (2021). *HSC Chemistry 10* [Computer software]. Pori, Finland. Available at: www.mogroup.com/hsc.

[19] Akhnazarova, S.L., & Kafarov, V.V. (1978). *Optimization of experiments in chemistry and chemical technology*. Moscow: Vysshaya Shkola, 319 p.

[20] Inkov, A.M., Tapalov, T., Umbetov, U.U., Hu Wen Tsen, V., Akhmetova, K.T., & Dyakova, E.T. (2003). *Optimization methods*. Shymkent: South Kazakhstan State University.

[21] Ochkov, V.F. (2007). *Mathcad 14 for students, engineers, and designers*. Saint Petersburg: BHV-Petersburg

Ирису кен орнындағы халькопирит-магнетит кенінен кальций хлориді қатысуында түсті металдарды хлоридті айдау процесінің термодинамикалық негіздемесі

М.А. Тулеев[1*], В.М. Шевко[1], Д.К. Айткулов[2], Ю.П. Удалов[3]

[1]М. Әуезов атындағы Оңтүстік Қазақстан университеті, Шымкент, Қазақстан
[2]Қазақстан Республикасының минералдық шикізатты кешенді өңдеу жөніндегі ұлттық орталығы, Алматы, Қазақстан
[3]Санкт-Петербург мемлекеттік технологиялық институты, Санкт-Петербург, Ресей

**Корреспонденция үшін автор: mustafa19930508@mail.ru*

Аңдатпа. Ирису кен орнындағы халькопирит-магнетит кенінің құрамында түсті металдардың, әсіресе мыстың болуы бұл кенді металлургиялық өндірісте тікелей пайдалануға мүмкіндік бермейді. Сондықтан кенді қолданар алдында одан металдарды алдын ала бөліп алу қажет. Мақалада Ирису кенінен түсті металдарды хлоридті айдау арқылы күйдіру әдісімен бөліп алу бойынша жүргізілген зерттеулердің нәтижелері келтірілген. Зерттеулер компьютерлік термодинамикалық модельдеу әдісімен, Гиббс энергиясының минимум принципіне негізделген HSC-10 бағдарламалық кешенін қолдану арқылы жүргізілді. Хлорлаушы реагент ретінде кальций хлориді пайдаланылды. Температура мен қысымның түсті металдардың хлоридті айдалуына, сондай-ақ темір мен күкірттің мінез-құлқына әсері анықталды. Ирису кені кальций хлоридімен әрекеттескенде келесі газ тәрізді хлоридтердің түзілетіні анықталды: $AgCl_{(г)}$, $CoCl_{2(г)}$, $Cu_2Cl_{2(г)}$, $Cu_3Cl_{3(г)}$, $Cu_4Cl_{4(г)}$, $CuCl_{(г)}$, $FeCl_{2(г)}$, $PbCl_{(г)}$, $PbCl_{2(г)}$, $ZnCl_{2(г)}$. Қысымды 0.1-ден 0.001 барға дейін төмендету мыстың толық хлоридті айдалу температурасын 683°C-қа, мырыштікін 597°C-қа, қорғасындікін 593°C-қа, ал күміс пен кобальттікін 700°C-қа дейін төмендететіні анықталды. 700°C температурада темірдің хлоридті айдалу дәрежесі небәрі 0.24% құрайды. Күйдіріндіде темір негізінен Fe_3O_4 және аз мөлшерде Fe_2O_3 мен FeO түрінде кездеседі. Бұл жағдайларда күкірттің басым бөлігі іс жүзінде толық (99.99%) SO_2 түрінде газ фазасына өтеді. 700°C температура және 0.001 бар қысымда түзілген хлоридті айдамалар құрамында 33.94% мыс, 11.57% қорғасын, 5.98% мырыш, 2.88% кобальт, 0.2673% күміс және 5.49% темір бар. Бұл полиметалл концентратында кенмен салыстырғанда мыс, мырыш және күміс мөлшері 44.6 есе, қорғасын 44.5 есе, кобальт 45.3 есе артқаны анықталды.

Негізгі сөздер: *халькопирит-магнетит кені, кальций хлориді, термодинамикалық модельдеу, температура, қысым, хлоридті айдау, мыс, қорғасын, мырыш, кобальт, күміс, күкірт.*

Термодинамическое обоснование хлоридовозгонки цветных металлов из халькопирит-магнетитовой руды Ирису в присутствии хлорида кальция

М.А. Тулеев[1*], В.М. Шевко[1], Д.К. Айткулов[2], Ю.П. Удалов[3]

[1]Южно-Казахстанский университет им. М. Ауэзова, Шымкент, Казахстан

[2]Национальный центр по комплексной переработки минерального сырья Республики Казахстан, Алматы, Казахстан

[3]Санкт-Петербургский государственный технологический институт, Санкт-Петербург, Россия

**Автор для корреспонденции: mustafa19930508@mail.ru*

Аннотация. Присутствие цветных металлов и особенно меди в халькопирит-магнетитовой руде месторождения Ирису не позволяет использовать эту руду в металлургическом производстве. Для этого необходимо предварительно извлечь металлы из руды. В статье приводятся результаты исследования по извлечению цветных металлов из Ирисуской руды хлоридовозгоночным обжигом. Исследования проводились методом компьютерного термодинамического моделирования и использованием программного комплекса HSC-10 основанного на принципе минимума энергии Гиббса. В качестве хлорирующего агента использовали хлорид кальция. Определялось влияние температуры и давления на хлоридовозгонку цветных металлов и поведение при этом железа и серы. Установлено, что взаимодействие руды Ирису с хлоридом кальция сопровождается образованием газообразных хлоридов: $AgCl_{(г)}$, $CoCl_{2(г)}$, $Cu_2Cl_{2(г)}$, $Cu_3Cl_{3(г)}$, $Cu_4Cl_{4(г)}$, $CuCl_{(г)}$, $FeCl_{2(г)}$, $PbCl_{(г)}$, $PbCl_{2(г)}$, $ZnCl_{2(г)}$. Уменьшение давления от 0.1 до 0.001 бар снижает температуру, полной хлоридовозгонки меди до 683°C, цинка - 597°C, свинца - 593°C, серебра и кобальта до 700°C. Степень хлоридовозгонки железа при 700°C составляет только 0.24%. В огарке оно в большей мере присутствует в виде Fe_3O_4 и в меньшей мере - в виде Fe_2O_3 и FeO. Сера в этих условиях практически полностью (99.99%) переходит в SO_2. Хлоридные возгоны, образующиеся при 700°C и 0.001 бар содержат 33.94% меди, 11.57% свинца, 5.98% цинка, 2.88% кобальта, 0.2673% серебра и 5.49% железа; В этом полиметаллическом концентрате в сравнении с рудой, содержание меди, цинка и серебра увеличилось в 44.6 раза, свинца – в 44.5 раза, кобальта – в 45.3 раза.

Ключевые слова: *халькопирит-магнетитовая руда, хлорид кальция, термодинамическое моделирование, температура, давление, хлоридовозгонка, медь, свинец, цинк, кобальт, серебро, сера.*

Publisher's note

SATBAYEV UNIVERSITY

Engineering Journal of Satbayev University

Volume 148 (2026), Issue 3, 16-23

https://doi.org/10.51301/ejsu.2026.i3.03

Application Practice of L-SX-EW in the Processing of Copper Ores from Kazakhstan Deposits

N. Yakushev*

VNIItsvetmet, a branch of the RSE «NC CPMRM RK», Oskemen, Kazakhstan

**Corresponding author: nikita.yakushev2112@mail.ru*

Abstract. The article provides an analytical review of the current state and development prospects of Leach-Solvent Extraction-Electrowinning (L-SX-EW) technology within the global and domestic copper industries. The study analyzes the mineral resource base of the Republic of Kazakhstan, including major copper deposits in the East and Central regions. Attention is given to solvent extraction flowsheets, the impact of mineralogical composition, and key technological challenges in processing oxidized and mixed copper ores. The paper highlights the historical role of «VNIItsvetmet» in the development of regional hydrometallurgical technologies and research approaches. The work systematizes data on modern technological schemes and principal efficiency factors of the L-SX-EW process, confirming its vital role in maintaining the long-term competitiveness of Kazakhstan's copper sector.

Keywords: *copper, heap leaching, solvent extraction, electrowinning, Kazakhstan mineral resources, oxidized copper ores*.

Received: 05 March 2026
Received in revised form: 08 June 2026
Accepted: 15 June 2026
Available online: 30 June 2026

1. Introduction

The global increase in copper consumption, including high-purity cathode grades and concentrates, together with the gradual depletion of high-grade sulfide ore reserves and the transition towards the development of off-balance resources and refractory oxidized and mixed ore, necessitates modernization and the development of more efficient ore processing technologies and enhanced recovery of valuable components. Under these conditions, heap leaching followed by solvent extraction and electrowinning (L-SX-EW), which enables the production of high-purity copper, has become one of the key technological solutions. According to the International Copper Study Group (ICSG), hydrometallurgical processes currently account for approximately 20-25% of total mine copper production worldwide [1].

The Republic of Kazakhstan possesses significant copper ore reserves – approximately 36 million tonnes of identified resources. The mineral resource base of copper in Kazakhstan is primarily represented by deposits of copper sandstones (Zhezkazgan), complex copper-pyrite and pyrite-polymetallic ores (Zyryanovskoye, Artemyevskoye, and others in the Rudny Altai, Eastern Kazakhstan), copper porphyry deposits (Aktogay and Aidarly, Bozshakol, Koksay, etc.), and copper skarn deposits (Sayak). Mine copper production in 2021 amounted to 520 thousand tonnes. The country accounts for approximately 2.5% of global mine production and refined copper output (second place within the CIS) [2]. The successful implementation of projects such as Aktogay, Kounrad, and Almaly has demonstrated the effectiveness of L-SX-EW technology. However, the involvement of ores with complex mineralogical compositions, as well as mixed ores, in hydrometallurgical processing presents a number of technological challenges.

The main issues encountered at operating plants include high concentrations of impurities (iron, silica, manganese, chlorides, etc.) in pregnant leach solutions (PLS), which complicate copper extraction by solvent extraction, as well as the formation of insoluble interfacial emulsions (crud). Optimization of the solvent extraction process is a critical stage for ensuring stable plant operation [3].

This article provides an overview of L-SX-EW technology, ranging from global trends to the specific operational features of domestic deposits. The paper examines the current state of the technology in international practice, technological flowsheets and key stages of heap leaching, as well as the factors affecting process efficiency. Particular attention is given to the industrial implementation of L-SX-EW in the processing of copper ores in Kazakhstan and to the historical role of VNIItsvetmet in the development of hydrometallurgical technologies in the region.

2. Research methodology

Over the past decade, SX-EW technology has demonstrated steady growth. According to analytical reports, total global copper mine production increased from 18.4 million tonnes in 2014 to approximately 22.4 million tonnes in 2023. Copper production by the L-SX-EW method also rose by about 17% over the same period. From 2026 onward, further growth of hydrometallurgical production is forecast at an average annual rate of about 2%, driven by the development of green technologies [4]:

– Renewable energy sources (RES): the construction of wind turbines and solar panels requires copper consumption volumes that are 3-4 times higher than those of conventional power plants;

– Transport sector: the production of electric vehicles requires 2-4 times more copper than the manufacture of conventional internal combustion engine vehicles;

– Urbanization: large-scale global investments in infrastructure development provide additional stimulus to the copper market;

– Copper produced by electrowinning (EW) consistently meets international LME Grade A standards (99.99% purity), enabling producers to market the product directly to end users without intermediate processing stages.

In several regions (for example, in Africa, including the Democratic Republic of the Congo), hydrometallurgical operations have demonstrated significant production growth, particularly against the backdrop of new project commissioning and capacity expansions [1, 5].

The key advantages of SX-EW technology include relatively low capital and operating costs, simplicity of process flowsheets and equipment design, and the possibility of reprocessing waste dumps previously considered uneconomic. However, the technology also has significant drawbacks: it is characterized by long metal recovery cycles that may extend over months or even years, as well as strong dependence on climatic conditions and the permeability of the ore heap [6, 7].

Global copper production is concentrated in several key regions [8]:

1). Chile – the undisputed world leader in both reserves and copper production. In 2023, the country's output amounted to approximately 5 million tonnes.

2). Peru – ranks second globally, with production of 2.6 million tonnes.

3). China – produces about 1.7 million tonnes of copper. It should be noted that China is not only a major producer but also the world's largest consumer.

4). United States – the U.S. mining sector produces approximately 1.1 million tonnes of copper annually. A significant share originates from operations in Arizona, where SX-EW technology has historically been widely applied for the processing of oxidized ores.

5). Russian Federation – consistently ranks among the top five global refined copper producers. Russian enterprises account for approximately 4.8% of total world output, highlighting the region's importance in maintaining global supply balance.

6). Democratic Republic of the Congo (DRC) – the fastest-growing region. The DRC reached second place globally in copper mine production (3.3 million tonnes in 2024). The principal contribution comes from the large-scale Kamoa-Kakula and Tenke Fungurume projects.

3. Results and discussion

3.1. Process flowsheets and key stages of heap leaching

Solvent extraction (SX) in copper hydrometallurgy is the process of recovering metal ions from pregnant leach solutions (PLS) generated during leaching and concentrating them into an electrolyte suitable for subsequent electrowinning (EW). The essence of the method lies in a reversible chemical reaction between the aqueous phase and an organic reagent (extractant) dissolved in a diluent. The process proceeds in two main stages:

Extraction. Contact between the pregnant leach solution (PLS) and the organic phase, during which copper ions transfer into the organic phase, replacing hydrogen ions of the extractant.

Stripping (re-extraction). Contact of the loaded organic phase with a strong sulfuric acid solution, resulting in the transfer of copper back into the aqueous phase, thereby producing a purified and concentrated electrolyte suitable for cathode production.

The overall L–SX–EW process chain, including leaching, solvent extraction, stripping, and electrowinning, is shown in Figure 1. The extraction–stripping reaction can be expressed as follows:

$$CuSO_4(aqueous) + 2RH(org.) \rightleftharpoons CuR_2(org.) + H_2SO_4 \qquad (1)$$

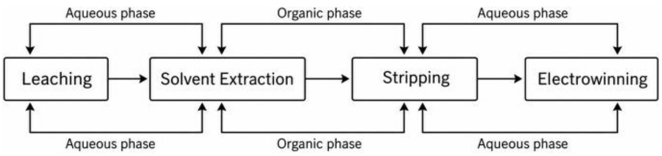

Figure 1. Process flowsheet of the L–SX–EW process chain

The selection of the process and equipment configuration for solvent extraction is determined by the copper concentration in the initial pregnant leach solution (PLS) and the required degree of recovery. During the life of a deposit and throughout the heap leaching process, the composition of the pregnant solution inevitably changes. At the initial stages, the solution typically contains higher concentrations of readily leachable components. As the reserves are depleted, however, the chemical composition of the minerals within the heap changes. As a result, the concentration of recoverable components in solution gradually decreases, and undesirable or secondary components may begin to appear. Changes in the composition of the pregnant solution represent one of the key factors influencing the dynamics of metal recovery from ores and the overall efficiency of the heap leaching process. Considering the combined impact of these factors, modification of the process flowsheet may become necessary [9, 10].

In modern practice, several basic solvent extraction configurations are used, each offering specific operational advantages. Series extraction configuration (2E – 1S) (Figure 2).

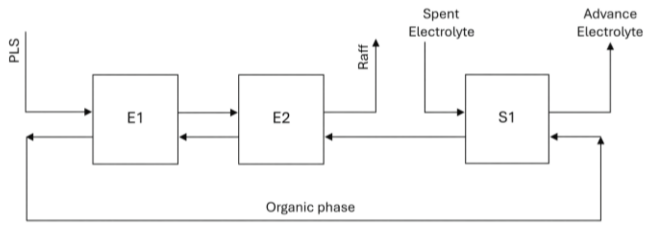

Figure 2. Sequential extraction circuit

Pregnant leach solution (PLS) sequentially passes through several extraction stages (E1 and E2), contacting the organic phase, generally in a counter-current arrangement. One of the key features of this configuration is ensuring the maximum possible copper recovery from the Pregnant leach solution (PLS) (approximately 90%) through deeper depletion of the aqueous phase at the second extraction stage. The efficiency of copper transfer can be enhanced by adding extraction and stripping stages to the circuit, increasing the extractant concentration, or modifying the relative flow rates of the organic and aqueous phases (O/A ratio). Depending on PLS characteristics (pH, copper concentration, impurities), up to three extraction stages and two stripping stages may be applied.

To increase copper production capacity, the standard sequential extraction circuit may be replaced with a parallel or combined configuration (Figures 3 and 4).

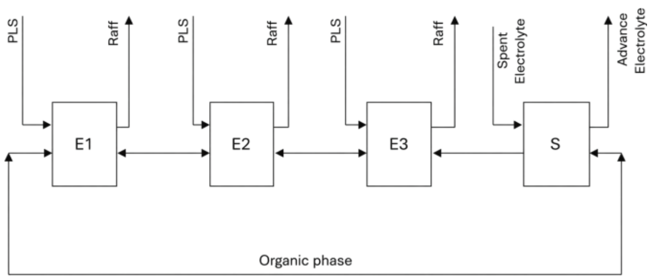

Figure 3. Parallel extraction circuit

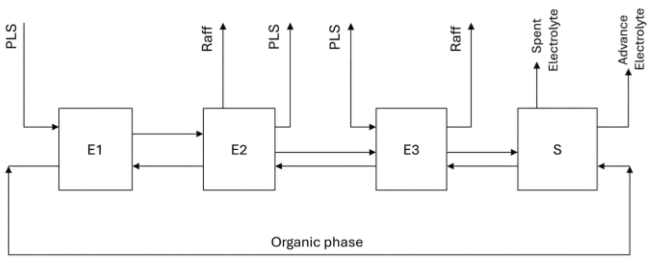

Figure 4. Sequential-parallel extraction circuit

In this example, the Pregnant leach solution (PLS) is fed in parallel to the mixers of both extraction stages, while the organic phase flow remains the same as in the sequential scheme. This arrangement allows the same circuit to process twice the PLS flow rate, provided that the extractant concentration can be increased to transfer the additional copper. As a result, the overall rate of copper transfer from the PLS to the electrowinning circuit can be increased. Implementing parallel flow in the circuit is a cost-effective way to enhance the productivity of an existing sequential-type plant. Plants are often converted from sequential to parallel or sequential-parallel configurations toward the end of the mine life [11].

Washing of the organic phase with water is an auxiliary operation in the solvent extraction process, positioned between the extraction and stripping stages. The primary purpose of this stage is to remove entrained aqueous phase and associated impurities that are carried by the organic phase from the pregnant leach solution (PLS) obtained by heap leaching.Under copper SX–EW conditions, the organic phase after extraction typically contains mechanically entrained PLS, including iron and manganese ions, chlorides, and other undesirable components that may adversely affect subsequent process stages and the quality of the electrolyte for electrowinning.

The organic phase washing is carried out by contacting it with a weak aqueous solution in a separate mixer-settler unit or a dedicated wash cell. As a result of this contact, both the mechanically entrained aqueous phase and a portion of impurities loosely held in the organic phase are removed. This significantly reduces the transfer of undesirable components to the stripping stage and subsequently to the EW electrolyte [12].

The selection of a specific extraction circuit is a compromise between the depth of metal recovery and the plant throughput in terms of solution flow rates. For a clear comparison of the advantages and disadvantages of sequential, parallel, and hybrid configurations, a summary table has been prepared (Table 1), reflecting the specifics of their application under various operating conditions.

Table 1. Brief characteristics of extraction circuits

Criterion	Sequential extraction circuit	Parallel extraction circuit	Sequential-parallel extraction circuit
Operating principle	Aqueous and organic phases move in full counter-current flow through all stages.	The PLS stream is split and fed simultaneously to different extraction stages.	Combination scheme: part of the PLS passes through one stage, while another part passes through two extraction stages.
Recovery	Maximum, as it enables ~90% copper recovery from the pregnant leach solution (PLS) due to deep depletion at the second stage.	Lower. The solution contacts the organic phase only once, resulting in higher copper content in the raffinate.	Adjustable. Provides a balance between recovery depth and processing volume.
PLS flow rate capacity	Limited. The entire solution volume must pass through each stage.	Maximum. Allow processing of up to twice the PLS volume.	High. Optimal for plants increasing throughput while copper grades decline.
Copper concentration in PLS	Suitable for medium concentrations (2–5 g/L Cu in pregnant leach solutions).	Effective for very low-grade solutions when maintaining high flow rates is required.	Optimal when copper concentration in ore decreases over time.
Examples of application	Zaldívar Mine (Chilie)	Used as a temporary measure for capacity expansion.	Morenci Mine (USA); Aktogay (Kazakhstan); Kansanshi Mine (Zambia)

3.2. Factors affecting process efficiency

The efficiency of the hydrometallurgical «leaching – solvent extraction – electrowinning» (L–SX–EW) technology is determined by a combination of physicochemical and process parameters. Primary importance is attributed to the mineralogical composition of the feed ore, which dictates the leaching regime selection and predetermines the kinetics of valuable metal transfer into the pregnant leach solution (PLS). However, as noted by researchers, an equally critical factor is the accumulation of impurity elements in circulating solutions, such as iron, manganese, chloride, and silica [13].

The presence of these components not only reduces extraction selectivity but also accelerates degradation of the organic phase, leading to increased operating costs and reduced cathode metal purity. The mineral composition of the primary raw material establishes the foundation for the entire process chain. Minerals determine which copper-bearing phases are available for leaching, how readily they dissolve, which by-products will enter the PLS, and the overall chemical environment of the solution. Different minerals exhibit varying solubility in sulfuric acid. For example, copper carbonates such as Malachite and Azurite dissolve readily, whereas minerals such as Chrysocolla, Cuprite, and Tenorite require higher sulfuric acid concentrations. Secondary sulfides may be leached in the presence of strong oxidants such as ferric sulfate (Fe^{3+}), while Chalcopyrite is the most refractory among common copper minerals [14, 15]. Gangue minerals also exert a significant influence. For instance, high contents of Calcite and Dolomite (typical of mixed ores in the Republic of Kazakhstan) lead to excessive sulfuric acid consumption.

The pregnant leach solution (PLS) derived from heap or tank leaching and fed to the solvent extraction stage represents a multicomponent system. In addition to copper ions (Cu^{2+}), the solution almost invariably contains impurities capable of significantly affecting extraction selectivity, organic phase stability, and electrolyte quality in the electrowinning (EW) stage. The most common impurities in PLS include iron (Fe^{2+}/Fe^{3+}), manganese (Mn^{2+}), aluminum (Al^{3+}), calcium (Ca^{2+}), magnesium (Mg^{2+}), chlorides, silicic acid, and colloidal particles. Their presence may result in both direct losses in SX efficiency and indirect operational issues related to organic degradation and electrolyte contamination [16].

The presence of ferric iron (Fe^{3+}) reduces current efficiency during electrowinning, as it is continuously reduced at the cathode and oxidized at the anode. Although modern oxime extractants exhibit high selectivity toward copper, Fe^{3+} may be partially co-extracted or interact with the organic phase, impairing phase separation and increasing the tendency for interfacial crud formation [17].

Manganese is typically present in solution as Mn^{2+} and is scarcely extracted into the organic phase. However, during electrowinning (EW), it may be oxidized to Mn^{3+} or Mn^{4+} species, which are strong oxidants. These compounds can accelerate degradation of both the extractant and the diluent, shortening organic phase life and increasing reagent losses.

The presence of chloride ions in PLS, and especially in the EW electrolyte, is considered a critical factor limiting process stability. Chlorides accelerate equipment corrosion, promote the formation of undesirable gaseous by-products during electrolysis, and impair cathode copper quality.

Colloidal particles of silicic acid, clay minerals, and metal hydrolysis products play a particular role in impairing SX circuit performance. They are capable of stabilizing emulsions. The accumulation of such impurities leads to increased phase separation time, higher organic phase losses, and overall plant instability [18].

3.3. Industrial implementation of L–SX–EW processes in the processing of copper ores in kazakhstan

The transition to industrial implementation of L–SX–EW technology marked a turning point for the copper industry of Kazakhstan, enabling the development of off-balance and refractory oxidized ore reserves. To date, the successful operation of hydrometallurgical complexes at the country's largest deposits confirms not only the technical reliability of the flowsheet but also its strategic importance in maintaining national competitiveness in the global cathode copper market.

3.3.1. Aktogay

The Aktogay deposit is the largest hydrometallurgical processing site for oxidized copper ores in the Republic of Kazakhstan and one of the most large-scale examples of industrial heap leaching implementation. Aktogay is a major porphyry copper deposit, where SX–EW technology was first introduced to process the oxidized «cap» overlying the primary sulfide ore body.

The first cathode copper from oxidized ore was produced in December 2015. The design capacity of the SX–EW facility is approximately 25,000 tonnes of copper per year from the oxide zone. This SX–EW complex became an essential component of the overall production strategy, as it enabled the integration of hydrometallurgy for processing low-grade oxidized ores that are inefficiently treated by conventional concentration methods [19].

At Aktogay, a multi-line extraction system is employed. Given the enormous volumes of circulating pregnant leach solution (PLS), the plant operates under a flexible configuration combining sequential and parallel extraction circuits (Figure 4). This approach ensures high productivity even under seasonal fluctuations in copper concentration in the PLS [20].

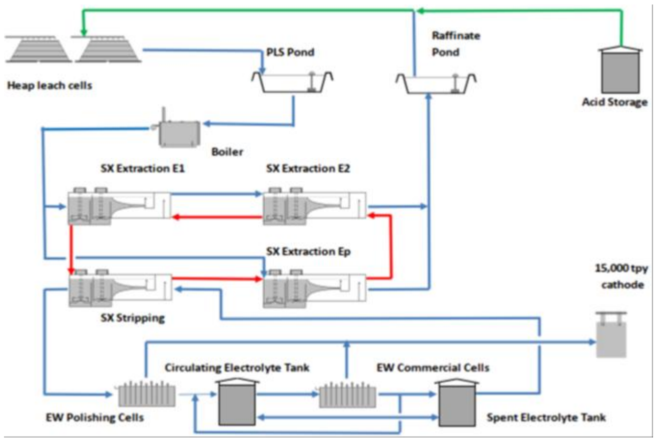

Figure 4. SX–EW Flowsheet of the Aktogay Mining and Processing Plant

By 2026, the depletion of oxidized ore reserves posed a significant threat to the continued operation of the oxide plant at Aktogay, implying a potential full shutdown of the production cycle – from heap leaching on active pads to cathode copper production. In order to extend the operational life of the facility, management initiated the search for innovative approaches to processing alternative feed materials, including off-balance ores and technogenic waste.

Conventional intensification methods, such as the use of percolation columns or agitated tank leaching, were rejected due to the enormous volumes of already stacked material. Underground leaching technology was also considered impractical given the open-pit mining configuration of the deposit.

The most promising development pathway identified was bioleaching, based on the activity of specialized microorganisms. This technology enables efficient recovery of valuable components from low-grade and mixed ores directly within existing heaps, minimizing capital expenditures for plant retrofitting. The implementation of bacterial leaching is regarded as a strategic solution capable not only of revitalizing the oxide plant's production capacity but also of significantly improving the overall resource efficiency of the Aktogay deposit in the long term [21].

3.3.2. Kounrad

The Kounrad project is unique not only for Kazakhstan but also in global practice. It represents one of the few successful and highly profitable examples of reprocessing historic technogenic dumps accumulated over decades (since the 1930s) of operation at the Kounrad copper mine. Historically, the Kounrad copper deposit was developed in the early 20th century, resulting in the formation of substantial waste rock dumps with relatively low copper grades (0.3% Cu).

The project was launched during 2010-2012, with the first cathode copper produced in April 2012. The initial SX–EW plant capacity was about 10 thousand tonnes of cathode copper per year. In subsequent years, production capacity was expanded: by 2015, additional extraction and electrowinning circuits were commissioned, increasing annual output to approximately 14 thousand tonnes of copper. The final product is M00K-grade cathode copper with a purity of at least 99.99% Cu, supplied both to the domestic market and for export [22].

The Kounrad project has earned a strong reputation for economic efficiency, as dump reprocessing requires relatively low capital and operating costs compared to conventional mining and concentrator complexes. As of the mid-2020s, cumulative cathode copper production since commissioning amounts to hundreds of thousands of tonnes, and the project is expected to remain in operation at least until 2034, processing significant volumes of copper-bearing material remaining from historical mining.

The dump material consists of oxidized copper ore with the following composition (%): 1.46 Fe; 0.17 S; 76.32 SiO_2; 11.86 Al_2O_3; 0.17 CaO; 0.13 MgO; 0.002 Zn; 0.001 Pb. Copper minerals are represented by approximately 76% oxide compounds, 13% secondary sulfides, 10.6% primary sulfides, and 0.4% sulfates. The maximum lump size in the dumps ranges from 0.6 to 1 m.

By 2025, the Kounrad dumps remain an economically viable source of copper. The company estimates remaining resources sufficient to sustain production at least until 2034. Copper recovery from the Eastern Dumps is estimated at approximately 45-50%, while recovery from the Western Dumps ranges from about 35-42% of the theoretical metal content [23, 24]. The Kounrad project became the first full-scale industrial SX–EW operation in Kazakhstan based on hydrometallurgical copper recovery from dump bodies, demonstrating the technological and economic viability of the flowsheet for low-grade copper resources.

3.3.3. Almaly

The Almaly deposit represents one of the most interesting and technically challenging cases for hydrometallurgy in Kazakhstan. Unlike Aktogay, where processes are already scaled up and well established, Almaly is frequently referenced in scientific studies as a site characterized by «complex» ores requiring non-standard approaches to solution purification.

The Almaly copper deposit is located in the Shetsky District of the Karaganda Region, approximately 150 km from the regional center. The resource potential is significant, amounting to about 30 million m^3 of ore. Since the end of 2018, a hydrometallurgical complex operated by Sary-Arka Copper Processing has been in operation at the site. The enterprise specializes in cathode copper production via heap leaching, producing up to 10 thousand tonnes of high-grade copper annually, primarily for export markets [25].

The technological scheme at Almaly is as follows: after heap leaching, copper is transferred into the pregnant leach solution (PLS), from which it is subsequently recovered by solvent extraction (SX) using organic extractants. The selection of the optimal extractant composition and operating conditions is a key task for this project.

Research has shown that from Almaly PLS (with Cu concentrations of approximately 0.26-2.35 g/dm^3), the most effective extractant for selective copper recovery under laboratory conditions was Acorga 5640 at a concentration of about 5%, providing copper recovery of up to ~94%. Other extractants, such as LIX 984N and Acorga 5910 / Acorga 5747, also demonstrated high selectivity; however, under the given conditions, Acorga 5640 proved to be optimal. This finding is important for designing efficient industrial SX–EW flowsheets tailored to the specific composition of Almaly PLS [26].

Recent publications indicate that, based on the current ore base, approximately 4.43 million tonnes of ore per year are planned to be processed to produce around 9 thousand tonnes of cathode copper annually, with potential for further capacity increases as infrastructure and technology develop [27].

At this deposit, a range of technological challenges has been identified, primarily associated with impurity components such as iron (Fe) and silica (SiO_2). These impurities may impair phase separation, promote crud formation, and negatively affect the quality of produced copper. Addressing these issues requires integrated technological solutions and strict control of SX–EW operating parameters [28].

3.3.4. Ayak-Kodjan

The Ayak-Kodjan deposit is located in the Ekibastuz District of the Pavlodar Region of the Republic of Kazakhstan, forming part of the regional copper belt. The project was developed by Eurasia Copper Operating with the objective of exploiting oxidized and low-beneficiation-grade ore bodies. These ores are traditionally difficult to process by flotation but are well suited for hydrometallurgical copper recovery [29].

At Ayak-Kodjan, a full production cycle of Grade A cathode copper was implemented based on the L–SX–EW flowsheet, with a production capacity of approximately 2.5 thousand tonnes of cathode copper per year (as of June 2014). However, according to the latest available information, production at the site is currently suspended.

3.3.5. Borly

The Borly deposit is located in the Aktogay District of the Karaganda Region of the Republic of Kazakhstan, approximately 30 km from the city of Balkhash and near the Balkhash–Kounrad railway line. It belongs to the copper–molybdenum (Cu–Mo) ore type, with the presence of both copper sulfide and oxide minerals. Historically, Borly has been recognized in geological exploration sources as a perspective copper (and molybdenum) deposit with moderate metal grades [30].

In the 2020s, a hydrometallurgical plant for the production of cathode copper using the SX–EW process was constructed and officially commissioned at the Borly deposit with the participation of Irkaz Metal Corporation. According to an official press release of the Government of the Republic of Kazakhstan, the enterprise in the Karaganda Region has a design capacity of 5 thousand tonnes of cathode copper per year and is expected to create approximately 140 jobs.

Production is carried out using a modern hydrometallurgical SX–EW cycle – from acid leaching to electrolytic deposition of high-purity M00k-grade cathode copper [31].

The annual ore consumption amounts to approximately 2.5 million cubic meters, equivalent to about 4.575 million tonnes. This volume ensures the stability and continuity of the production process, enabling the plant to achieve its planned output targets. The enterprise operates around the clock in two 12-hour shifts, using a rotational work schedule with 15-day shifts [32].

3.3.6. Berkarinskoye

The Berkarinskoye deposit is located in the East Kazakhstan Region of the Republic of Kazakhstan, approximately 350 km east of the city of Karaganda and in proximity to Semey. It represents an industrially significant copper ore project where an integrated mining and processing scheme based on the L–SX–EW flowsheet is being implemented.

The project has been developed by Arx Minerals through its subsidiary Nouvelle Mining. The mineral reserves have been registered on the state balance of Kazakhstan in accordance with the JORC Code classification (2012 edition).

The estimated annual production parameters include mining of approximately 600 thousand tonnes of ore and production of about 5 thousand tonnes of cathode copper per year. The projected mine life is 8-9 years, with potential extension subject to reserve expansion.

The nearest settlements are the villages of Algabas (approximately 9.5 km north of the site) and Kaynar (approximately 40 km east). The region is characterized by a sharply continental climate, with short hot summers and long severe winters, which significantly influences logistics and the technological organization of production, particularly heap leaching operations and solution management [33].

As of the end of 2024, public hearings were also conducted regarding environmental aspects of operations at the «North Berkara» site, which forms part of the Berkarinskoye deposit. This process is a mandatory stage for obtaining an Environmental Impact Permit (EIP/ERV). The hearings addressed geological boundaries, ore body characteristics, and planned exploration activities, including drilling and chemical-analytical studies [34].

3.4. The role of VNIItsvetmet in the development of hydrometallurgical technologies for processing oxidized and mixed copper ores in Kazakhstan

The establishment of a scientific and methodological framework for applying solvent extraction technologies to the processing of Kazakhstan's mineral resources began at VNIItsvetmet in 1997. Research activities were carried out under long-term programs aimed at introducing environmentally safe hydrometallurgical solutions for oxidized and mixed non-ferrous metal ores.

A significant milestone was international scientific and technical cooperation between the Republic of Kazakhstan and Japan, through which the institute obtained an automated pilot-scale plant. This facility enabled large-scale testing of beneficiation and hydrometallurgical processes under conditions close to industrial operation.

In subsequent years, comprehensive studies were conducted on more than twenty copper deposits across Kazakhstan, including Aktogay, Kounrad, Benkala, Zhezkazganskoye, Borly, Ayak-Kodjan, Ai, Vavilonskoye, Karchiga, Almaly, and Berkarinskoye Deposits. These deposits are characterized by diverse geological, mineralogical, and technological parameters.

The research results formed the basis for the development of design regulations for approximately fifteen industrial facilities. As a result, a practice-oriented model was established for adapting the L–SX–EW technology to raw materials with low to moderate copper grades and varying gangue mineral compositions.

One of the earliest examples of industrial validation was the processing of tailings from the Kounrad mine. Despite the extremely low copper content in the feed material (0.1-0.2%), the favorable mineralogical composition (predominantly quartz) resulted in relatively low sulfuric acid consumption and limited impurity accumulation in pregnant leach solutions. Based on these studies, a technological regulation was developed, leading to the commissioning in 2008 of the country's first solvent extraction facility operating on technogenic raw materials.

Based on research conducted at VNIItsvetmet, recommendations were also developed for implementing the L–SX–EW technology at the Benkala deposit. The proposed flowsheet was subsequently successfully introduced into industrial operation.

A new stage in technological development was associated with the exploitation of oxidized ores at the Aktogay deposit. This site is characterized by significant variability in material composition (volcanogenic formations, porphyry and granodiorite varieties) with an average copper grade of approximately 0.3%. Research findings from 2007-2013 were used in developing industrial process solutions by KAZ Minerals PLC (formerly Kazakhmys PLC) for heap leaching followed by solvent extraction and electrowinning. The commissioning of the plant in 2015 and achievement of a design capacity of about 25 thousand tonnes of cathode copper per year confirmed the technological feasibility and economic efficiency of the selected solutions.

In 2016-2017, VNIItsvetmet conducted research on heap leaching of oxidized copper ores from the Almaly deposit in the Karaganda Region. The studies demonstrated the necessity of a more complex technological configuration due to low copper grades and specific mineralogical characteristics. The developed process procedure included three-stage crushing, increased sulfuric acid consumption (up to 12 kg/t), and an extended leaching period combined with parallel solvent extraction of solutions. Implementation of these solutions at Sary-Arka Copper Processing enabled the launch of cathode copper production with a capacity of up to 10 thousand tonnes per year. The plant was commissioned in 2018.

Further expansion of L–SX–EW application in Kazakhstan is associated with the commissioning in 2022 of a hydrometallurgical facility operated by KAZ Metal Corporation for processing ores from the Borly deposit (Karaganda region). The design capacity of the facility is up to 5 thousand tonnes of cathode copper per year. Between 2017 and 2022, a comprehensive research program was completed for processing oxidized and mixed ores from the Berkarinskoye Deposit (East Kazakhstan), culminating in the development of a technological regulation and subsequent industrial implementation of the project by Arx Minerals in 2023 [35].

4. Conclusions

The conducted review has demonstrated that heap leaching followed by selective solvent extraction and electrowinning of copper (L–SX–EW) represents one of the most efficient and economically justified approaches for processing oxidized and mixed copper ores in the Republic of Kazakhstan. The widespread industrial implementation of this technology is driven by the substantial resources of low-grade copper ores, the specific features of their mineralogical composition, and the possibility of incorporating technogenic formations and previously uneconomic reserves into production.

Analysis of mineralogical factors and pregnant leach solution composition indicates that the efficiency of L–SX–EW processes is largely determined by ore material composition, the nature of copper-bearing minerals, the ratio of gangue phases, and the presence of impurity components. Mineralogical differences between oxidized and mixed ores, as well as variability in iron, aluminum, manganese, silicon, and other element contents, significantly influence leaching kinetics, reagent consumption, organic phase stability, and copper extraction selectivity.

Industrial practice in Kazakhstan at deposits such as Aktogay, Kounrad, Almaly, Borly, and Berkarinskoye Deposit confirms that even with low copper grades in the feed material, acceptable recovery rates and high-purity cathode copper production can be achieved, provided that appropriate technological schemes, crushing parameters, leaching regimes, and extraction conditions are selected. A key factor in successful project implementation is the adaptation of technological solutions to the specific geological and mineralogical conditions of each deposit.

A special role in the development of hydrometallurgical copper processing technologies in Kazakhstan belongs to VNIItsvetmet, which for several decades has carried out comprehensive research and pilot-scale studies in heap leaching and solvent extraction.

Overall, the results of this review indicate that further development of the L–SX–EW technology in Kazakhstan is associated not only with expansion of the resource base through the inclusion of new deposits and technogenic materials, but also with improvement of solution quality control methods, reduction of organic phase losses, enhancement of extraction selectivity, and increased stability of operating regimes.

Author contributions

The author confirms that they are the sole contributor to this work.

Funding

This research received no external funding.

Acknowledgements

The author gratefully acknowledges the editor and reviewers for their helpful comments and suggestions.

Conflicts of interests

The authors declare no conflict of interest.

Data availability statement

The original contributions presented in this study are included in the article. Further inquiries can be directed to the corresponding author.

References

[1] International Copper Study Group. (2024). *World Copper Factbook 2025*. https://icsg.org/copper-factbook/

[2] Chernykh, A.I., Girfanov, M.M., Istomin, V.A., Fedorov, D.T., Pashkov, V.S., & Svatkov, A.S. (2023). Mineral resource base of the CIS countries of the Central Asian region: Status and directions of interaction and development. *Ores and Minerals*, (3), 6-36. https://doi.org/10.47765/0869-5997-2023-10011

[3] Ritcey, G.M. (1980). Crud in solvent extraction processing: A review of causes and treatment. *Hydrometallurgy*, *5*, 97-107. https://doi.org/10.1016/0304-386X(80)90031-6

[4] Dong, D., van Oers, L., Tukker, A., & van der Voet, E. (2020). Assessing the future environmental impacts of copper production in China: Implications of the energy transition. *Journal of Cleaner Production*, *274*, 122825. https://doi.org/10.1016/j.jclepro.2020.122825

[5] PW Consulting Chemical & Energy Research Center. (2025). Global copper solvent extraction reagent market size, share & trends analysis 2026–2032. *Available at:* https://pmarketresearch.com/chemi/copper-solvent-extraction-reagent-market/

[6] Khalezov, B.D. (2013). *Heap leaching of copper and copper-zinc ores (domestic experience)*. Yekaterinburg.

[7] Masloboev, V.A., Makarov, D.V., Svetlov, A.V., Fokina, N.V., Yanishevskaya, E.S., & Goryachev, A.A. (2018). Problems and prospects of hydrometallurgical processing of low-grade sulfide ores and technogenic waste in northern regions. *Proceedings of the Kola Science Centre of the Russian Academy of Sciences*, *9*(1), 58-64. https://doi.org/10.25702/KSC.2307-5252.2018.9.1.58-64

[8] Wood Mackenzie. (2024). *Global copper market outlook: Supply, demand, and price trends* (Metals & Mining Report). *Retrieved from:* https://www.woodmac.com/

[9] Dudley, K.A., Readett, D.J., Crane, P.A., & Mackenzie, J.M.W. (2002). *Copper hydrometallurgy process evolution: Changing operating parameters and philosophies throughout the life of Girilambone Copper Company's solvent extraction circuit.* ISEC 2002, Cape Town, South Africa.

[10] Miller, G. (2011). Methods of managing manganese effects on copper solvent extraction plant operations. *Solvent Extraction and Ion Exchange*, 29(5-6), 837-853. https://doi.org/10.1080/07366299.2011.595647

[11] Readett, D.J., Hanlon, M., Dudley, K.A., Crane, P.A., & Mackenzie, J.M.W. (2002). *Evolution of a copper solvent extraction circuit: Management of operating parameters under varying leach solution conditions*. International Solvent Extraction Conference (ISEC 2002), Cape Town, South Africa.

[12] Schlesinger, M.E., King, M.J., Sole, K.C., & Davenport, W.G. (2011). *Extractive metallurgy of copper* (5th ed.). Elsevier.

[13] Kordosky, G.A. (2002). Copper recovery using leach/solvent extraction/electrowinning technology: Forty years of innovation. *Journal of the Southern African Institute of Mining and Metallurgy*, *102*(8), 445-450.

[14] Solís Marcial, O.J., Nájera-Bastida, A., Soriano-Vargas, O., Ruelas Leyva, J.P., Talavera-López, A., Inchaurregui, H., & Zárate Gutiérrez, R. (2025). Recovery of copper from pregnant leach solutions of copper concentrate using aluminum shavings. *Minerals*, *15*(10), 1048. https://doi.org/10.3390/min15101048

[15] Naboychenko, S.S., & Smirnov, V.I. (1974). *Hydrometallurgy of copper.* Metallurgiya Publishing House.

[16] Wang, C.Y. (2005). *Crud formation and its control in solvent extraction*. International Solvent Extraction Conference 2005, Beijing, China.

[17] Ritcey, G.M. (2006). Equipment in solvent extraction processing. *Solvent extraction: Principles and applications to process metallurgy*, *2*, 253-419.

[18] Crane, F. (2004). Extraction in copper hydrometallurgy: Development and current status. *Complex Use of Mineral Resources*, (2), 36-55.

[19] Kazakhstan Today. (2015). KAZ Minerals produced first cathode copper at the Aktogay deposit. *Available at:* https://www.kt.kz/rus/ekonomika/kaz_minerals_proizvela_pervuju_katodnuju_medj_na_mestorozhdenii_aktogaj_1153613338.html

[20] KAZ Minerals. (2024). *Aktogay SX/EW flowsheet*.Technical drawing. https://www.kazminerals.com/media/17040/aktogay-sxew-flowsheet.pdf

[21] Kozhek, M., Mamezhanov, B., & Amarzayaa, U. (2025). Study of copper recovery from oxidized and low-grade ores of the Aktogay Mining and Processing Plant using heap and bacterial leaching and implementation of the "Heap Bioleaching at AGOK" project. *World Science*, *99*(6). https://doi.org/10.5281/zenodo.16792897

[22] Kursiv. (2024). Kazakhmys temporarily suspends one of its oldest copper mines. *Available at:* https://kz.kursiv.media/2024-07-04/zhnb-kazakhmyskounradconserv/

[23] Central Asia Metals PLC. (2025). *Annual report and accounts 2024*. https://www.centralasiametals.com/operations/kounrad/

[24] Discovery Alert. (2026). *Copper mining operations: Market dynamics 2026*. https://discoveryalert.com.au/copper-mining-operations-market-dynamics-2026/

[25] Chepushtanova, T.A., Yesirkegenov, M.I., Mamyrbayeva, K.K., Merkibayev, E.S., & Nikoloski, A. (2023). Testing of the opti-

mum extractant for solvent extraction of Almaly deposit copper. *Complex Use of Mineral Resources*, *324*(1), 43-49. https://doi.org/10.31643/2023/6445.06
[26] Mamyshev, Z. (2024). *Copper company reconstructs a mine in the Karaganda Region.* Kursiv. https://kz.kursiv.media/2024-07-16/zhnb-coppercompanyreconst/
[27] Mamyshev, Z. (2024). *Copper company reconstructs a mine in the Karaganda Region.* Kursiv. https://kz.kursiv.media/2024-07-16/zhnb-coppercompanyreconst/
[28] Chepushtanova, T.A., Yesirkegenov, M.I., Mamyrbayeva, K.K., & Merkibayev, E.S. (2023). Investigations of copper extraction and crud formation components of productive solution of the Almaly deposit. *Non-Ferrous Metals*, *54*(1), 11-19. https://doi.org/10.17580/nfm.2023.01.02
[29] Mining and Metallurgical Industry. (2014). Copper using SX–EW technology. *MMP*, (8), 11.
[30] National Geological Service. (n.d.). Teasers for 42 deposits of Kazakhstan. Investment overview. *Available at:* www.geology.kz
[31] Ministry of Industry and Construction of the Republic of Kazakhstan. (2022). Launch of a cathode copper production plant in the Karaganda Region. *Available at:* www.gov.kz
[32] Paletsky, V.A. (2025). Design of an aspiration system to reduce emissions at a hydrometallurgical complex of a mining deposit Bachelor's thesis, Satbayev University.
[33] Arx Minerals. (n.d.). Projects: Berkara Deposit. *Available at:* https://www.arxminerals.kz/
[34] Department of Natural Resources and Environmental Management of the Abai Region. (2024, December 4). Announcement of public hearings (North Berkara). *Available at:* www.gov.kz
[35] Sizikova, N.V., & Kushakova, L.B. (2023). Participation of VNIItsvetmet in the development of hydrometallurgical technology for processing oxidized and mixed copper ores of Kazakhstan deposits. *Innovations and integrated processing of mineral raw materials as key components of economic diversification: Proceedings of the international scientific and practical conference*, *1*, 42-44.

Қазақстан кен орындарының мыс кендерін өңдеу кезінде L-SX-EW қолдану тәжірибесі

Н. Якушев*
«ҚР МШКҚӨ ҰО» РМК «ВНИИцветмет» филиалы, Өскемен, Қазақстан
**Корреспонденция үшін автор:* nikita.yakushev2112@mail.ru

Аңдатпа. Мақалада әлемдік және отандық мыс өнеркәсібі контекстіндегі үймеде шаймалау, сұйық экстракция және электролиз (L-SX-EW) технологиясының қазіргі жағдайына аналитикалық шолу берілген. Шығыс және Орталық Қазақстанның ірі кен орындарын қоса алғанда, Қазақстан Республикасының минералдық-шикізат базасы талданған. Экстракция сызбаларына, минералогиялық құрамның әсеріне, сондай-ақ тотыққан және аралас мыс кендерін өңдеудегі технологиялық қиындықтарға назар аударылды. «ВНИИцветмет» институтының өңірдің гидрометаллургиясын қалыптастырудағы тарихи рөлі баяндалды. Жұмыс Қазақстанның мыс саласының бәсекеге қабілеттілігін қолдау үшін оның маңыздылығын растай отырып, L-SX-EW процесінің ағымдағы технологиялық сызбалары мен тиімділік факторлары туралы деректерді жүйелейді.
Негізгі сөздер: *мыс, үймеде шаймалау, сұйық экстракция), электролиз, Қазақстанның минералдық-шикізат базасы, тотыққан мыс кендері*.

Практика применения L-SX-EW при переработке медных руд месторождений Казахстана

Н. Якушев*
Филиал РГП «НЦ КПМС РК» «ВНИИцветмет», Усть-Каменогорск, Казахстан
**Автор для корреспонденции:* nikita.yakushev2112@mail.ru

Аннотация. В статье представлен аналитический обзор современного состояния технологии кучного выщелачивания, жидкостной экстракции и электролиза (L-SX-EW) в контексте мировой и отечественной медной промышленности. Проанализирована минерально-сырьевая база Республики Казахстан, включая крупные месторождения Восточного и Центрального Казахстана. Уделено внимание схемам экстракции, влиянию минералогического состава, а также технологическим вызовам при переработке окисленных и смешанных медных руд. Освещена историческая роль института «ВНИИцветмет» в становлении гидрометаллургии региона. Работа систематизирует данные о текущих технологических схемах и факторах эффективности процесса L-SX-EW, подтверждая его значимость для поддержания конкурентоспособности медной отрасли Казахстана.
Ключевые слова: *медь, кучное выщелачивание, жидкостная экстракция, электролиз, минерально-сырьевая база Казахстана, окисленные медные руды*.

Publisher's note

Engineering Journal of Satbayev University
Volume 148 (2026), Issue 3, 24-32

https://doi.org/10.51301/ejsu.2026.i3.04

Geospatial Model for Land Degradation Assessment in the Caspian region based on Integrated Multifactor Indicators

M.E. Amirkhanov[1], Y. Zhakypbek[1*], Sun Hao[2]
[1]Satbayev University, Almaty, Kazakhstan
[2]China University of Mining and Technology, Beijing, China
*Corresponding author: y.zhakypbek@satbayev.university

Abstract. Land degradation and desertification are major environmental challenges in the arid Caspian region (Pri-Caspian) of Kazakhstan. This study assesses desertification susceptibility in the Mangystau region using an integrated GIS and remote sensing approach. Four controlling factors were analyzed: distance to active tectonic faults, terrain slope, vegetation cover derived from the Normalized Difference Vegetation Index (NDVI), and soil moisture conditions represented by the Water Requirement Index (WRI). Euclidean distance analysis was used to evaluate tectonic influence, slope gradients were derived from SRTM data, and NDVI and WRI were calculated from Landsat 8 OLI imagery. All factors were reclassified into standardized ordinal classes and integrated using a weighted sum multi-criteria evaluation model to generate a composite desertification susceptibility map. The results indicate strong spatial heterogeneity in degradation conditions. Areas near tectonic faults with steeper slopes, low NDVI, and low WRI values show the highest susceptibility to desertification, while regions with gentle slopes, higher vegetation cover, and better soil moisture exhibit greater environmental stability. The study demonstrates that land degradation in Mangystau is controlled by the combined effects of geological, geomorphological, and ecological factors. The proposed integrated framework provides a reliable tool for desertification assessment and supports sustainable land management in arid and semi-arid environments.

Keywords: *land degradation, desertification, tectonic faults, terrain slope, NDVI, WRI, reclassification*.

Received: 19 January 2026
Received in revised form: 10 June 2026
Accepted: 15 June 2026
Available online: 30 June 2026

1. Introduction

The Caspian region, which includes Atyrau and Mangystau of Kazakhstan has been experiencing increasing desertification over the past decades; this phenomenon threatens both the environment and local livelihoods. Land degradation is considered one of the main drivers of desertification, as it reduces fertility and vegetation cover.

Remote sensing data, such as Landsat images, have been widely used to monitor changes in vegetation and soil moisture; they provide valuable information for large and inaccessible areas. In addition, the digital elevation models (SRTM) allow researchers to analyze slopes, which affects erosion and water retention; these factors contribute to land degradation.

The Euclidean distance tool was used to determine the distance to active tectonic fault lines, which can influence soil moisture and land degradation. Vegetation indices, such as NDVI, have been applied to detect the loss of plant cover, whereas the Water Ratio Index (WRI) is used to assess soil moisture. Previous studies have shown that areas with steep slopes or low vegetation density are more vulnerable to degradation, which highlights the need for integrated assessments.

In this study, remote sensing indices, slope analysis, and distance metrics are combined to evaluate land degradation, providing a comprehensive view of desertification patterns. Active tectonic faults, which influence groundwater distribution, are also considered as contributing factors to the spatial variability of soil moisture and vegetation, although this aspect is often overlooked in conventional studies.

The study is devoted to the important issue of land degradation and desertification in the Caspian region. The study is highly relevant because the increasing impacts of climate change and human activities have accelerated environmental degradation, threatening ecosystems and local livelihoods. One of the main problems is the lack of an integrated approach to accurately assess land degradation using multiple environmental factors and geospatial technologies.

The results of this research are expected to support sustainable land management strategies and help mitigate desertification risks in the Pri-Caspian region of Kazakhstan.

2. Materials and methods

2.1. Study area

The study area is in the Caspian region of Western Kazakhstan and mainly covers the territory of the Mangystau region (approximately 43.40°–45.70° N, 50.00°–55.00° E) with partial inclusion of adjacent areas of the Atyrau region

m.amirkhanov@satbayev.university; y.zhakypbek@satbayev.university; sunhao@cumtb.edu.cn
Engineering Journal of Satbayev University. eISSN 2959-2348. Published by Satbayev University

(approximately 46.00°–48.00° N, 50.00°–53.00° E) [1]. Mangystau region is situated in the southwestern part of Kazakhstan along the eastern coast of the Caspian Sea (Pri-Caspian area) and represents one of the most arid and environmentally sensitive regions of the country [2].

Geographically, Mangystau region is characterized by a complex relief that includes coastal lowlands, plateaus, depressions, and isolated mountain massifs [3]. A significant part of the territory lies below sea level, including the Karagiye Depression (approximately 44.02° N, 51.33° E), one of the deepest continental depressions in Central Asia [4]. The Mangystau Plateau and the Ustyurt Plateau dominate the eastern and northeastern parts of the region, forming elevated flat and dissected surfaces with steep escarpments [5]. The climate is sharply continental and extremely arid, with very low annual precipitation, high summer temperatures, strong winds, and intense evaporation. These climatic conditions contribute to soil salinization, sparse vegetation cover, and high susceptibility to desertification [6].

Geologically, the Mangystau region is influenced by complex tectonic structures related to the Caspian basin [7]. Numerous faults in Figure 1 and lineaments control groundwater movement and may affect spatial variations in soil moisture and vegetation distribution. These tectonic features, together with the fragile surface conditions, increase the sensitivity of landscapes to degradation processes [8].

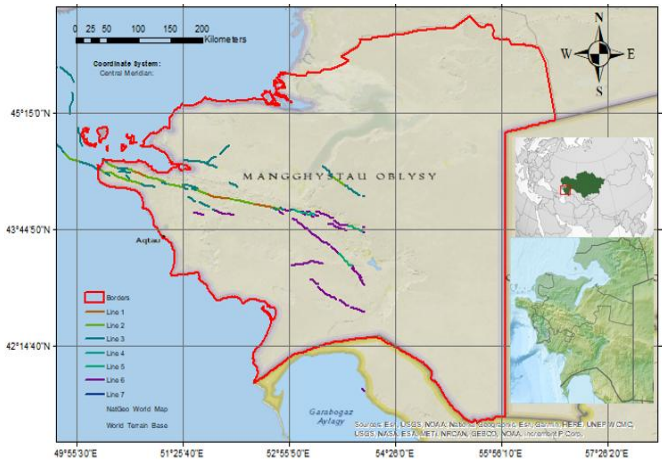

Figure 1. Active tectonic fault lines of Mangystau Pri-Caspian region

Due to the combined influence of arid climate, complex relief, tectonic activity, and fragile ecosystems, the Mangystau and adjacent parts of Atyrau regions represent a highly suitable area for investigating land degradation, desertification, and associated geomorphological processes using integrated GIS and remote sensing approaches.

2.2. Methodological framework

The methodological framework in Figure 2 of this study is based on an integrated GIS and remote sensing approach for assessing land degradation, desertification, and landslide susceptibility in the Caspian region. The workflow consists of several sequential stages, including data acquisition, factor extraction, reclassification, spatial integration, and final susceptibility mapping. The interaction between tectonic faults, slope, vegetation cover (NDVI), and soil moisture (WRI) forms an integrated system controlling soil degradation and desertification processes.

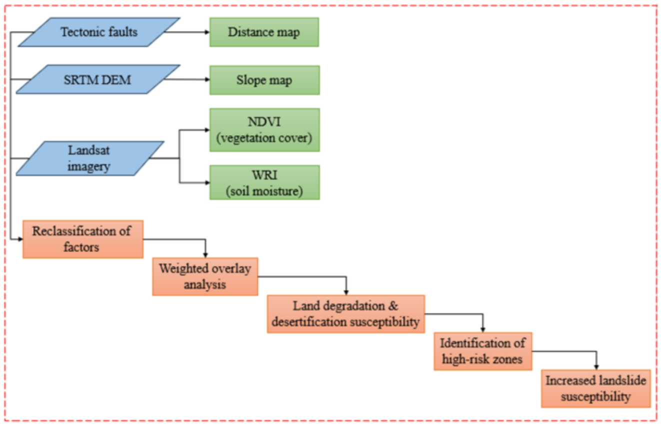

Figure 2. Workflow of the GIS-based methodological framework for assessing land degradation and desertification in the Mangystau region

Tectonic structures affect groundwater distribution, slope determines erosion intensity, vegetation protects soil from degradation, and soil moisture reflects surface stability. The combined influence of these factors increases the susceptibility of landscapes to degradation and landslide processes.

2.3. Assessment of tectonic fault control on land degradation processes

Previous studies have demonstrated that tectonic structures and associated geological processes influence vegetation distribution and soil conditions. For instance, Li et al. (2023) found that vegetation index values (NDVI) vary in relation to fault length density and elevation, suggesting that fault zones affect hydrothermal and ecological conditions – with lower NDVI in areas close to faults at certain elevations and contrasting patterns at higher altitudes [9]. Additionally, tectonic activity coupled with lithological controls has been shown to shape spatial patterns of soil and vegetation parameters in fault-controlled landscapes [10]. Tectonic and internal geomorphological dynamics also significantly contribute to erosion and sediment production rates, linking structural geology to soil degradation processes [11]. Moreover, fault zones tend to exhibit increased fracture density and reduced rock strength, which can enhance susceptibility to mass movement and surface instability under external triggers such as rainfall [12].

Figure 3 illustrates the relief of the Mangystau region in relation to the distribution of active tectonic faults and recorded seismic events. The terrain is predominantly represented by gently undulating plains and dissected plateaus, with local elevated areas corresponding to structural uplifts and residual mountain ridges.

Tectonic faults are shown as linear features of different colors, indicating their relative activity and confidence levels. The major fault zones form elongated, predominantly northwest–southeast trending structures, which reflect the regional tectonic framework of the Caspian basin. These fault systems control the structural pattern of relief and contribute to the formation of escarpments, depressions, and plateau boundaries. Seismic events are represented by blue circles, classified into major, middle, and minor categories according to earthquake magnitude. The concentration of seismic points near fault intersections suggests a strong spatial relationship between tectonic activity and seismicity. This spatial coincidence confirms the ongoing tectonic activity of the region and highlights the role of fault zones as zones of crustal weakness.

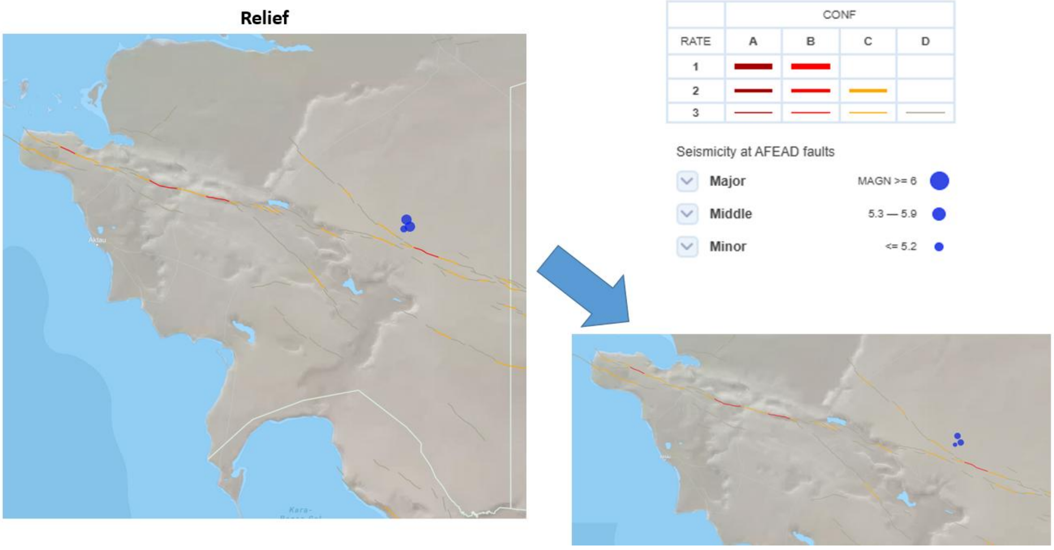

Figure 3. Relief and distribution of active tectonic faults and seismic events in the Mangystau region

The relief shading emphasizes elevation differences and slope variations, which are more pronounced in areas adjacent to major fault lines. These zones are characterized by increased surface dissection and geomorphological instability, making them more susceptible to erosion, soil degradation, and slope failure processes. The integrated visualization of relief, tectonic faults, and seismicity demonstrates that tectonic structures play a key role in shaping the landscape of the Mangystau region. Their influence extends beyond geological formation and directly affects surface stability, hydrological conditions, and land degradation patterns.

Tectonic faults are represented by colored linear features corresponding to different confidence and activity classes. The major fault zones extend predominantly in a northwest–southeast direction, forming continuous structural corridors across the region. These fault systems divide the territory into distinct geomorphological blocks and control the spatial organization of surface features. The satellite image reveals that fault zones often coincide with linear valleys, subtle relief breaks, drainage anomalies, and variations in surface reflectance, indicating their strong control over geomorphological and hydrological processes shown in Figure 4.

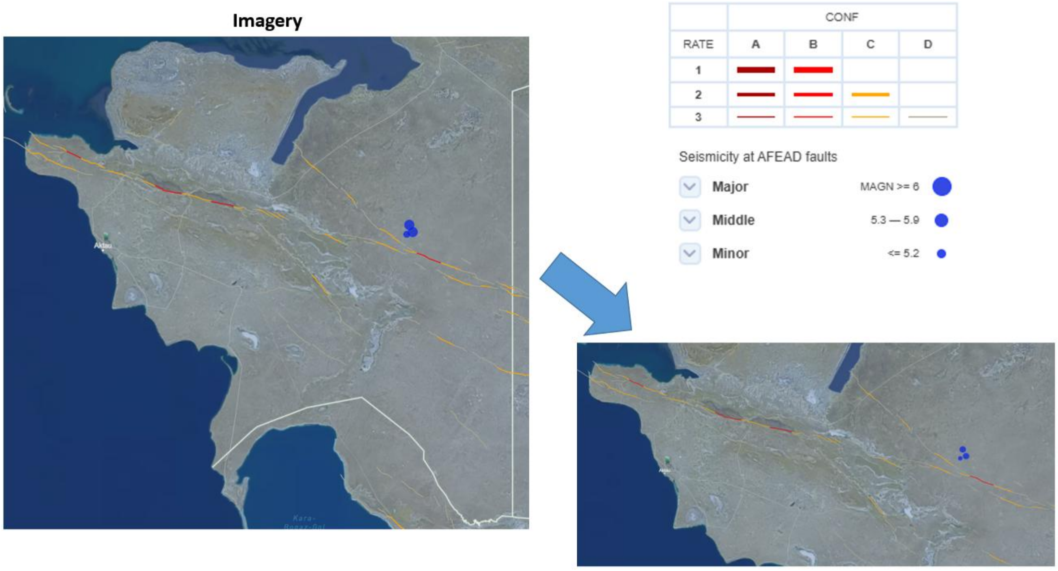

Figure 4. Satellite imagery of the Mangystau region shows the spatial distribution of active tectonic faults and seismic events

These zones act as preferential pathways for groundwater movement and influence soil moisture distribution.

Seismic events are shown as blue circles and are spatially clustered near the major fault intersections. This spatial association confirms the tectonic activity of the region and supports the reliability of the mapped fault structures. The integrated analysis of satellite imagery and tectonic data indicates that fault zones represent key controlling factors for surface instability, soil degradation, and landscape fragmentation in the Mangystau region.

Tectonic faults represent an important geological factor influencing groundwater circulation, soil moisture conditions, and surface stability. Therefore, the distance to tectonic fault zones was considered as a controlling parameter in the assessment of land degradation and desertification susceptibility.

Euclidean distance analysis was applied to measure the proximity of each pixel to active tectonic fault lines, which were obtained from regional geological surveys and have been shown to affect groundwater availability in arid environments. Before processing, all raster datasets were resampled and aligned into a unified coordinate system to avoid spatial mismatches; however, minor discrepancies in pixel boundaries were encountered, and these were corrected through geometric adjustment. Each index was classified into degradation-related categories based on thresholds commonly reported in similar studies, which allowed meaningful comparison across variables.

2.4 Role of terrain slope in soil degradation and desertification processes in the Mangystau region

Several studies have demonstrated that topographic factors, particularly slope gradient, play a crucial role in soil degradation processes. Steeper slopes tend to enhance surface runoff and increase sediment yield, thereby accelerating soil erosion and the loss of soil particles under rainfall events (Chen et al., 2022) [13]. Wind and water erosion processes interacting with slope characteristics further intensify soil property changes, with upper slope areas losing soil organic matter and nutrients more rapidly than lower slope positions [14]. Research also shows that slope gradients influence the distribution of soil organic carbon, indicating that slope contributes not only to physical erosion but also to chemical and biological aspects of soil degradation [15]. Studies in hilly landscapes reveal significant impacts of slope gradient on soil physicochemical properties, underlining the need to consider topographic variations in land degradation assessments [16].

The images were acquired for the vegetation period to ensure consistent phenological conditions, and cloud-contaminated scenes were excluded to maintain data reliability. Shuttle Radar Topography Mission (SRTM) elevation data with 30-meter resolution were incorporated to generate slope values, since terrain inclination is known to influence erosion processes and water redistribution.

2.5 NDVI and WRI for assessing land degradation and desertification in the Mangystau region

NDVI is widely used as an indicator of vegetation condition and has been extensively applied to assess land degradation and desertification patterns in arid and semi-arid environments [17]. In addition, spectral water indices provide indirect information on surface wetness and soil moisture (WRI) conditions, which are closely linked to degradation processes in drylands [18].

In the arid environments of the Mangystau region, vegetation degradation and surface drying are key manifestations of soil degradation and desertification. The Normalized Difference Vegetation Index (NDVI) derived from Landsat imagery is widely applied to quantify vegetation cover and its decline, which is commonly interpreted as an indicator of land degradation and desertification dynamics. At the national scale, desertification-sensitive areas in Kazakhstan are concentrated in the western and southwestern regions, including Mangystau and Atyrau, highlighting the relevance of vegetation-based remote sensing monitoring for the Caspian zone [19].

To complement NDVI-based vegetation assessment, spectral water indices can be used to characterize surface wetness conditions associated with soil moisture variability. The Water Ratio Index (WRI) is defined using visible, NIR, and SWIR bands and is commonly used for water/wetness detection in multispectral data; comparative assessments of water indices explicitly include WRI and discuss its sensitivity to moisture-related spectral contrasts [20]. Because soil moisture strongly controls vegetation productivity and erosion resistance in drylands, combining NDVI with WRI provides an integrated view of vegetation stress and surface wetness patterns that are relevant for mapping land degradation and desertification susceptibility in Mangystau.

3. Results and discussion

3.1 Spatial distribution distances to active tectonic faults

The spatial distribution of the Euclidean distance to active tectonic faults in the Mangystau region is shown in Figure 5. Nine major active fault lines (Line 1 – Line 9) were considered in the analysis. For each grid cell, the minimum Euclidean distance to the nearest fault line was calculated, producing a continuous distance surface.

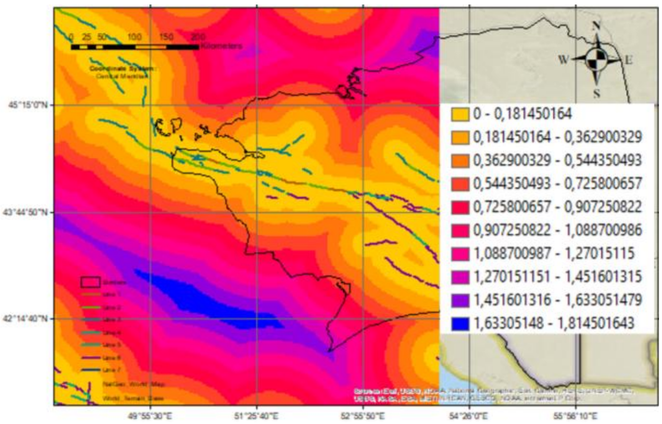

Figure 5. Proximity map to active tectonic faults in Mangystau

The results indicate a clear spatial gradient in distance values across the study area. Areas located near the fault systems are represented by low distance values (yellow to light orange colors), while regions situated farther from the tectonic structures exhibit higher distance values (purple to blue colors).

Short distances to active faults are mainly concentrated in the central and northern parts of the region, reflecting the dense distribution of tectonic structures in these zones. In contrast, the southern and southwestern parts of the study area are characterized by relatively larger distances, indicating weaker direct tectonic influence.

The generated distance map provides a quantitative spatial representation of tectonic proximity and serves as an important geomorphological indicator for subsequent spatial analyses of land surface processes in the Mangystau region.

The Euclidean distance values to active tectonic faults were further reclassified into ten ordinal classes to facilitate spatial interpretation and comparative analysis (Figure 6). The reclassification scale ranges from Class 1 to Class 10, where Class 1 (Red) represents the shortest distance to active fault lines, and Class 10 (Blue) corresponds to the greatest distance.

The reclassified map reveals a clear spatial pattern of tectonic proximity across the Mangystau region. Zones classified as Classes 1-3 are primarily distributed along the central tectonic fault systems, indicating strong spatial association with active structural features. Intermediate classes (Classes 4-7) form transitional belts surrounding the major fault zones. The highest distance classes (Classes 8-10) are mainly concentrated in the southern and southwestern parts of the study area, reflecting weaker tectonic influence.

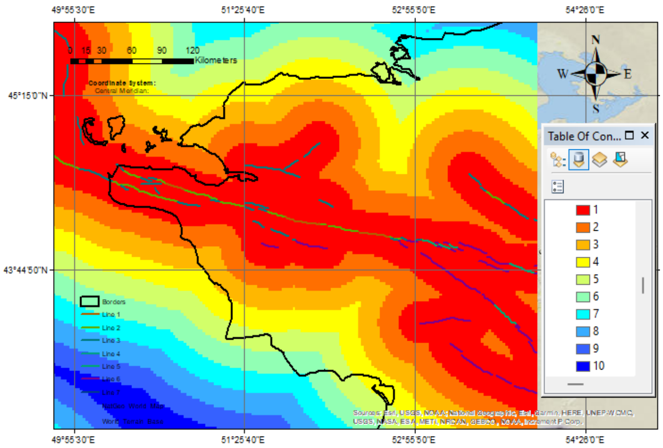

Figure 6. Reclassified distance to active tectonic faults

This classification scheme provides a standardized spatial framework for distinguishing areas with different levels of proximity to active tectonic structures and improves the interpretability of the distance surface for subsequent spatial analyses.

The combined analysis of the continuous Euclidean distance surface and its reclassified version demonstrate a consistent and reliable spatial pattern of proximity to active tectonic faults in the Mangystau region. Both representations confirm that tectonic structures exert a strong spatial control on the regional geomorphological framework.

3.2. Slope gradient distribution

Figure 7 presents the spatial distribution of terrain slope in the Mangystau region. The slope values were derived from the digital elevation model and classified into ten ordinal categories ranging from flat surfaces to strong slope gradients, to enhance spatial interpretation and geomorphological differentiation.

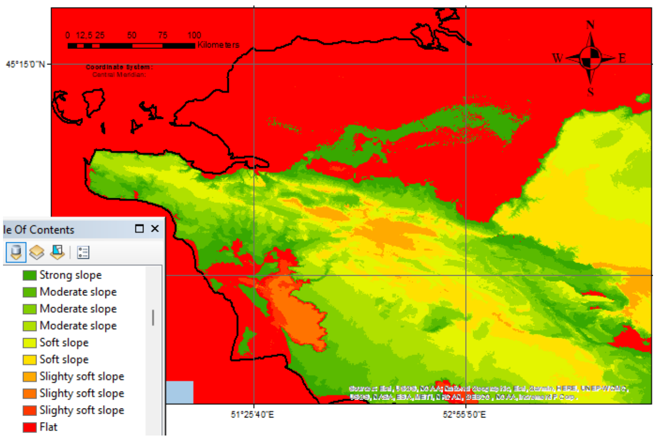

Figure 7. Slope gradient distribution derived from DEM in the Mangystau region

Flat and very gentle slope classes dominate the northern and coastal parts of the region, indicating extensive low-relief plains. These areas are characterized by minimal elevation variation and relatively stable geomorphological conditions. Gentle and moderately gentle slope classes are widely distributed across the central part of the study area, forming transitional zones between plains and elevated terrains.

Moderate slope classes are mainly concentrated along elongated belts in the central and southeastern parts of the region, reflecting the presence of structural and erosional landforms. Slightly steep and steep slope classes are limited to spatial extent and are primarily associated with hilly terrains, escarpments, and tectonically influenced zones.

The steepest slope classes occupy only a small proportion of the total area and are mainly restricted to localized topographic highs and dissected relief features. These areas represent zones of enhanced geomorphological activity and increased surface instability.

Overall, the slope classification reveals a clear spatial differentiation of relief conditions in the Mangystau region and provides an important quantitative basis for further geomorphological, hydrological, and environmental analyses.

The slope gradient map of the Mangystau region reveals a predominance of flat to gently sloping terrains, indicating that low-relief plains constitute a major part of the study area. These landforms reflect relatively stable geomorphological conditions and limited vertical dissection of the surface. Moderate slope classes form transitional belts that correspond to structural and erosional landforms, while steep and strongly sloping areas are spatially restricted and mainly associated with localized uplands and tectonically influenced zones. The limited extent of high-slope areas suggests that intense geomorphological processes are confined to specific topographic features. The spatial pattern of slope gradients demonstrates clear geomorphological heterogeneity across the region and provides an essential basis for assessing surface processes, land stability, and environmental sensitivity in the Mangystau region.

3.3. NDVI and WRI spatial distribution

Figure 8 illustrates the spatial distribution of the Normalized Difference Vegetation Index (NDVI) in the Mangystau region. The NDVI values were classified into ten categories to enhance visual interpretation and to distinguish surface types based on vegetation density.

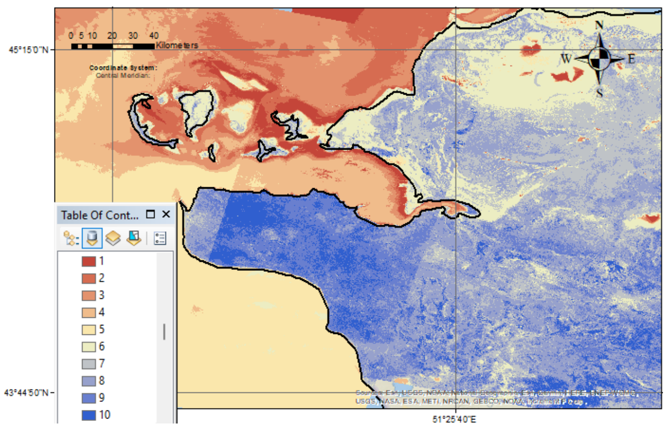

Figure 8. NDVI-Derived vegetation distribution in the Mangystau region

Low NDVI values (red tones) are primarily associated with water bodies and non-vegetated surfaces, indicating minimal or absent vegetation cover. These zones are mainly located along coastal and lacustrine areas. Moderate NDVI classes represent sparsely vegetated or mixed surface conditions, reflecting transitional environments between barren land and vegetated areas.

High NDVI values (blue tones) dominate the central and southern parts of the region, corresponding to areas with relatively dense and healthy vegetation cover. These zones indicate more favorable ecological conditions for plant growth compared to surrounding arid surfaces.

The NDVI map demonstrates a clear spatial contrast between water, barren land, and vegetated surfaces, highlighting the heterogeneity of land cover in the Mangystau region. This spatial pattern provides an important basis for further ecological and environmental assessments.

Figure 9 shows the spatial distribution of the Water Requirement Index (WRI) in the Mangystau region. The WRI values were classified into ten ordinal classes, where Class 1 (red) represents the lowest soil moisture conditions and Class 10 (blue) indicates the highest soil moisture levels.

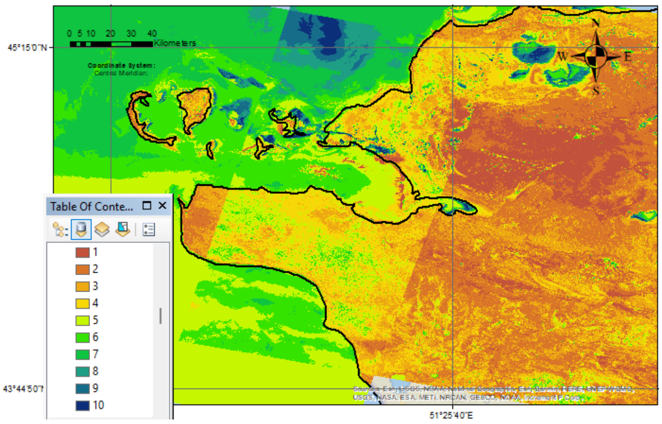

Figure 9. Water requirement index (WRI) map of the Mangystau region

Low WRI values (Classes 1-3) dominate large parts of the eastern and southeastern regions, reflecting arid surface conditions and limited soil water availability. These areas are characterized by high dryness and weak moisture retention capacity. Moderate WRI classes (Classes 4-7) form transitional zones, indicating intermediate soil moisture conditions.

High WRI values (Classes 8-10) are mainly concentrated in localized northern and coastal zones, as well as near water bodies and low-lying terrains. These areas represent relatively humid soil conditions and higher water availability for vegetation.

Overall, the WRI map demonstrates strong spatial heterogeneity in soil moisture conditions across the Mangystau region and provides an important indicator for evaluating hydrological and ecological variability within the study area.

The combined analysis of NDVI and WRI maps reveals a strong spatial consistency between vegetation distribution and soil moisture conditions in the Mangystau region. Areas characterized by high WRI values, indicating elevated soil moisture, generally correspond to zones with higher NDVI values, reflecting healthier and denser vegetation cover. This spatial agreement confirms the dominant role of soil moisture availability in controlling vegetation development under arid and semi-arid climatic conditions.

Conversely, regions with low WRI values are mainly associated with low NDVI levels, indicating sparse or absent vegetation cover. These areas represent environmentally stressed zones where limited water availability restricts plant growth. Transitional zones with moderate WRI values exhibit intermediate NDVI levels, highlighting gradual ecological gradients across the landscape.

Overall, the integrated interpretation of NDVI and WRI demonstrates that soil moisture is a key limiting factor for vegetation distribution in the Mangystau region. The strong correlation between these two indices provides a reliable basis for ecological monitoring, land degradation assessment, and environmental management in arid environments.

Figure 10 presents the overall modeling framework used to assess land degradation and desertification sensitivity in the Mangystau region. The model integrates geomorphological, geological, and ecological indicators within a GIS-based multi-criteria evaluation approach.

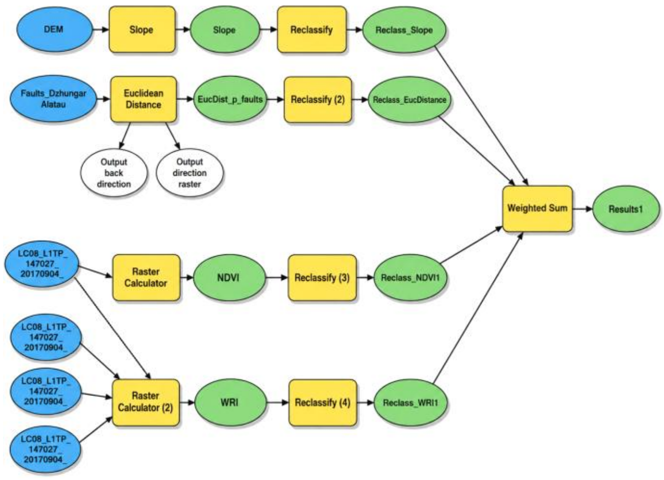

Figure 10. Integrated spatial modeling framework for desertification assessment

Four main thematic factors were included in the model:

1. Terrain slope, derived from the digital elevation model (DEM) using the *Slope* tool and subsequently reclassified into ordinal classes.

2. Distance to active tectonic faults, calculated using the *Euclidean Distance* tool based on mapped fault lines and then reclassified to represent different levels of tectonic influence.

3. Vegetation cover, represented by the Normalized Difference Vegetation Index (NDVI), calculated from Landsat 8 OLI imagery using the raster calculator and reclassified into vegetation density classes.

4. Soil moisture conditions, represented by the Water Requirement Index (WRI), also derived from Landsat 8 OLI imagery and reclassified into soil moisture classes.

Each factor layer was standardized through reclassification to ensure a uniform scale and comparability among variables. The reclassified layers were then integrated using the *Weighted Sum* method, where each factor contributes proportionally to the final composite index based on its relative importance.

4. Conclusions

The integrated analysis of tectonic faults, terrain slope, vegetation cover (NDVI), and soil moisture conditions (WRI) demonstrates that land degradation and desertification processes in the Mangystau region are controlled by a complex interaction of geological, geomorphological, and ecological factors.

Active tectonic faults significantly influence groundwater movement, soil moisture distribution, and slope stability. As a result, areas located in proximity to tectonic structures are more prone to soil instability and surface degradation due to enhanced structural weakness and hydrological disturbances.

Terrain slope plays a key role in regulating surface runoff and erosion intensity. Increasing slope gradients lead to higher runoff velocity, stronger soil erosion, and accelerated loss of fertile soil layers. Consequently, steeper areas exhibit greater susceptibility to land degradation.

Vegetation cover, represented by NDVI, reflects the protective function of plant communities. Low NDVI values indicate sparse vegetation, which reduces soil protection, increases evaporation, and enhances erosion processes. This results in reduced ecosystem stability and increased vulnerability to degradation.

Soil moisture conditions, expressed by WRI, represent the hydrological status of the land surface and the availability of water for vegetation growth. Low WRI values correspond to dry soil conditions, which directly promote soil degradation and intensify desertification processes.

When analyzed together, these factors form an integrated environmental system: tectonic structures control hydrological conditions, terrain slope determines erosion intensity, vegetation cover regulates surface stability, and soil moisture reflects the current degradation state. Their combined interpretation provides a comprehensive framework for assessing land degradation and desertification processes in arid and semi-arid regions. This integrated approach allows a more reliable identification of environmentally vulnerable zones and offers a scientific basis for sustainable land management and desertification control strategies in the Mangystau region.

The final output represents the spatial distribution of land degradation and desertification sensitivity, reflecting the combined influence of tectonic, topographic, vegetation, and hydrological conditions.

This integrated modeling framework allows a comprehensive and systematic evaluation of land degradation processes and provides a robust spatial basis for environmental assessment and land management planning in arid and semi-arid regions.

Author contributions

Conceptualization: MEA, YZ; Data curation: YZ, MEA; Formal analysis: MEA, YZ, SH; Funding acquisition: YZ, MEA; Investigation: YZ, MEA; Methodology: MEA, YZ; Project administration: YZ, MEA; Resources: YZ, SH; Software: MEA, SH; Supervision: YZ, SH; Validation: MEA, YZ; Visualization: MEA, SH; Writing – original draft: MEA, YZ; Writing – review & editing: SH, YZ. All authors have read and agreed to the published version of the manuscript.

Funding

This research was funded by the Science Committee of the Ministry of Science and Higher Education of the Republic of Kazakhstan under the framework of the program (Grant No.BR24993218).

Acknowledgements

The authors express their sincere gratitude to the editor and anonymous reviewers for their constructive comments and valuable suggestions, which have significantly improved the quality of this manuscript.

Conflicts of interests

The authors declare no conflict of interest.

Data availability statement

The original contributions presented in this study are included in the article. Further inquiries can be directed to the corresponding author.

References

[1] Amirkhanov, M., Zhakypbek, Y., Tursbekov, S., & Nurpeissova, T. (2025). Comparative analysis of the state of desertification of the lands of West and East Kazakhstan. *Engineering Journal of Satbayev University*, *147*(2), 40-49. https://doi.org/10.51301/ejsu.2025.i2.06

[2] White, K.D. (2019). Environmental Issues in Kazakhstan. *Global Encyclopedia of Public Administration, Public Policy, and Governance. Springer, Cham*, 1-7. https://doi.org/10.1007/978-3-319-31816-5_3854-1

[3] Li, J., Ye, M., Pu, R., Liu, Y., Guo, Q., Feng, B., Huang, R., & He, G. (2018). Spatiotemporal Change Patterns of Coastlines in Zhejiang Province, China, Over the Last Twenty-Five Years. *Sustainability*, *10*, 477. https://doi.org/10.3390/su10020477

[4] Issanova, G., Saduakhas, A., Abuduwaili, J., Tynybayeva, K., & Tanirbergenov, S. (2020). Desertification and land degradation in Kazakhstan. *Scientific Journal of Pedagogy and Economics*, (5), 95-102.

[5] Salmurzauly, R., Zulpykharov, K., Tokbergenova, A., Kaliyeva, D., & Bilalov, B. (2025). Ecological Vulnerability of Lands of Western Kazakhstan: Analysis Based on MEDALUS Model and Remote Sensing. *Sustainability*, *17*, 9990. https://doi.org/10.3390/su17229990

[6] Yesmagulova, B.Z., Assetova, A.Y., Tassanova, Z.B., Zhildikbaeva, A.N., & Molzhigitova, D.K. (2023). Determination of the Degradation Degree of Pasture Lands in the West Kazakhstan Region Based on Monitoring Using Geoinformation Technologies. *Journal of Ecological Engineering*, *24*, 179-187. https://doi.org/10.12911/22998993/155167

[7] Shinkarenko, S., Berdengalieva, A., Doroshenko, V., & Naichuk, Y. (2023). An Analysis of the Dynamics of Areas Affected by Steppe Fires in Western Kazakhstan on the Basis of Earth Remote Sensing Data. *Arid Ecosyst.*, *13*, 29-38. https://doi.org/10.1134/S2079096123010122

[8] Bazarbayeva, S.M. (2024). Dataset on Industrial Waste Compositions in West Kazakhstan and Conditions for Processing Them into Construction Materials. *Data Brief*, *54*, 110265. https://doi.org/10.1016/j.dib.2024.110265

[9] Li, H., Liu, X., Zhao, X., Zhang, W., Liu, J., Luo, X., Wang, R., & Xing, L. (2023). Contrasting Effects of Tectonic Faults on Vegetation Growth along the Elevation Gradient in Tectonically Active Mountains. *Forests*, *14*, 2336. https://doi.org/10.3390/f14122336

[10] Ludat, A. L., & Kübler, S. (2023). Tectonic controls on the ecosystem of the Mara River basin, East Africa, from geomorphological and spectral index analysis. *Biogeosciences*, *20*(10), 1991-2012. https://doi.org/10.5194/bg-2022-206

[11] Shojaei, S., Reza Noura, M., & Moslempour, M.E. (2022). Study of the effect of geological and geomorphological parameters on soil erosion and sediment yield of Gabrik River basin, S.E Iran. *Nexo Revista Científica*, *35*(01), 97-110. https://doi.org/10.5377/nexo.v35i01.13920

[12] Ehteshami-Moinabadi, M. (2022). Properties of fault zones and their influences on rainfall-induced landslides, examples from Alborz and Zagros ranges. *Environmental Earth Sciences, 81*, 168. https://doi.org/10.1007/s12665-022-10283-2

[13] Chen, T., Shu, J., Han, L., Tian, G., Yang, G., & Lv, J. (2022). Modeling the effects of topography and slope gradient of an artificially formed slope on runoff, sediment yield, water and soil loss of sandy soil. *Catena*, *212*, 106060.. https://doi.org/10.1016/j.catena.2022.106060

[14] Tuo, D., Lu, Q., Wu, B., Li, Q., Yao, B., Cheng, L., & Zhu, J. (2023). Effects of Wind-Water Erosion and Topographic Factor on Soil Properties in the Loess Hilly Region of China. *Plants (Basel)*, *12*(13), 2568. https://doi:10.3390/plants12132568

[15] Nozari, S., Boruvka, L. (2023). The effects of slope and altitude on soil organic carbon and clay content in different land-uses: A case study in the Czech Republic. *Soil & Water Res*, *18*(3), 204-218. https://doi:10.17221/105/2022-SWR
[16] Ewunetu, T., Selassie, Y.G., Molla, E., Admase, H., & Gezahegn, A. (2025). Soil properties under different land uses and slope gradients: Implications for sustainable land management in the Tach Karnuary watershed, Northwestern Ethiopia. *Frontiers in Environmental Sciences, 13*, 1518068. https://doi:10.3389/fenvs.2025.1518068
[17] Rivera-Marin, D., Dash, J., & Ogutu, B. (2022). The use of remote sensing for desertification studies: A review. *Journal of Arid Environments*, *206*, 104829.. https://doi.org/10.1016/j.jaridenv.2022.104829
[18] Al-Ali, Z., Abulibdeh, A., Al-Awadhi, T., Mohan, M., Al Nasiri, N., Al-Barwani, M., & Abdullah, M. (2024). Examining the potential and effectiveness of water indices using multi-spectral sentinel-2 data to detect soil moisture as an indicator of mudflow occurrence in arid regions. *International Journal of Applied Earth Observation and Geoinformation*, *130*, 103887.https://doi.org/10.1016/j.jag.2024.103887
[19] Hu, Y., Han, Y., & Zhang, Y. (2020). Land desertification and its influencing factors in Kazakhstan. *Journal of Arid Environments*, *180*, 104203.https://doi.org/10.1016/j.jaridenv.2020.104203
[20] Guo, B., Zhang, R., Lu, M., Xu, M., Liu, P., & Wang, L. (2024). A New Large-Scale Monitoring Index of Desertification Based on Kernel Normalized Difference Vegetation Index and Feature Space Model. *Remote Sensing*, *16*, 1771. https://doi.org/10.3390/rs16101771

Интегралды көпфакторлы көрсеткіштер негізінде Каспий маңы өңірі жерлерінің деградациясын бағалаудың геокеңістіктік моделі

М.Е. Амирханов[1], Ы. Жакыпбек[1*], Сунь Хао[2]
[1]*Satbayev University, Алматы, Қазақстан*
[2]*Қытай тау-кен және технологиялар университеті, Бейжің, Қытай*
**Корреспонденция үшін автор:* y.zhakypbek@satbayev.university

Аңдатпа. Шөлейттену және жер деградациясы Қазақстанның Каспий маңы өңіріндегі негізгі экологиялық проблемалардың бірі болып табылады. Бұл зерттеуде интеграцияланған ГАЖ және қашықтықтан зондтау әдістерін пайдалана отырып Маңғыстау облысының шөлейттену үрдісіне ұшырауы бағаланады. Төрт бақылаушы фактор ретінде: белсенді тектоникалық жарылымдарға дейінгі қашықтық, жер бедерінің еңістігі, өсімдіктердің нормаланған айырмашылық индексі (NDVI) негізінде есептелген өсімдік жамылғысы және су қажеттілігі индексі (WRI) ұсынған топырақ ылғалдылығы шарттары. Тектоникалық әсерді бағалау үшін евклидтік қашықтықты талдау қолданылды, жер бедерінің еңістік градиенттері SRTM деректерінен алынды, ал NDVI және WRI Landsat 8 OLI суреттерінен есептелді. Барлық факторлар стандартты реттік класстарға қайта жіктелді және шөлейттенуге ұшырау картасын жасау үшін анықталған нәтижені көп критерийлік бағалау үлгісін пайдалана отырып біріктірілді. Нәтижелер жер деградация жағдайларының күшті кеңістіктік гетерогенділігін көрсетеді. Тік беткейлері, төмен NDVI және WRI мәндері бар тектоникалық жарылымдарға жақын аймақтар шөлейттенуге бейім, ал жұмсақ беткейлері, жоғары өсімдік жамылғысы және топырақтың ылғалдылығы жақсы аймақтар экологиялық тұрақтылықты көрсетеді. Зерттеу Маңғыстаудағы жердің деградациясы геологиялық, геоморфологиялық және экологиялық факторлардың жиынтық әсерімен бақыланатынын көрсетеді. Ұсынылған жүйе шөлейттенуді бағалаудың сенімді құралы болып табылады. Сонымен қатар, құрғақ және жартылай құрғақ жерлерде жер ресурстарын тұрақты басқаруды қолдайды.

Негізгі сөздер: *топырақ деградациясы, шөлейттену, тектоникалық жарылымдар, жер бедерінің еңістігі, NDVI, WRI, қайта жіктеу*.

Геопространственная модель оценки деградации земель Прикаспийского региона на основе интегральных многофакторных показателей

М.Е. Амирханов[1], Ы. Жакыпбек[1*], Сунь Хао[2]
[1]*Satbayev University, Алматы, Казахстан*
[2]*Китайский университет горного дела и технологий, Пекин, Китай*
**Автор для корреспонденции:* y.zhakypbek@satbayev.university

Аннотация. Деградация земель и опустынивание являются основными экологическими проблемами в засушливом Прикаспийском регионе Казахстана. В данном исследовании оценивается подверженность Мангистауской области опустыниванию с использованием, интегрированной ГИС и дистанционного зондирования. Были проанализированы четыре контролирующих фактора: расстояние до активных тектонических разломов, уклон местности, растительный покров, рассчитанный на основе нормализованного разностного индекса растительности (NDVI), и условия влажности почвы, представленные индексом потребности в воде (WRI). Для оценки тектонического воздействия был использован анализ евклидовых расстояний, градиенты склонов были получены на основе данных SRTM, а NDVI и WRI были рассчитаны на основе снимков Landsat 8 OLI. Все факторы были реклассифицированы в стандартные порядковые классы и интегрированы с использованием модели многокритериальной оценки взвешенной суммы для создания карты подверженности опустыниванию. Результаты указывают на сильную пространственную неоднородность условий деградации. Районы вблизи тектонических разломов с более крутыми склонами, низкими значениями NDVI и WRI наиболее подвержены опустыниванию, в то время как регионы с пологими склонами, более высоким растительным покровом и лучшей влажностью почвы демонстрируют большую экологическую стабильность. Исследование демонстрирует, что деградация земель в Мангистау контролируется совокупным воздействием геологических, геоморфологических и экологических факторов. Предлагаемая система представляет собой надежный инструмент для оценки опустынивания и поддерживает устойчивое управление земельными ресурсами в засушливых и полузасушливых районах.

Ключевые слова: *деградация земель, опустынивание, тектонические разломы, уклон местности, NDVI, WRI, переклассификация.*

Publisher’s note

All claims expressed in this manuscript are solely those of the authors and do not necessarily represent those of their affiliated organizations, or those of the publisher, the editors and the reviewers.

Engineering Journal of Satbayev University
Volume 148 (2026), Issue 3, 33-52

https://doi.org/10.51301/ejsu.2026.i3.05

Meta-analysis and systematic review of drone technology in mining and geotechnical engineering

M.Z. Emad*
King Fahd University of Petroleum and Minerals, Dhahran, Saudi Arabia
**Corresponding author:* muhammadzaka.emad@kfupm.edu.sa

Abstract. Unmanned Aerial Vehicles (UAVs) have revolutionized geotechnical and mining operations by enabling fast, high-resolution, and inexpensive spatial data acquisition, terrain modeling, and monitoring. The current review and meta-analysis integrate observations from over 133 peer-reviewed articles to present a comparison of the accuracy of UAV-based surveying methods, i.e., photogrammetry and LiDAR, and traditional methods such as total stations and terrestrial LiDAR. This study focuses on application of UAVs and drone use in mining and geotechnical engineering in terms of finding stockpile volumes, mining subsidence, mine tailings and dump site, and rock mass identification. UAVs are capable of achieving decent accuracy on a regular basis, as indicated by meta-analysis, if optimized flight parameters, RTK/PPK positioning, and GCPs are utilized. Improved accuracy in UAV LiDAR surveys and balance between visual accuracy and cost-recovery in UAV photogrammetry are feasible. However, error magnitude is dependent on complexity of terrain, flight planning, and meteorology, emphasizing methodical accuracy. Bibliometric analysis indicates exponential publication development per year since 2017 for UAVs, and China once more emerges as the leading contributor with funding, authorship, and research. Keyword and co-authorship network visualization demonstrates increasing adherence to machine learning, 3D reconstruction, and digital twin technologies. SWOT analysis determines UAVs' efficiency of operations, safety benefit, and visual outcome as its major strengths but bottlenecks to data processing, inconsistent accuracy, and difficulties in unfavorable terrain conditions as its weaknesses. Shortages of skills are listed as major weaknesses to extensive deployment. The findings are reinforced by an industry validation survey in which 100% of respondents testified to UAV-improved efficiency and 71% to significant cost savings. There are some concerns regarding the amount of data processing and UAV response in slopes or complex environments. UAVs are transitioning from test equipment to geotechnical equipment of choice, providing real-time actionable information for monitoring, site planning, and hazard analysis. Sensor fusion, artificial intelligence-driven analytics, and normalization of workflow destinies are UAVs to be a major driver of mining digitalization. Future research will focus on underground mapping, automation, and standardization of the regulation to open up the full potential of UAVs across the mining value chain.

Keywords: *drones, UAVs, UAS, photogrammetry, mine waste, volumetrics, accuracy, subsidence, landslide, mapping.*

Received: 29 April 2026
Received in revised form: 20 June 2026
Accepted: 23 June 2026
Available online: 30 June 2026

1. Introduction

Unmanned Aerial Vehicles (UAVs) are currently an affordable equipment of civilian application, transforming the model of acquiring geoscientific information through high spatial resolution, ease of operation, and enhanced safety [1]. Mineral exploration and geological mapping conventionally rely on time-consuming ground surveys, low-resolution satellite images, and costly airborne geophysics, frequently being incapacitated by logistic limitations and availability [2]. UAV technology directly plugs this observation gap, since low-altitude, generic platforms for miniaturized sensors and rendering remote sensing a focused, precise solution to mineral identification and other geoscientific applications [3]. A highlight of UAVs in mineral prospecting is that they possess the ability to mount hyperspectral and thermal sensors. Spectral signatures are specific for every mineral, these help with identification of minerals on earth. While satellite sensors like ASTER are a favorite for lithological mapping at the regional level, their resolution is often too coarse for deposit-scale investigation in detail [4]. UAV-borne hyperspectral sensors, however, acquire this data at centimeter resolutions, enabling the identification of subtle mineralogical variations and key mineral assemblages (e.g., phyllosilicates, carbonates, iron oxides) that are pathfinders to ore deposits [5]. This facilitates the rapid delineation of alteration zones, reducing the discovery to resource definition timeframe by orders of magnitude.

In addition to direct mineral recognition, UAVs provide a multi-toolset for the modern geoscientist. Coupling high-resolution optical cameras with Structure-from-Motion (SfM) photogrammetry software enables the creation of precise Digital Outcrop Models (DOMs). These 3D models provide essential spatial context to geological interpretation, allowing for the measurement of structural features, bedding attitudes, and fracture intensity with accuracy [6]. Magnetometer and gamma-ray spectrometer equipped UAVs are also proving to be useful tools for high-resolution geophysical surveying, mapping anomalies related to subsurface mineralization [6]. The technology adds value across the entire mine lifecycle, from pre-exploration baseline mapping to operational tasks like stockpile volumetrics, pit slope stability monitoring, and post-mining land reclamation assessment.

The advantages of UAVs in a mine site are numerous and primarily hinge on personnel safety, operational efficiency, and data quality [7, 8]. Their ability to access hazardous or logistically challenging areas such as unstable highwalls [9], deep pits, and active blast areas, without endangering human life is a major benefit [10]. They are hence extremely essential for geotechnical applications like landslides and slopes where conventional technologies such as levelling, total stations, and terrestrial laser scanning are time-intensive, labor demanding, and hazardous [11]. UAVs, when equipped with high-end sensors like LiDAR, multispectral, and thermal cameras, provide cheaper, faster, and safer alternatives [12-14] with centimeter-level topographic mapping precision [15], near real-time volume calculations, and remote sensing of dangerous environments [16]. Fast advancement in UAV applications like pit wall stability monitoring, waste dump monitoring, blast fragmentation analysis, and tailings dam monitoring is highlighted in industry reports [7, 17]. Both UAV LiDAR and photogrammetry possess the ability to produce high-resolution Digital Elevation Models (DEMs) and point clouds with greater than 0.1% volumetric accuracy, often outperforming traditional GPS surveys at a cost saving of more than 60% in time and labour [18-21]. This is of specific value in large open-pit mines where routine volumetric monitoring of waste dumps and ore is integral to resource estimation and logistics planning [8, 22]. UAVs also allow real-time monitoring of ground movement and earthworks, with operators able to validate progress to project schedules without the need to interrupt work [23].

The sector is moving toward full autonomy and more integration of data. Drone-in-a-Box (DiaB) technology, under which fully autonomous inspection flights are possible without pilots, is being adopted by industry leaders for routine monitoring of critical infrastructure. UAVs are increasingly being incorporated into more extensive digital platforms that leverage artificial intelligence (AI), machine learning (ML), and IoT-enabled sensor networks [24, 25]. The intersection of UAV hardware, advanced remote sensing algorithms, and autonomous flight platforms is facilitating a new revolution of innovation [26-28]. Deep learning algorithms are being applied routinely to drone imagery for rock fragmentation measurement automation [29, 30], defect detection on conveyor belts [31], and prognostic ground deformation modeling [32]. Moreover, the availability of beyond-visual-line-of-sight (BVLOS) flight and 5G connectivity is facilitating real-time data streaming and centralized control of large-scale mining fleet operations [33-35].

Several detailed reviews capture this range of technology. Vishweshwaran and Sujatha [36] document usage of drones in geotechnical engineering for slope, pavement, and excavation monitoring, complete with methodology guidelines for integrating photogrammetry, SfM, LiDAR, and multispectral imaging. They also note the potential for AI/ML in automating crack detection and rock mass classification. Jackisch [37] has an interest in mineral exploration, demonstrating how drone-borne hyperspectral and magnetic surveys can delineate ore zones at a fraction of the cost of conventional methods, with examples from Greenland and Namibia. Shahmoradi et al. [38] cover applications at abandoned, active, and reclaimed mines, noting the value of collision-tolerant drones like the Elios series for GPS-denied underground mine voids. To these prospects, Andresen and Schultz-Fellenz [39] introduce UAV-facilitated change detection, while Perikleous et al. [40] cover the employment of UAVs in combination with geophysical sensors for subsurface mapping in a review of 59 mining case studies. Hussain et al. [41] and Chen et al. [42] explore the utilization of UAVs in landslide studies, documenting workflows for hazard evaluation. Arif et al. [43] outline the synergistic benefit of integrating InSAR and Global Navigation Satellite System (GNSS) with UAVs in a multi-sensor strategy to the quantification of mining-induced deformation.

To bridge these limitations, this study attempts a structured review of UAV application in mining and geotechnical engineering with particular reference to terrain modeling, stockpile volumetrics, real-time monitoring, and unsafe-site inspection. It is guided by the research question: "How accurate and efficient is terrain modeling and stockpile volumetrics using drones versus traditional surveying methods in various mining environments (open-pit, underground, tailings)?". Through a multi-method approach adopting the meta-analysis of UAV performance metrics, examining biblio-metric research trends mapping, SWOT analysis, and industry survey, this review seeks to provide an evidence-based synthesis of the current state and future prospects of UAVs in mining. Empirical evidence is used to guide research and make operational guidelines accessible to industry parties interested in optimizing use of UAVs for safety, efficiency, and sustainability. To validate the findings of a preceding meta-analysis and gauge current industry sentiment, a survey was distributed to thirty-three experienced practitioners (with experience of 3 years or more) in the mining and geotechnical fields. The seven responses, as being a specialized segment of the industry, confirm the meta-analysis's hypothesis of pervasiveness on the basis of higher efficiency. The survey also identifies the main issues preventing further integration, with data processing as the most significant technical barrier and sloping terrain as the most limiting environmental constraint.

2. Literature review

2.1. PPK vs RTK

The pursuit of centimeter-level positioning accuracy in Unmanned Aerial Systems (UAS) has made Real-Time Kinematic (RTK) and Post-Processed Kinematic (PPK) GNSS methodologies equally vital. Despite both employing carrier-phase differential corrections for integer ambiguity resolution and achieving high accuracy, their operational paradigms, infrastructure dependence, and robustness are quite disparate, dictating their applicability. The main distinction is the timing of the application of the corrections. RTK is a real-time method. It requires a continuous communication link, typically a radio modem, from a fixed base station to the UAS (rover). This base station, whose location is known, calculates error corrections based on comparing its known location to its location obtained by GNSS. These corrections are transmitted back to the rover in real time, allowing its onboard computer to resolve integer ambiguities immediately and output a corrected, centimeter-level position for direct geotagging of images [44]. The base station could be a user-mounted unit or, more typically, a network of Continuously Operating Reference Stations (CORS). While CORS networks are easy, their availability is dependent on good cellular data coverage at the flight location. The greatest weakness of RTK is that it depends on a continuous communication link; any break can trigger a re-initialization of the ambiguity resolution, leading to periods of degraded accuracy. Conversely, PPK is a post-mission method that decouples the process of correction from flight operation. The base station and the UAS rover both separately record the raw, time-stamped GNSS observation data, i.e., the carrier-phase and pseudo-range measurements. After flight, these data sets are integrated post-processing software to determine the true path of the drone. This approach is understandably more tolerant to faults because it eliminates the risk of in-flight radio link failure and is thus extremely well suited for operation in adversarial environments such as hilly terrain, dense forests, or near infrastructure where the line-of-sight communication is disrupted [45]. The correction origin will typically be a user-defined base station as the timing synchronization for processing with CORS data can be more complex.

The core algorithm for both approaches is the solution for the integer ambiguity in carrier-phase measurements. The Least-Squares Ambiguity Decorrelation Adjustment (LAMBDA) algorithm is the default algorithm for this purpose, where it is widely regarded for its effectiveness and resilience in determining correct integer ambiguities [46]. The global positioning solution is normally accomplished using a Kalman Filter, which combines optimally the GNSS carrier-phase measurements with the Inertial Measurement Unit (IMU) measurements. Sensor fusion is critical since the IMU provides high-rate velocity and attitude measurements that fill short-term gaps in GNSS signal availability and smooth the trajectory. Accuracy of the combined GNSS-IMU system, that is, calibration of the lever arm (physical distance between GNSS antenna and IMU) and sensor biases of the IMU itself, is a primary driver of end accuracy. With advancing sensor technology, cheaper, tactical-grade IMUs are more and more useful for high-accuracy PPK/RTK applications, closing the performance gap to more expensive systems.

2.2. Photogrammetry process

The modern photogrammetric pipeline, driven by SfM algorithms, breaks up a collection of overlapping 2D images into a precise 3D model in the guise of an iteratively performed computationally intensive pipeline. The initial step includes feature detection and matching, where the features are detected by algorithms like SIFT (Scale-Invariant Feature Transform), SURF (Speeded-Up Robust Features), or the computer friendlier ORB (Oriented FAST and Rotated BRIEF), which identify distinctive key points in each image that are scale, rotation, and illumination invariant [47]. By matching those features between a series of images, the program generates a series of tie points, establishing the first correspondence for the entire reconstruction. This sparsely textured point cloud and corresponding image points are fed into the core of SfS/ bundle adjustment and pose estimation. The approach first estimates the exterior orientation (camera location and orientation) of each camera and the 3D coordinates of the tie points simultaneously. This is optimized using bundle adjustment, a top-level optimization that minimizes the reprojection error, the difference between observed 2D feature positions and reprojected 3D points into the images [48]. Bundle adjustment is necessary to achieve a globally consistent and internally accurate model. In the context of rolling-shutter cameras on drones, a rolling-shutter correction needs to be incorporated at this stage. Since every scanline of an image is captured at a varying moment when the drone moves, perspective geometry is distorted. SfM software mimics this phenomenon by calculating the camera path for exposure of a single frame significantly improving accuracy, especially for fast-moving platforms.

Following sparse reconstruction, dense matching algorithms produce a dense point cloud. Semi-Global Matching (SGM) obtains disparity maps inexpensively by maximizing a pixel-wise cost of matching on numerous one-dimensional paths, while more recent approaches like PatchMatch scatter good matches randomly and in parallel, achieving high detail and effectiveness [49]. The dense cloud serves as input to Multi-View Stereo (MVS), which continues to optimize the geometry and generally outputs the final surface mesh or textured model. Along this pipeline, there are two things that are most critical to absolute, especially vertical, accuracy. First, precise camera calibration, measurement of the internal parameters like focal length, principal point, and lens distortion is not possible. Systematic errors due to uncalibrated or poorly calibrated cameras cannot be eliminated at all through bundle adjustment, usually being manifested as a doming or bowing of the model [50]. Second, ground control point (GCP) distribution and quantity are key. GCPs provide reproducible coordinates within a world-wide reference system, positioning the bundle adjustment and eliminating residual errors within the direct georeferencing solution. A uniformly distributed set of GCPs, particularly on the boundaries and at various heights within the study area, is required to control and minimize vertical error propagation. Independent check points are then required to objectively assess the resulting achieved accuracy.

2.3. UAV-LiDAR systems

UAV LiDAR systems integrate a number of sensors, a laser scanner, a GNSS receiver, and an IMU, to directly sense 3D points in space. To reduce the raw data to a coherent, correct point cloud, there is a set of fundamental calibration and alignment procedures to correct for systemic errors that are inherent in the multi-sensor system. Boresight and lever-arm calibration are the simplest calibrations. The lever-arm is the same 3D vector offset between the origin of the IMU and the LiDAR scanner, and the boresight consists of angular misalignments (roll, pitch, yaw) among the body frame of the IMU and the coordinate system of the scanner. Minor inconsistencies in the parameters, particularly in boresight angles, may result in significant positional errors, which manifest as "double walls" or overlapping flight strip misalignments [51]. Calibration is typically achieved by flying over a region with clearly defined planar features (e.g., rooftops of buildings, roads) in multiple directions and adjusting the parameters iteratively until multiple strips' point clouds merge perfectly. Following initial calibration, scan strip adjustment is often a subsequent requirement. This process refines the path and/or boresight angles by minimizing differences between overlapping LiDAR strips. By finding common planar or linear features between strips, a bundle adjustment-type optimization is performed to reduce vertical and horizontal offsets, producing a more consistent data set internally [52].

To register several flights or UAV-LiDAR and ground point cloud scans, point cloud registration algorithms are used. Among the well-known algorithms is the Iterative Closest Point (ICP) algorithm which iteratively computes the optimal rigid transformation (rotation and translation) between two-point clouds in the sense of minimizing the distance between the corresponding points [53]. A more robust alternative is the Normal Distributions Transform (NDT), which models the target point cloud as a set of probability density functions and can achieve better performance with unstructured scenes and partial overlaps [54]. Classic

GNSS/IMU positioning is out of function in GNSS-denied situations such as forests, canyons, or indoors. For these situations, SLAM algorithms fill the gap. LiDAR SLAM relies on the point cloud as a spatial reference. By registering piecewise incoming laser scans to a map of the scene that is incrementally growing, the algorithm simultaneously estimates the 6-degree-of-freedom trajectory of the sensor and builds the 3D model in real-time. This allows one to walk and collect data continuously without using external localization, making it extremely useful in mining, geotechnical, forestry, and infrastructure inspection tasks where GNSS signals do not reach [55]. UAV-LiDAR performance thus lies in an efficient processing pipeline that aligns sensor geometry, data stripping coinciding, and incorporates sophisticated registration or SLAM techniques to achieve metric accuracy for a broad variety of scenes.

2.4. Sensor fusion

The intrinsic limitations of remote sensing and personal navigation sensors become pronounced in challenging terrain, where signal blockage and poor geometries exacerbate error. Sensor fusion is an effective paradigm to overcome these limitations by synergistic integration of the strengths of complementary systems. The integration of GNSS and IMU using advanced filtering algorithms forms the basis of precise direct georeferencing in both LiDAR and photogrammetry, and combining LiDAR and photogrammetric data yields a stronger and more reliable end product. The spirit of GNSS/IMU integration is typically achieved by using an Extended Kalman Filter (EKF) or an Unscented Kalman Filter (UKF). The EKF linearizes the system dynamics and measurement models to propagate the state (position, velocity, attitude) and covariance, whereas the UKF uses deterministic sampling to better handle extreme non-linearities. The GNSS provides absolute position but with low update rate and susceptibility to signal loss. The IMU, by contrast, offers high-rate acceleration and angular rate measurements, which allow for precise dead reckoning between GNSS updates but are subject to unbounded drift due to sensor biases. The Kalman filter combines these data streams most effectively. The IMU propagates the state, and the GNSS measurements update and refine this prediction, estimating and correcting the IMU sensor biases simultaneously [56]. This integration is the primary defense against drift. In complex country side like deep valleys or under forest canopy, where GNSS signals are intermittently shadowed, the tightly coupled IMU is maintaining an accurate short-term track, drastically reducing the positional errors that would otherwise accumulate and manifest as distorted models.

This robust performance is then translated directly to improved elevation precision in bad terrain. A poorly navigated platform will mis-project laser returns or photographs, leading to smearing, “doming” or inability to accurately represent steep slopes and ridges. The combined GNSS/IMU solution provides a robust geometric foundation such that the precise range measurements from the LiDAR or the triangulated points from photogrammetry are properly positioned in space. Additionally, the merging of the end data products, LiDAR and photogrammetry, contributes to accuracy. Photogrammetry loses matches on texturally flat ground (e.g., sand, snow, or high canopy) where feature matching fails, creating voids in the data. LiDAR bridges small gaps in the vegetation and is immune to a lack of texture, providing solid ground points in these areas. LiDAR sacrifices point density and loses fine edges that high-resolution photography preserves. By co-registering the two data sets, systematic errors in LiDAR data can be eliminated using the photogrammetric point cloud, and Digital Terrain Model from LiDAR can be used as an absolute height reference for tying in the photogrammetric bundle adjustment and minimizing vertical error propagation [57]. Such synergy integration creates a better, more robust, and reliable 3D landscape model, directly countering the accuracy trends that single-sensor systems exhibit in challenging environments.

The conversion from measured to true coordinates of drone-based mapping, often reflected in doming or shearing in 3D models, is caused by an intersection of the error sources in the integrated navigation and photogrammetric system. A main contributor is the degradation of the direct georeferencing solution. Errors in onboard GNSS, i.e., multi-path or incorrect resolution of carrier-phase integer ambiguities in RTK/ PPK systems, translate directly to the exterior orientation of captured images [45]. Also, in the absence of good ground control, IMU errors, specifically, frame misalignment between GNSS and IMU frames, as well as gyro and accelerometer biases, introduce significant rotational errors. These rotational errors are non-linear and will lead to significant deformations, particularly on the vertical- or z-axis, creating the expected “doming” effect in the output point cloud [58]. The photogrammetric process itself causes additional shifts. Incomplete calibration of the camera, where the residual principal point and focal length errors remain, distort the internal geometry of the image bundle. Combined with insufficient image network geometry, like an insufficient flight plan with too few cross-strips, the bundle adjustment cannot derive the external platform position and orientation reliably from the internal camera parameters. This results in a non-rigid transformation with the system addressing navigation and calibration errors by deforming the 3D scene so that points of objects are transformed from their real positions [50].

2.5. Future of drone technology

The future of drone technology is in a very robust direction of more autonomy, integration, and intelligent data analysis. The future is not in stand-alone platforms, but in coupled systems, flocks of drones flying in coordination, and drones alongside other platforms like satellites, airborne LiDAR, and ground sensors creating multi-scale digital copies of the environment [59]. The principal driver is the necessity to propel edge computing, where data is calculated onboard in real time. This will enable real-time decision-making, such as a drone altering its flight path upon finding an anomaly in the mineralogy or identifying a structural defect, rather than merely collecting data to analyze afterward. Also, miniaturization and reduced cost of advanced sensors, in particular, solid-state LiDAR and hyperspectral cameras, are making high-fidelity remote sensing affordable, taking drones out of basic imaging into the realm of full-size 3D and chemical analysis.

Whether or not sensors or algorithms require more research is not an either/or question, but rather a question of recognizing that they are inter-dependent. When sensor technology advances, the most pressing research needs fall within the domain of algorithms to process, manage, and understand the enormous, disparate data streams generated by these sensors. The current state of the art moves towards generating data bottlenecks, in which terabytes of data are accumulated but remain slow and computationally intensive to analyze. All of the top research priorities are algorithmic. One, there is a pressing requirement for robust onboard SLAM in GPS-degraded environments such as underground tunnels or dense forests, from multi-sensor fusion of cameras, IMUs, and LiDAR. Second, advanced machine learning and artificial intelligence algorithms are required for real-time anomaly detection and feature extraction [60]. These include automatic detection of mineral assemblages in hyperspectral images, infrastructure cracks, or invasive species in agriculture without manual intervention. Third, one needs to study efficient data transmission and compression algorithms to mitigate the bandwidth limitation of real-time streaming of data from the edge [61]. In practice, although upgraded, lighter, and more effective sensors are always welcome, the edge currently is computational. The real potential in drone technology will be delivered not by sensors that collect the data, but by intelligent algorithms that transform this raw data into useful intelligence, autonomously and in near real-time.

2.6. Dense reconstruction in UAV-based mapping

The combination of SfM, dense image matching, LiDAR based Simultaneous Localization and Mapping (SLAM), and GNSS/INS fusion has constituted the core of UAV-based geospatial data collection, offering stable 3D reconstruction and navigation in different operation environments. SfM pipelines with bundle adjustment (BA) support high-accuracy scene modeling via incremental pose estimation and geometric refinement. There have been new advances, such as the graph-indexed Bag-of-Words approach with parallelized Schur complement-based BA (PSCBA) by Liu et al. [62] that improved efficiency while preserving the accuracy. Similarly, feature-matching techniques based on grid-based motion statistics have been demonstrated to be quite useful for suppressing drift in SfM processing [63]. Bergado and Nex [64] transferred UAV images to implement disparity shifting and occlusion masking. This was achieved through stereo networks using unsupervised learning models. Jannati et al. [65] introduce complementary studies seeking computationally efficient alternatives to Semi-Global Matching (SGM) through the introduction of a two-stage disparity estimation process removing image pyramids without sacrificing depth accuracy. In GNSS-denied real-time SLAM, UAV SLAM systems have employed LiDAR-IMU fusion more and more. Wang et al. [60] explained major features such as loop closure and pose graph optimization of outdoor SLAM systems, while Yin et al. [66] employed a two-step iterative calibration strategy to tackle LiDAR-IMU misalignments caused by rotation motion for SLAM robustness. GNSS/INS integration remains at the center of global navigation, but susceptibility to out-ages necessitates multi-sensor augmentation. Elamin et al. [67] demonstrated that tightly integrated GNSS/INS/LiDAR-SLAM systems regain fairly well the navigation performance in GNSS-denied environments, and Abdelaziz and El-Rabbany [68] also gained even better positional stability when incorporating stereo visual SLAM. Although, differing in their sensor dependency and computational topologies, these methods are converging towards hybrid fusion of vision, inertial, and LiDAR observables. SfM is effective with highly structured scenes that have high feature density. LiDAR-SLAM offers texture-poor or dynamic scene robustness, and GNSS/INS offers absolute georeferencing. Dense image matching is shifting from hand-crafted metrics to learning-based pipelines with growing emphasis on domain adaptation, occlusion, and acceleration. Together, these developments point to a common trend for UAV mapping: scalable, real-time, sensor-fused solutions that can provide high-accuracy spatial intelligence in various terrain and operating conditions.

3. Materials and methods

This review adheres to a rigorous, multi-stage methodology that seeks to minimize selection bias, maximize reproducibility, and provide an exhaustive synthesis of innovations in drone technology for mining and geotechnical uses. Unlike conventional narrative reviews that rely on subjective selection of literature and lack open search processes, the current study follows the PRISMA [69] preferred Reporting Items for Systematic Reviews guidelines to ensure methodological transparency, systematic examination of literature, and quantitative synthesis where applicable. The review answers three key research questions:

1). How do drone-based terrain modeling and stockpile volumetrics in terms of accuracy and efficiency compare with conventional surveying methods in other geotechnical and mining environments?

2). What technological (LiDAR vs. photogrammetry) and operational (flight planning, sensor fusion) factors influence UAV performance in real-time mining and geotechnical monitoring?

3.1. Literature search strategy

A systematic search strategy was employed in three major databases including Scopus (last searched on September 10th 2025), Web of Science (last searched on September 10th 2025), Google Scholar (last searched on September 10th 2025) to find peer-reviewed papers from journals, conference proceedings, and industry reports between 2010 and 2025. The search term used Boolean operators and keyword combinations like ("UAV" OR "drone" OR "UAS") AND ("mining" OR "open-pit" OR "Quarries" OR "Coal" OR "Exploration" OR "tailings" OR "Waste") AND ("Landslide" OR "Slope" OR "Deformation" OR "Highway" OR "Sink hole") AND ("Accuracy" OR "Precession"), with broad coverage of the studies.

Additional backward and forward citation tracking was conducted on significant papers to seek out early papers not caught in the initial search. To minimize selection bias, predetermined inclusion/exclusion criteria were applied and only empirical quantification studies (e.g., accuracy tests, efficiency measures) were retained, while purely theoretical or simulation-based studies were excluded except where they suggested novel methodological designs. Non-English publications were also excluded which includes Chinese, French and Russian languages. The PRISMA framework guided the four-stage screening process (Figure 1):

– identification;
– screening;
– eligibility assessment;
– inclusion.

All of the retrieved records (n = 338) were initially retrieved. The de-duplicated records were removed by Endnote. Review papers and meta-analysis studies were also excluded, leaving an initial dataset of 162 articles. The author screened title/abstract, resolving disagreements at three points and subsequently combining the remainder. The remaining full-text articles were screened for eligibility, and 94 studies were found eligible for qualitative synthesis and 18 for meta-analysis. A data extraction form with a uniform pattern documented key variables: study year, location, mining type (open-pit, underground, tailings), drone information (sensor type, flight altitude, ground sample data), and comparison metrics (Mean Error, RMSE, Standard Error, Standard Deviation, Minimal Error).

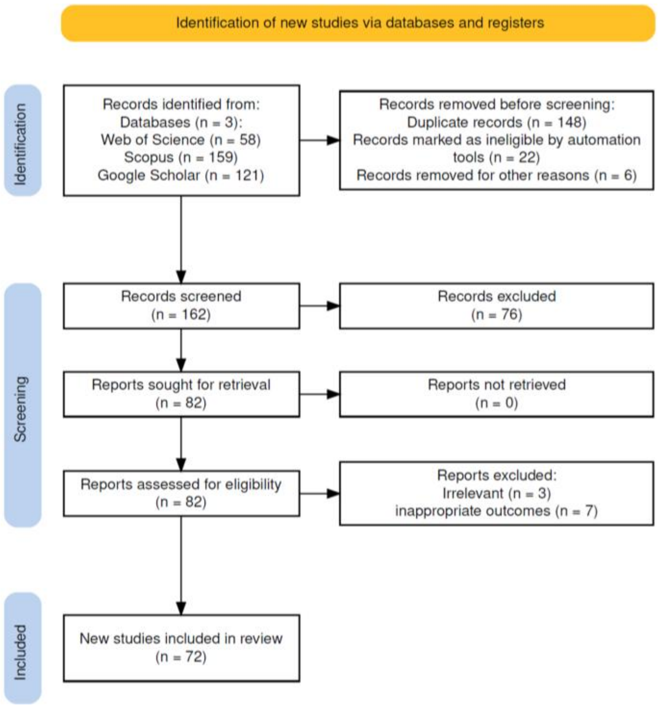

Figure 1. Prisma flowchart

To quantitatively contrast UAV performance with traditional methods (total stations, terrestrial LiDAR), meta-analysis was conducted on those papers reporting subsidence, stockpile volume, accuracy analysis and slope deformation measurement error.

Data was split by sensor type (LiDAR vs. photogrammetry) and mining environment to establish context-dependent differences. The magnitude of efficiency of UAVs in terms of time and cost saving is quantified by calculating effect sizes. Funnel plot, helped with determining subgroup analysis and publication bias. Co-occurring keywords, author collaborations and research trends were shown using Bibliometric maps developed by VOS viewer [70]. Evolving areas of interest were presented by forming clusters. Thematic analysis categorized the studies into technological (sensor technology advances), operational (flight planning concerns) themes, and it noted gaps such as the absence of representation of applications for underground mining.

Strengths-Weaknesses-Opportunities-Threats (SWOT) analysis combined qualitative evidence from existing literature. Strengths included acquiring high-resolution data and avoiding human exposure to hazards, while weaknesses listed battery life limitations and processing of data constraints. Opportunities identified AI-aided predictive modeling and real-time streaming facilitated by 5G, while threats included cybersecurity exposure and fluctuating global regulations. To make findings practically relevant, these were cross-checked with seven mining industry experts through semi-structured interviews, focusing on actual-world implementation issues. Interview findings were utilized as an industry validation for this research.

4. Results and discussion

The results are discussed in five main sections starting with systematic literature review addressing the research questions followed by meta-analysis, Bibliometric analysis, SWOT analysis, and industry survey.

4.1. Systematic review

Accurate measurement is the core of sciences behind mining and geotechnical engineering. For centuries, this relied on the meticulous work of surveyors with theodolites and tripods [71]. There is a revolution in technology currently underway with UAVs, or drones, revolutionizing volumetric analysis and terrain modeling [72-75]. This is founded on unparalleled efficiency and enhanced safety, while providing accuracy that matches the demanding standards of modern industrial uses. The greatest advantage of drone surveying is its efficiency in terms of economy, time and safety [76, 77]. Conventional ground-based methods, using total stations or Differential GPS (DGPS), require crews to physically visit every point of interest. In a large open-pit mine or over very extensive stockpiles, this can take weeks or days of laborious work. In contrast, a drone captures the same area in several hours [78], traveling a pre-programmed grid and automatically capturing thousands of overlapping, high-resolution images [79]. Automation creates digital surface models and 3D models using photogrammetry software [80, 81]. There is a chance of minimal disruption of operations with quicker turnaround times leading to enablement of real-time data monitor [82] at site with much improved mining rate [8] and stockpile volume computations. Mining is a hazardous environment with unstable highwalls, heavy equipment, and unstable stockpiles. Measurement from such environments [83] is far riskier in nature. UAVs are a perfect application for leaching pads, dangerous areas, high and steep slopes or difficult terrain where free access is limited. Drones do not expose men to hazardous conditions on site which greatly improve project safety during mapping and surveying [84]. This ability of drones makes them stand out as they can potentially save human lives at a much lower price compared to ground-based methods. In terms of application in industries requiring high accuracy, the accuracy of data collected from drones has paramount importance [84-86]. While traditional surveying still holds a slight edge in ultra-high-definition point measurement, the difference has narrowed by a significant margin. Modern drone platforms, especially those with RTK or PPK GPS capability and assisted by accurately positioned GCPs, are consistently delivering vertical and horizontal accuracies [87]. This is more than adequate for the majority of mining and geotechnical applications.

For critical operations such as stockpile volume calculations studies have reported drone error rates of between 0 and 3% [11], compared to 1% for conventional methods. Both fall within industry acceptable tolerance of ±3% to make drone-derived data fit for purpose. Industry practitioners and researchers have reported that the accuracy of measurement by drone is influenced by terrain, vegetation, and GCP location [1, 88, 89] but reliability of outputs remains sufficient for operational decision making. Open-pit mines, quarries, slopes, and spoil piles are where drones are best applied, with the ability to image large areas very rapidly being a perfect match for operational needs. They are seeing increased use in geotechnical engineering for slope monitoring, erosion studies, and project monitoring [90, 91]. Notably, drones are typically synergistically coupled with traditional methods [92], providing macro-context with ground-truthed micro-details.

Drone technology application is a quantum leap for the field of geotechnincal and mining engineering. It shatters the traditional trade-off between accuracy and efficiency, with improved safety, accessibility, and rapid data acquisition without compromising accuracy [9, 93, 94]. As sensor technology, LiDAR, and artificial intelligence evolve, the use and usefulness of drones in challenging and complex environments should expand. Drone surveys are also susceptible, to compounding sources of error [95, 96], which is absent in traditional surveying. Incorrect placement of GCPs, poor satellite visibility, or multipath effects can undermine positional accuracy [88]. Inadequate flight planning like an incorrect altitude or insufficient image overlap can reduce model resolution and introduce errors [97]. Severe winds, variable lighting, and difficult terrain (i.e., highly reflective or featureless surfaces) are also environmental conditions that affect data quality. Software processing choices also affect volumetric outputs, and these need to be firmly verified with independent checkpoints [98, 99]. At the core of UAV-based remote sensing is the decision between LiDAR and photogrammetry, each with its own particular strengths. Higher precision is achievable with LiDAR technology with the ability to penetrate vegetation cover [100] and create models. The LiDAR systems provide laser pulses at high speed which offers accurate results and is immune to light conditions, thus suitable for operation in the shade or underground application. Such systems as expensive computationally and otherwise as the payload requirements are huge making them suitable for employment in mega projects. In contrast, photogrammetry builds three-dimensional models by mosaicking overlapping high-resolution images [100] taken from multiple perspectives. Photogrammetry is superb for generating photorealistic site models and is economically viable [101] for use cases such as monitoring haul road surfaces, stockpile inventory volumes, and structural inspections. Some limitations of photogrammetry are its lighting-sensitiveness [102], it cannot penetrate in dense vegetation [100], and it may be less accurate in elevation modeling, particularly in regions of complex terrain [89].

Sensor selection is the starting point, while flight planning is essential for data quality. The main parameters are flying height, speed, image overlap, and direction [103]. Good stereo reconstruction with improved resolution is ensured by sufficient overlapping (80% front and 60% side), reduced ground sample distance (GSD), and lower flying heights. Elevation accuracy is greatly improved for complex terrains by adaptive flight planning [104]. Without such planning, even the most sophisticated sensors can yield suboptimal data. Data fusion is emerging as a frontier in UAV application. The integration of LiDAR point clouds with photogrammetric textures, thermal imaging, or multispectral data enhances visualization and quantitative analysis together [105, 106]. Accelerated data processing can be achieved by using RTK or PPK systems [89] which may eliminate requirement for many GCPs. Now it does not take too much time to assess slope stability or stockpile volume or generate a map thanks to the cloud-based systems and automation. Drones offer an extremely powerful means of volumetric surveying with unmatched speed and safety. Nevertheless, they require rigorous mission planning, flight, and data verification to balance intrinsic inaccuracies. If used correctly, not only do they enhance surveying but also contribute to a safer, more efficient, and data-driven mining industry.

4.2. Meta-analysis

Figure 2 presents a summary of several studies involving UAV photogrammetry and LiDAR for topographic modeling and the reported mean errors. The reported accuracies by results are significantly diverse, ranging from 0.00 m to 0.45 m mean error. Such extreme diversity indicates that achievable accuracy significantly depends upon sensor orientation, flight conditions, terrain characteristics, and data processing techniques.

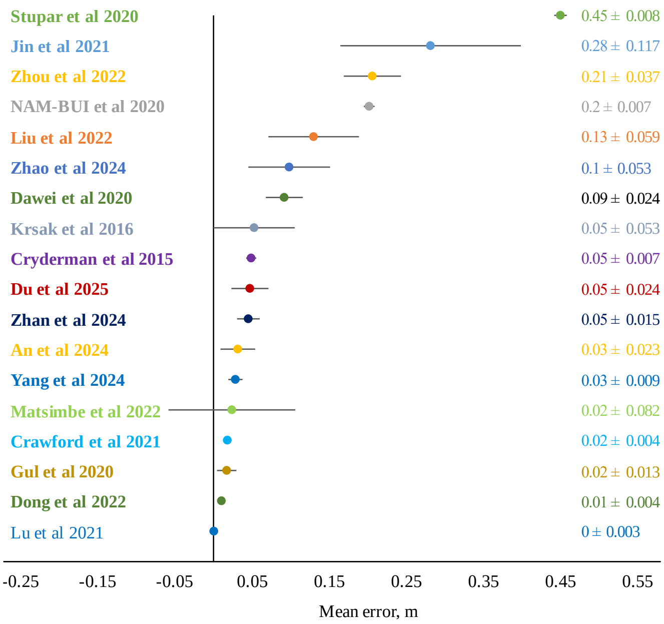

Figure 2. Forest plot showing mean errors as reported in multiple studies available from literature [108-110, 112-126]

An extremely high percentage of research studies achieved high accuracy with mean error below 0.05 m. Strangely enough, Lu et al. [107] reported a mean error value of 0.00 ± 0.003 m, then Dong et al. [108] at 0.01 ± 0.004 m, and Gul et al. [109] at 0.02 ± 0.013 m. This cluster of very close results with tight confidence limits is a demonstration of good methodology. These typically involve the use of high-resolution sensors with RTK/PPK GNSS integration, optimal GCP networks, and advanced SfM algorithms. There is a range in the middle which produced mean errors between 0.05 m and 0.15 m, like Zhao et al. [110] (0.10 ± 0.053 m) and Liu et al. [111] (0.13 ± 0.059 m). A complex terrain and less dense GCP network are likely the cause of obtaining a wider confidence interval. Large scale mapping of geomorphology, classification of land, environmental monitoring can accommodate small errors and low accuracies are sufficient for these applications.

The Figure shows few outliers like Stupar et al. [112] (0.45 ± 0.008 m) and Jin et al. [113] (0.28 ± 0.117 m). These high error levels reflect methodological limitations, perhaps the application of uncorrected consumer drones, poor GCP coverage, or unfavorable environmental conditions during data capture (e.g., high cover density, uniform terrain features, or lighting conditions). Such data can be sufficient for reconnaissance-level mapping but have limited application in quantitative geotechnical studies. A time-wise assessment of the results shows an apparent trend of improvement in accuracy in more recent study articles (2021-2025). This upgrade is likely the result of mass usage of RTK/PPK drones, sophisticated flight planning software, and sophisticated automated processing procedures.

This influence demonstrates UAV surveys can achieve sub-decimeter accuracy under rigorous methodology. The results verify the application of important tasks like volumetric measurements, surface deformation and creation of DEM which require higher precision. Above all, the range of accuracy noted emphasizes that accuracy is not inherent to the platform but rather under systematic survey design. Sensor calibration, image overlap, flight altitude, GCP design, and post-processing approach are essential parameters affecting outcomes. Consequently, rigorous adherence to best practices for data acquisition and processing is necessary for the use of UAVs in mission-critical mining and geotechnical operations.

Figure 3 is a pie chart representing country-level trends of publication of research with focus on the accuracy of UAV and drone technology in geotechnical engineering and mining practices. The figure indicates a highly skewed pattern of publication, which is a representation of the geopolitical imbalance in the output of research and advancement of technology. The chart clearly shows that China is the dominant research country with 55.6% of the overall production. Such dominance is a proof of China's consistent strategic leap in autonomous systems, remote sensing, and digital geotechnical methods. Such dominance justifies China's dominance in rare earth element (REE) value chains, mining digitalization, and UAV manufacturing, emphasizing a national overall direction towards technology independence and innovation in extractive industries. Contrasting Chinese dominance, the following eight nations including Canada, Slovakia, Slovenia, Vietnam, Turkey, USA, Malawi, and China & Mongolia (general category) share 5.6% of global production in research.

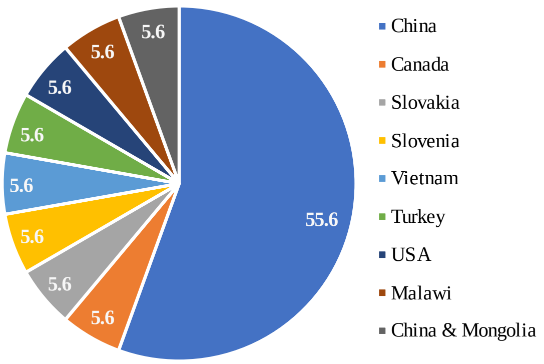

Figure 3. Pie chart showing percentage of country wise publications with China securing top slot

It is a sign of research clusters on nothing but China and others with modest yet increasing attention to precise mapping and volume calculation in mining with the help of UAVs. From the strategic point of view, this graph provides the following critical two observations:

1). Unipolarity by any nation poses risk in global knowledge exchange, standardization, and frontier transfer of technology. This has tremendous significance to mining operations based on the accuracy of UAV for environmental monitoring and regulatory compliance.

2). Having geographically and economically diverse contributors (e.g., Turkey, Vietnam, Malawi) implies untapped potential for North-South and South-South collaborations, particularly in the use of UAV technology to terrain, climatic regimes, and mineralization in their nations.

3). Overrepresentation of top mining economies (e.g., Australia, South Africa, Chile) in this dataset necessitates further bibliometric analysis and may be an indication of language limitation, unpublished industrial knowledge, or dispersed scholarly work not amounting to a recoverable quantity.

Overall, Figure 3 not only indicates variable publication levels but also reflects the need for more diversified and balanced global research setting for UAV geospatial mining applications. Multinational collaboration, sponsorship funding, and open-access publishing can accelerate innovation and render research into UAV precision vulnerable to multinational skills and field-observing contextualization.

Figure 4 shows a funnel plot summarizing the distribution of key application themes explored in UAV-based research within the mining and geotechnical engineering sectors. The data is presented as a percentage share of the total studies reviewed (N = 100% base for normalization). The five dominant themes include accuracy analysis, mining subsidence monitoring, dumpsite surveillance, stockpile volumetrics, and rock mass identification. The largest and highest portion of the funnel is "Accuracy analysis" (100%), representing the ubiquitous applicability within the literature examined. This is the fundamental nature of accuracy benchmarking in remote sensing applications, where ground-truth validation, mean error analysis, and comparison against traditional surveying methods (e.g., total stations, RTK-GNSS) are inevitable. High accuracy is the necessary prerequisite to all subsequent work such as volumetric calculation, slope analysis, or feature classification and hence the methodological pillar of UAV-based surveying.

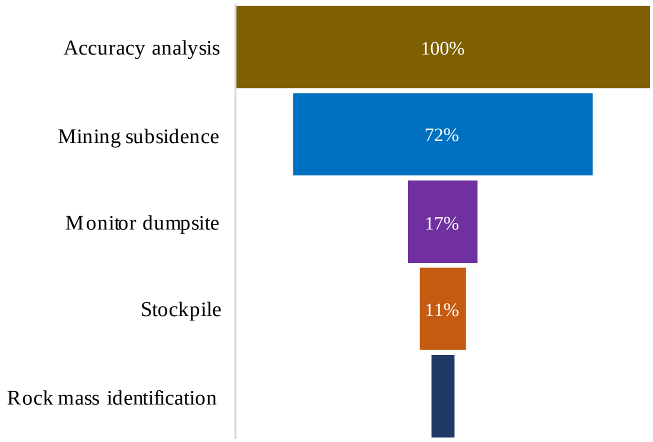

Figure 4. Funnel plot showing distribution of topics studied in the domain

This wide-ranging emphasis (e.g., Zhou et al., [114]; Jin et al., [113]), illustrate that more than 90% of mining drone applications utilize some form of geospatial accuracy validation through GCPs or advanced correction systems like PPK/RTK. The second category, accounting for 72% of research, is "Mining subsidence monitoring". Such high frequency reflects growing concern over ecological risks from surface deformation due to underground mining, particularly in coal and salt mining districts. UAVs provide regular and high-resolution orthomosaics and DSMs, allowing temporal change detection of millimeter-order ground deformation. Compared to traditional leveling or InSAR, UAVs are more adaptable and can survey larger areas, especially in mountainous or remote terrain. Examples mentioned include subsidence bowl monitoring, fault reactivation zones, and room-and-pillar mining pillar failure, indicating high usage of UAVs for geotechnical risk evaluation.

The "monitor dumpsite" has an increasing focal area but is considered as a secondary factor with 17%. There are greater geo-environmental and geotechnical challenges associated with spoil dumps, tailing storage facilities, and waste rock piles. UAVs increasingly survey slope angles, monitor erosion or storm-driven change, and aid the safe development of landforms. The low figure suggests that this can be a new field of research, possibly because dumped material needs to be discriminated from natural ground in photogrammetry, or visual clutter and surface instability problems. The other top category, "Stockpile monitoring" (11%), is unexpected in light of its crucial role in stock management and logistics. UAV-based photogrammetry estimation of stockpile volume has been demonstrated to be faster, safer, and often less expensive [9] than terrestrial laser scanning or GPS surveying. The low share of this category in the funnel is likely a result of underreporting in peer-reviewed literature since most stockpile surveys are conducted as in-house industrial practice rather than academic research. This indicates a research-to-practice gap, with a possible future standardization and publication of industrial processes. "Rock mass identification" (6%) is at the bottom of the funnel, the least researched amongst UAV applications. Its low occurrence is understandable as the technical potential of UAV photogrammetry and conventional RGB images to extract lithological heterogeneity is low. However, enhancement of sensor fusion, particularly hyperspectral and multispectral imagery, is beginning to push the horizon for remote geological mapping. Initial research has indicated promise in fracture trace mapping, joint orientation analysis, and lithological boundary definition but still remains in its infancy [127]. The low ratio presents a high-potential research frontier, especially with AI-enhanced classification algorithms for spectral and visual UAV-collected data. This funnel chart illustrates a standard "top-heavy" research distribution where anchor topics like accuracy and deformation monitoring are dominating, with less-screened operational and frontier uses lagging behind. The taper from 100% to 6% reveals an advanced-validate-but-nascent-integrate-and-innovate ecosystem of research. This trend replicates technology adoption life cycle, with lead adopters first piloting reliability (accuracy), then in particular applications (subsidence, dumps), followed by blanket application in logistics (stockpiles) and finally into cutting-edge frontiers (rock mass classification).

A multi-dimensional comparison of UAV research applications in geotechnical engineering and mining was conducted with a bubble chart visualization (Figure 5) that integrates three prominent metrics: the amount of data points collected (study volume, x-axis), Root Mean Square Error (RMSE, accuracy, y-axis), and research focus (bubble size). The integrated strategy reveals distinct patterns of research investment and performance for five prominent application areas (Figure 4). The Mining Subsidence Monitoring application has the largest data volume (>250 points) and largest research footprint (largest bubble size), and hence is the most researched application. However, it also has the largest RMSE in all categories (~0.12 m). This combination suggests large-scale use because of regulatory and security requirements in underground mining regions but also indicates significant technical challenges.

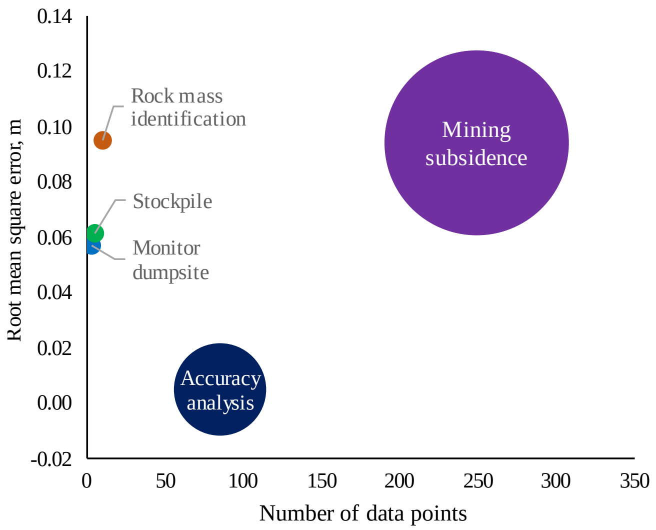

Figure 5. Bubble plot showing multi-parameters including RMSE, number of data points and number of studies on a particular topic

The high error is likely caused by complexity of terrain, ongoing surface deformation, vegetation disturbance, and low-contrast surfaces, all of which interact to make change detection as well as accurate elevation modeling more challenging. These findings emphasize the need for urgent methodological advances, such as multi-sensor data fusion (e.g., fusion of LiDAR and photogrammetry) and better ground control, to achieve higher measurement accuracy in this socially and operationally significant application.

On the other hand, "Accuracy Analysis" research mirrors the highest precision with a very low RMSE of ~0.005 m, in addition to a high volume of data (~90 points). This indicates UAV systems can utilize high precision in controlled situations under validation and benchmarking study conditions, where they are typically applied in rigorous flight planning, high GCPs, and optimized processing parameters. The wide research interest shows the academic community's desire to establish the base-level trustworthiness of UAV-based information. This field is a pivotal building block for the validation of applications in operational environments such as volumetric estimation and deformation monitoring.

The applications of "Stockpile Management" (RMSE ≈ 0.02 m) and "Dumpsite Surveillance" (RMSE ≈ 0.01 m) are both positioned in the high-accuracy, low-data-volume sector of the graph. Their high accuracy confirms that UAVs are very suitable for volumetric measurement and material monitoring in these structured environments. The relatively small bubble sizes guarantee that these applications are perfectly underreported in the literature. This discrepancy most likely results from industrial processes being monitored proprietarily and from a journal bias towards new rather than usual operational monitoring activity. The disagreement confirms a definite trajectory from mere experimentation towards broad-scale uptake, and then a potential wave of innovation again. Greater academic effort is surely an opportunity to develop and standardize automated, high-frequency monitoring pipelines for these high-value commercial applications.

Rock Mass Identification is the smallest bubble, which indicates that it is the least studied application, and it has a moderate RMSE of ~0.06 m (Figure 5). Challenges in lithology conversion here are largely due to the inherent limitations of standard RGB imagery in handling texture-poor or spectrally uniform rock surfaces, exacerbated in numerous instances by challenging lighting conditions. The modest level of error and low research effort constitute a significant opportunity for improvement. Future efforts can attempt to leverage various sensors (e.g., multispectral or thermal cameras) and new machine learning techniques for lithological classification and structural feature extraction. It is a promising area for cross-disciplinary collaboration between remote sensing, computer science, and engineering geology.

Figure 6 shows that UAV photogrammetry was the most researched method (n = 9), as it had the highest mean error at 17.11 centimeters. Such inaccuracy is most likely due to its susceptibility to environmental influences (e.g., variation of light, wind blur) and challenging processing of low-texture or vegetated surfaces. The absence of RTK or PPK georeferencing in the majority of photogrammetric processes also contributes to reduced accuracy. The findings show that while low-cost and of general utility, standard photogrammetry requires strict ground control and calibration in order to be sufficient in high-precision uses such as volumetric accounting or small-scale deformation monitoring. The blend of photogrammetry and LiDAR (UAV LiDAR Photogrammetry) delivered a much lower mean value of error at 6.11 cm. The hybrid approach takes advantage of the merits of both technologies:

– LiDAR vegetation penetration;
– height accuracy;
– photogrammetric high-resolution visual texture.

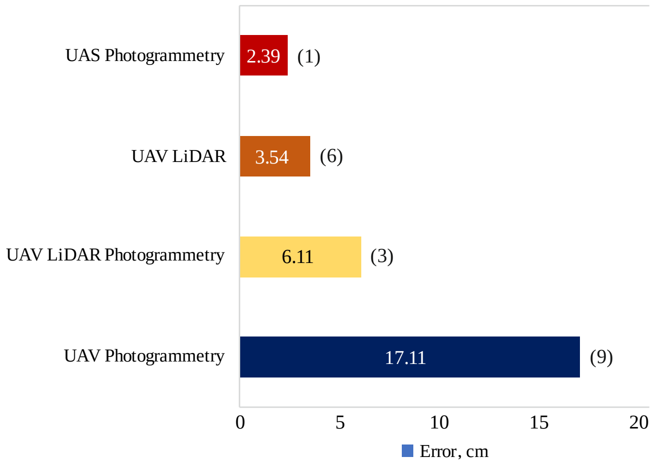

Figure 6. Comparison of error for different methods, showing UAV photogrammetry incurs greater errors

The perceived accuracy gain suggests the benefits of sensor fusion for applications that represent a trade-off between dimensional accuracy and visual information content, i.e., geotechnical change detection and early geological modeling. The lowest mean error of 2.39 cm was obtained by UAS Photogrammetry, typically larger fixed-wing systems in this case.

UAV LiDAR achieved greater accuracy with a mean error of 3.54 cm, based on results of six studies (n = 6). This performance demonstrates LiDAR's strong points, both in its independence from ambient illumination and in the generation of distortion of digital terrain models beneath complex topography. The residual error is likely to be dominated by post-processing constraints or calibration problems rather than sensor inaccuracy itself. UAV LiDAR is therefore well-suited to applications demanding high spatial precision, including engineering-grade topographic mapping and slopes stability analysis in detail. UAS Photogrammetry, which in this case typically refers to larger fixed-wing systems, had the lowest average error of 2.39 cm. This result relies on a small sample size of (n = 1) and thus lower statistical power. The high accuracy is most likely gained through optimized operating conditions, i.e., RTK-capable positioning, very stable flight, and high-resolution cameras under optimal conditions. While such results indicate potential for high accuracy using photogrammetry, reproduction in a variety of studies is required to confirm results and allow for standards of performance to be generalized. There is evidence for a consistent cost vs ease-of-use vs accuracy trade-off. Photogrammetry remains popular with lower cost and high-resolution visual outputs, yet unpredictable accuracy demands rigorous methodological planning. LiDAR-based methods, being more costly, yield a much improved and uniform level of accuracy. The future focus areas can include sensor fusion to achieve high precision, also optimization studies for UAS platforms will be helped by standard workflows and a vide validation across mining and geotechnical fields and environment.

4.3. Bibliometric & thematic analysis

The pattern of publications over the period from 2010 to 2025 reflects distinct phases of technological and academic progress in the application of UAVs in geotechnical engineering and mining (Figure 7). The disagreement confirms a definite trajectory from mere experimentation towards broad-scale uptake, and then a potential wave of innovation anew.

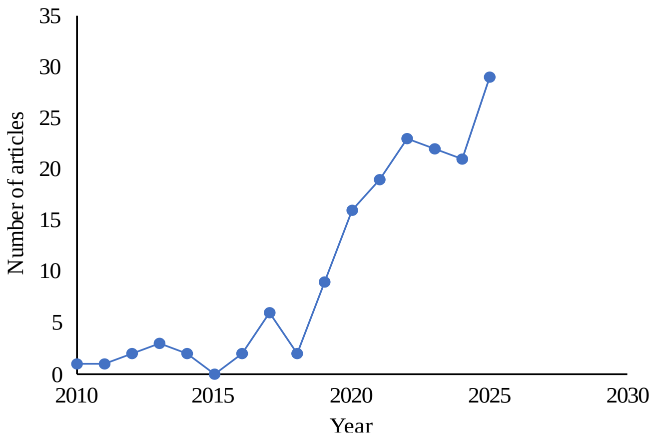

Figure 7. Publication trend over the years showing that the UAV research is increasing tremendously owing to the accessibility of the equipment lately

The first or infancy period of UAV technology is clearly from 0 to 4 annual publications which is considered as a low productivity range. This can be attributed to uncertainties, some developments in technology and commercial immaturity. Research during this period was largely exploratory and consisted of isolated feasibility studies and early case reports. There was a definite point of inflection observed between 2017 and 2019, with annual publication numbers rising from 1 to 9. This growth is coincident with significant developments in UAV affordability, platform stability, and commercial availability of integrated sensors (i.e., photogrammetric, LiDAR, and thermal cameras). The focus of research shifted from fundamental feasibility to applied validation, with studies demonstrating utility in stockpile volumetrics, slope stability monitoring, and high-resolution topographic mapping. Stronger academia-industry partnerships helped with increased pilot deployments. The publications count becomes three times between the year 2019 to 2022. Two factors can be attributed to this growth:

– the maturity of AI-based data processing software for point cloud classification and feature detection;

– COVID-19-induced accelerated uptake of remote monitoring solutions.

The technology is being translated into a valuable geospatial application for industrial and research use. There is a plateau of publication numbers, levelling out at a figure of about 21-23 papers each year, from 2022 to 2024. This would suggest a phase of methodological consolidation and maturity. The research focus would appear to have changed from demonstrating potential for application to improving accuracy, optimizing workflows, and incorporating UAV-derived data into more comprehensive mine planning and management systems, including early digital twin systems.

A record high of 29 publications in the year 2025 (till october) suggests a new era of innovation. This peak is likely the result of innovations in multi-sensor fusion (e.g., hyperspectral LiDAR), novel applications such as underground mine mapping and predictive subsidence modeling, and the integration of UAV data into large-scale digital twin systems. Such a peak would also be driven by increasing regulatory and societal pressure for sustainable mining activities, for which UAVs offer affordable monitoring solutions.

Figure 8 presents the publication pattern of academic papers by their funders, indicating the dominant status of Chinese funding institutions in sponsoring geospatial and UAV studies.

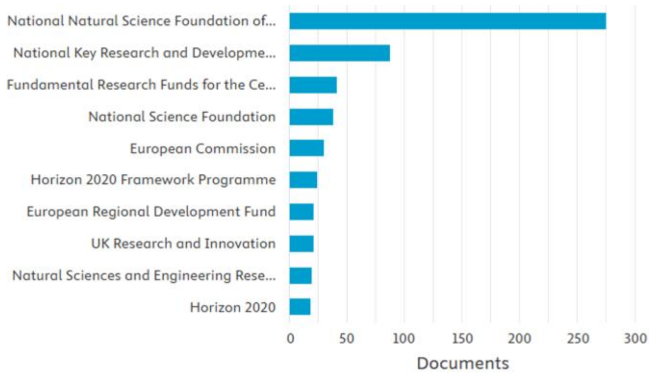

Figure 8. Distribution of scholarly documents by their funding sponsors highlighting the research focus of various organizations and countries

The NNSFC is the dominant one with nearly 300 funded articles, followed by the National Key Research and Development Program of China with about 90 articles. Other Chinese sources, such as the Fundamental Research Funds for the Central Universities, also contribute significantly. On the other hand, the international funders, such as the U.S. National Science Foundation, European Commission, and Horizon 2020 Framework Programme, sponsor relatively fewer documents (between 20 to 50 each). This distribution is proof of China's strategic investment in scientific research in such areas as remote sensing, UAV technology, and geotechnical applications and a reflection of its global leadership position in research output in these fields.

Figure 9 generated using VOSviewer, is a visualization of a co-authorship network of researchers in the field of UAV-based surveying and geotechnical applications. Every node is one author, and the edges between them indicate co-authored papers. The colors indicate different collaboration groups or research teams.

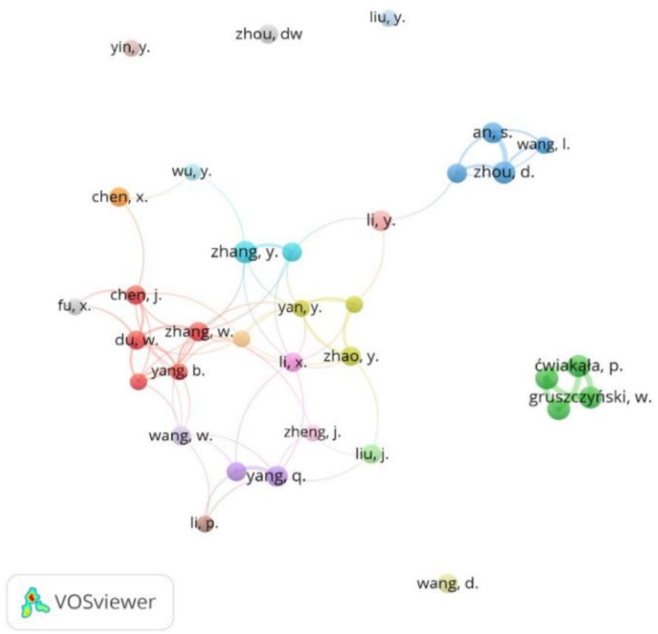

Figure 9. Co-authorship network visualization of researchers working in the domain showing very little collaboration in UAV research

Several highly connected clusters can be seen, which suggests extensive intra-group collaboration most significantly between Chinese researchers (center-left), which possesses the largest network, indicating high output as well as collaborative work. Another green cluster on the right is separate and smaller, representing European authors such as Ćwiakąła, Pawel [128] and Gruszczyński [129], with distribution at regional level. Individual authors such as Yin, [130] and Zhou [114, 131] continue to be isolated at the periphery, reflecting a weak collaborative link in this data set. This visualization is highlighting cross-institutional and cross-country coordination to facilitate innovation in UAV geotechnical research.

Figure 10 illustrates a keyword co-occurrence network visualization developed using VOSviewer, displaying the thematic context of UAV research in the geotechnical and mining sector.

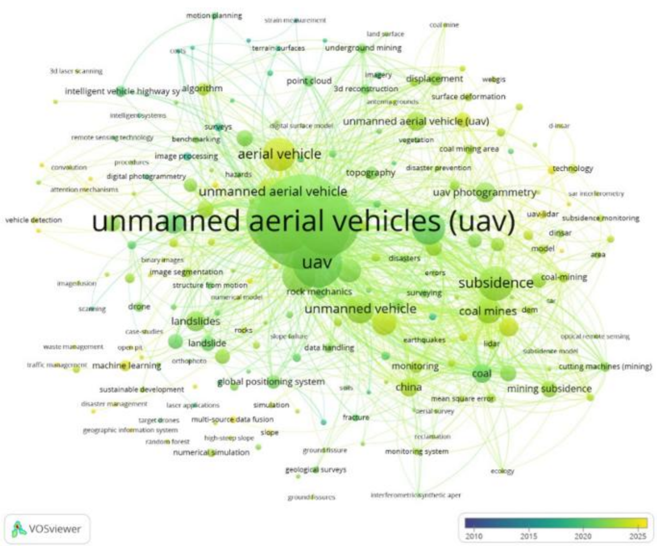

Figure 10. Keyword co-occurrence network visualization showing joint core concepts, topics, and ideas of the researchers in UAV research relevant to geotechnical and mining fields

The size of each node is based on how often the keyword is used in the literature, while the closeness and thickness of the lines connecting them are based on the intensity of keyword co-occurrence.

The central dominance of words "unmanned aerial vehicles (UAV)", "UAV photogrammetry", "subsidence", and "coal mining" indicates that the majority of academic focus is on UAV applications in subsidence monitoring in mining, terrain modeling, and safety inspection. Peripheral clusters reveal closely related subtopics such as "LiDAR", "monitoring system", "GPS", and "machine learning", indicating new intersections between UAV technology, spatial analysis, and AI-based analytics.

Purple to yellow-green color gradation shows temporal development of research interest, demonstrating that terms like "subsidence monitoring", "3D reconstruction", and "laser scanning" have been increasing during the past five years (2020-2025). Overall, this map shows a dynamic multidisciplinary development of UAV-based mining research with huge potential for further innovations in precision surveying and geotechnical monitoring.

4.4. SWOT Analysis of UAV adoption

4.4.1. Strengths

The most widely accepted strength of UAVs is their spectacular reduction in data collection time. Many authors [132, 133] indicated UAVs are "much faster and more efficient", making weekly or even daily monitoring of sites possible, which is not feasible by conventional means [134].

Figure 11. SWOT analysis highlighting key features

One of the best features of these equipment are they remove human exposure to a dangerous or hazardous areas such as steep slopes [9], fires, waste dumps, accident or harmful radiation sites. The zero harm goal of the industry is clearly targeted through the UAV use in mines and geotechnical sites. The major researches found UAVs to be "much more cost-effective", driven by reduced labor expenses, reduced site downtime, and the ability to conduct surveys with a small team. UAV photogrammetry not only generates point data but also rich, visually appealing outputs like 3D digital surface models (DSMs), and digital terrain models (DTMs) that are extremely valuable for visualization, planning, and stakeholder management.

4.4.2. Weaknesses

The most commonly cited technical challenge is "data processing and software" [135, 136]. Handling high amounts of data requires significant computational capacity and sophistication [137], thus adding latency between data acquisition and knowledge actionable enough to inform key decisions. This indicates that accuracy is very susceptible to operator experience, equipment quality (e.g., RTK/PPK GPS), and processing technique [89, 138]. The technology creates a "skill gap" which means operators must be skilled in flight planning, data processing, and spatial analysis beyond the task of a traditional surveyor. Mohsan et al. [10] identified "skill gaps or deficiency in trained manpower" as the biggest problem. Another challenge is the limited penetration capabilities of the standard photogrammetry through vegetation [100] to model the bare earth surface. This is considered as a key flaw in exploration or forested regions.

4.4.3. Opportunities

Besides RGB cameras, integration of data from LiDAR (vegetation penetration and accurate height), multispectral/hyperspectral (detection of minerals) and thermal sensors (machine monitoring) [139] can be achieved in developing a more comprehensive digital twin of the site [140]. Machine learning processes can be utilized to process UAV data automatically for specific applications [141, 142], such as automatic crack detection in slopes, stockpile volume measurement, and time-series change detection, reducing the processing bottleneck. Autonomous mapping of underground mines using small and collision-free UAVs is an enormous growth prospect and renders such perilous spaces safer [143]. UAV designs provide the perfect spatial configuration for the development of dynamic digital twins of mines with real-time observation and simulation through sensor network integration.

4.4.4. Threats

This is the most significant external risk. MCTegg [144] described regulations as "Very significant", mentioning problems with flight permissions and airspace rules. This adds bureaucratic overhead, can decelerate missions, and fluctuates enormously by geography, making operations for firms operating in numerous jurisdictions difficult. The facts clearly indicate two settings where UAVs are least efficient:

1). Steep slopes and highwalls disrupt GPS signals and is usually the very spot that most need to be monitored for safety reasons, and it is a highly dangerous data shortage.

2). Traditional photogrammetry cannot photograph ground cover below the canopy and thus limits its use in woodland exploration or mines.

"Weather conditions" (rain, high winds, fog) are the primary technical problem [145, 146]. Weather conditions that will not ground a traditional survey team will frequently cancel UAV flights, and thus it can lead to delay in acquiring important information. The ease of gathering information will provide surveys being conducted without any particular intent, creating massive amounts of information that are never actually examined or converted into actionable business intelligence, watering down the value proposition.

4.4.5. Industry validation survey results

To cross-check the meta-analysis trends against current industry practice, a customized survey was circulated among practitioners with direct experience in applying UAV technology to mining and geotechnical projects. The survey attempted to quantify the opinions regarding the key areas: application prevalence, adoption level, performance metrics (accuracy, efficiency, cost), and operational challenges. The target sample was 33 practicing engineers, consultants, researchers, and technicians worldwide, selected on the basis of confirmed project experience. Seven full responses were returned, a return rate of 21.2%. Although small in number, the group of returners is specialist and expert, and their contribution represents a qualitative, expert-laid understanding of the practice situation. Collectively, they provide a necessary reality check for the verification of the wider trends in the literature.

The survey confirmed the meta-analysis finding that topographic modeling is the dominant application of UAVs in this industry, as it was cited by 85.7% of the respondents as a significant application. Stockpile volume estimation was second with a rate of 14.3%. With regard to integration with existing workflows, the results exhibit a strong paradigm shift with a combined 85.7% of practitioners confirmed UAVs have 'significantly replaced' (71.4%) or 'fully replaced' (14.3%) traditional surveying methods, whereas a minority (14.3%) regard them as complementary. This reinforces the meta-analysis observation of UAVs having shifted from an emerging tool to a cornerstone operation technology. A strong contrast between perceptions of data accuracy and perceptions of operational efficiency existed. All across the board (100%), the interviewee respondents vows that UAV-based techniques are much faster and require fewer people than traditional surveys. Efficiency has a straightforward effect on perceived savings in cost, with 85.7% of the respondents answering that UAVs are 'fairly more' or 'much more' cost-saving. Perceptions of accuracy were highly polarized and a point of disagreement. Nearly half of the respondents (42.9%) placed UAV-based information as less accurate than traditional survey methods, and the same percentage placed them in bulk as being equivalent (28.6%) or better (28.6%). This gap represents a huge discrepancy between technical accuracy reported in controlled studies of the meta-analysis and its observed place in typical field operations.

The survey also provided insightful comment on the actual-world impediments to UAV uptake, confirming and prioritizing issues which have been identified within the literature. The greatest technical barrier was software and data handling, at 71.4% of the sample. This identifies an obvious bottleneck that exists from data gathering through to handling and interpretation. In addition, respondents provided specific environmental and regulatory constraints. Steep slopes and highwalls (57.1%) and vegetation-laden areas (42.9%) were found to be the most challenging terrain to use UAVs. Finally, regulation systems were also considered a most critical factor where 42.9% and 57.1% of the population considered regulations as a 'very crucial' and 'somewhat crucial' obstacle respectively. The survey results significantly support the meta-analysis inferences of widespread application of UAVs rooted in unparalleled efficiency and cost-effectiveness. More importantly, they provide an able practitioner-based wisdom that refines the literature. They confirm that the largest concerns are now no longer concerned with technology viability per se but with how it is integrated, namely, perceived correctness verification, data procedures, and operation performance under challenging terrains and regulations. The findings redirect future development needs away from hardware design to applications software, standardized practices for correctness verification, and regulatory convergence.

5. Conclusions

This review integrates much more extensively the state-of-the-art in UAV technology application in mining and geotechnical engineering comprehensively, closing knowledge gaps based on an integrated multi-fethod research design that includes meta-analysis, bibliometric mapping, SWOT analysis, and industry confirmation. Clearly, the findings reveal how UAV technology has evolved from an innovative prospecting aid to a critical component of the digital mine and the ways in which data gathering operations have changed. The primary conclusion is that UAVs are able to successfully overcome the age-old trade-off between accuracy, efficiency, and safety. While the traditional survey methods maintain a narrow edge for highest-inaccuracy point measurement, the meta-analysis has shown that modern UAV platforms, particularly when equipped with RTK or PPK technology combined with strict ground control, are able to provide sub-decimeter accuracy. This level of precision, where faults are generally less than 0.05 meters, is highly adequate for the vast majority of industry applications, e.g., stockpile volumetrics, where faults will typically be comfortably within the industry-acceptable range of ±3%. Above all else, this accuracy comes at quick speeds, compressing data gathering time to hours from weeks and minimizing human exposure to hazardous conditions such as collapsing highwalls, active pit walls, and tailings storage facilities.

Bibliometric analysis shows an accelerating discipline with uncontrolled rates of publication after 2017, suggesting a redirection from proof-of-concept experiments towards widespread applications. But it is geographically localized expansion, and China dominates study production, simultaneously potentially undermining diversified knowledge production and providing a potential incentive for even more globalized coordination. Thematic analysis also identifies a research climate with a top-heavy, stable foundation in accuracy verification and subsidence monitoring but diminished exploration of operational applications like automated stockpile management and frontier topicality like AI-based rock mass identification.

SWOT analysis and industry survey both offer a reality check to the extent that technological capability alone is not going to translate into mass success. As much as industry experts on all sides recognize the advantages of UAVs such as speed, safety, affordability, and profusion of data output, there are major hurdles in the path. The most significant problems are not sensor capabilities but operational and man-factors like computing and expertise requirement of processing data, regulatory obstacles to Beyond Visual Line of Sight (BVLOS) flight, and vulnerability to bad weather. The industry survey is consistent in that data processing is viewed as the most serious technical bottleneck, and areas with steep terrain and high vegetation remain problematic environments. Hence, future integration of UAVs is not so much technological hardware but slim automated processing streams, regulatory streamlining, and squaring the skills gap with industry-relevant training programs.

This review supports that UAV technology is a revolutionizing driver of change in geotechnical engineering and mining by paradigm shift to safer, more efficient, and data-centric operations. The technology has lived up to its potential to provide repeat, high-rate geospatial data that form the core of resource estimation, activity planning, and risk mitigation. The way forward is to validate such success by overcoming major gaps and risks outlined above, particularly through investment in automation, building human capital, and policy activism. In this way, the sector can realize the complete potential of UAVs not only to enhance productivity but also drive its operational excellence, safety, and sustainability in the age of digitization.

Author contributions

The sole author was responsible for all aspects of the study and manuscript preparation. The author has read and agreed to the published version of the manuscript.

Funding

The research was funded by King Fahd University of Petroleum and Minerals, under Early Career Research Grant project number ECR 241035.

Acknowledgements

The author acknowledges the support provided by the King Fahd University of Petroleum and Minerals, Saudi Arabia under the Deanship of Research project Early Career Research number ECR 241035.

Conflicts of interest

Author VL declared that he was Deputy Editor in Chief of the Engineering Journal of Satbayev University at the time of submission. This had no impact on the peer review process and the final decision.

Data availability statement

The original contributions presented in this study are included in the article. Further inquiries can be directed to the corresponding author.

Abbreviations

The following abbreviations are used in this manuscript:

BVLOS	Beyond Visual Line of Sight
DGPS	Differential Global Positioning System
DIB	Drone in Box
DSM	Digital Surface Model
GCP	Ground Control Points
GNSS	Global Navigation Satellite System
GPS	Global Positioning System
IMU	Inertial Measurement Unit
LiDAR	Light Detection and Ranging
NNSFC	National Natural Science Foundation of China
PPK	Post-Processed Kinematics
PRISMA	Preferred Reporting Items for Systematic reviews and Meta-Analyses
RMSE	Root Mean Square Error
RTK	Real Time Kinetics
SfM	Structure from Motion
SGM	Semi Global Matching
SLAM	Simultaneous Localization and Mapping
TLS	Terrestrial Laser Scanner
UAV	Unmanned Aerial Vehicle
UAS	Unmanned Aircraft System
TLS	Terrestrial Laser Scanner

References

[1] Zhong, W., Rasouli, S., Singh, A.K., Mohandes, S.R., Antwi-Afari, M.F., Cheung, C., Manu, P., & Agrawal, U. (2025). The adoption of UAVs for enhancing safety in construction industry: A systematic literature review. *Intelligent Infrastructure and Construction*, *1*(1), 3. https://doi.org/10.3390/iic1010003

[2] van der Meer, F.D., van der Werff, H.M.A., van Ruitenbeek, F.J.A., Hecker, C.A., Bakker, W.H., Noomen, M.F., van der Meijde, M., Carranza, E.J.M., de Smeth, J.B., & Woldai, T. (2012). Multi- and hyperspectral geologic remote sensing: A review. *International Journal of Applied Earth Observation and Geoinformation*, *14*(1), 112-128. https://doi.org/10.1016/j.jag.2011.08.002

[3] Jackisch, R., Heincke, B.H., Zimmermann, R., Sørensen, E.V., Pirttijärvi, M., Kirsch, M., Salmirinne, H., Lode, S., Kuronen, U., & Gloaguen, R. (2022). Drone-based magnetic and multispectral surveys to develop a 3D model for mineral exploration at Qullissat, Disko Island, Greenland. *Solid Earth*, *13*(4), 793-825. https://doi.org/10.5194/se-13-793-2022

[4] Kruse, F.A. (2012). Mapping surface mineralogy using imaging spectrometry. *Geomorphology*, *137*(1), 41-56. https://doi.org/10.1016/j.geomorph.2010.09.032

[5] Kirsch, M., Lorenz, S., Zimmermann, R., Tusa, L., Möckel, R., Hödl, P., Booysen, R., Khodadadzadeh, M., & Gloaguen, R. (2018). Integration of terrestrial and drone-borne hyperspectral and photogrammetric sensing methods for exploration mapping and mining monitoring. *Remote Sensing*, *10*(9), 1366. https://doi.org/10.3390/rs10091366

[6] Bemis, S.P., Micklethwaite, S., Turner, D., James, M.R., Akciz, S., Thiele, S.T., & Bangash, H.A. (2014). Ground-based and UAV-based photogrammetry: A multi-scale, high-resolution mapping tool for structural geology and paleoseismology. *Journal of Structural Geology*, *69*, 163-178. https://doi.org/10.1016/j.jsg.2014.10.007

[7] Minh, D.T., & Dung, N.B. (2023). Applications of UAVs in mine industry: A scoping review. *Journal of Sustainable Mining*, *22*(2), 128-146. https://doi.org/10.46873/2300-3960.1384

[8] Shrivastava, A. (2025). Unmanned aerial vehicles (UAV) in mining sector: Enhancing productivity and safety. *Proceedings of the Institution of Mechanical Engineers, Part G: Journal of Aerospace Engineering*, *239*(15), 2219-2235. https://doi.org/10.1177/09544100251352429

[9] Tsachouridis, S., Pavloudakis, F., Sachpazis, C., & Tsioukas, V. (2025). Monitoring slope stability: A comprehensive review of UAV applications in open-pit mining. *Land*, *14*(6), 1193. https://doi.org/10.3390/land14061193

[10] Mohsan, S.A.H., Khan, M.A., Noor, F., Ullah, I., & Alsharif, M.H. (2022). Towards the unmanned aerial vehicles (UAVs): A comprehensive review. *Drones*, *6*(6), 147. https://doi.org/10.3390/drones6060147

[11] Alsayed, A., & Nabawy, M.R.A. (2023). Stockpile volume estimation in open and confined environments: A review. *Drones*, *7*(8), *537*. https://doi.org/10.3390/drones7080537

[12] Tysiąc, P., Moskalewicz, D., & Janowski, Ł. (2025). Development of UAV-based LiDAR and multispectral measurement techniques for monitoring sediment intrusion in coastal wetlands. *Measurement*, *253*, 117459. https://doi.org/10.1016/j.measurement.2025.117459

[13] Dadrass Javan, F., Samadzadegan, F., Toosi, A., & van der Meijde, M. (2025). Unmanned aerial geophysical remote sensing: A systematic review. *Remote Sensing*, *17*(1), 110. https://doi.org/10.3390/rs17010110

[14] Wanner, D., Hashim, H.A., Srivastava, S., & Steinhauer, A. (2024). UAV avionics safety, certification, accidents, redundancy, integrity, and reliability: A comprehensive review and future trends. *Drone Systems and Applications*, *12*, 1-23. https://doi.org/10.1139/dsa-2023-0091

[15] Dlamini, S.M., & Ouma, Y.O. (2025). Large-scale topographic mapping using RTK-GNSS and multispectral UAV drone photogrammetric surveys: Comparative evaluation of experimental results. *Geomatics*, *5*(2), 25. https://doi.org/10.3390/geomatics5020025

[16] Perera, G.S.N., & Nalani, H.A. (2022). UAVs for a complete topographic survey. *The International Archives of the Photogrammetry, Remote Sensing and Spatial Information Sciences*, *XLIII-B2-2022*, 441-447. https://doi.org/10.5194/isprs-archives-XLIII-B2-2022-441-2022

[17] Park, S., & Choi, Y. (2020). Applications of unmanned aerial vehicles in mining from exploration to reclamation: A review. *Minerals*, *10*(8), 663. https://doi.org/10.3390/min10080663

[18] Leitão, J.P., Moy de Vitry, M., Scheidegger, A., & Rieckermann, J. (2016). Assessing the quality of digital elevation models obtained from mini unmanned aerial vehicles for overland flow

modelling in urban areas. *Hydrology and Earth System Sciences, 20*(4), 1637-1653. https://doi.org/10.5194/hess-20-1637-2016

[19] Dai, S., Wei, G., & Liang, B. (2021). Influence of control point number on UAV low-altitude photogrammetry and its application: A case study in subsidence monitoring of a tailing dam area in northwestern China. *The Chinese Journal of Geological Hazard and Control, 32*(5), 113-120. https://doi.org/10.16031/j.cnki.issn.1003-8035.2021.05-14

[20] Dai, W., Hu, J., Wang, B., Fan, M., Zhou, Y., & Zhang, M. (2024). Effects of digital elevation model resolution on unmanned aerial vehicle-based topographic change detection in human-altered landscapes. *Drones, 8*(11), 610. https://doi.org/10.3390/drones8110610

[21] Curcio, A.C., Peralta, G., Aranda, M., & Barbero, L. (2022). Evaluating the performance of high spatial resolution UAV-photogrammetry and UAV-LiDAR for salt marshes: The Cádiz Bay study case. *Remote Sensing, 14*(15), 3582. https://doi.org/10.3390/rs14153582

[22] Ostermann, L., Gobachew, A., Schwung, A., & Lier, S. (2025). Planning of logistic networks with automated transport drones: A systematic review of application areas, planning approaches, and system performance. *Logistics, 9*(3), 111. https://doi.org/10.3390/logistics9030111

[23] Hasegawa, H., Sujaswara, A.A., Kanemoto, T., & Tsubota, K. (2023). Possibilities of using UAV for estimating earthwork volumes during process of repairing a small-scale forest road, case study from Kyoto Prefecture, Japan. *Forests, 14*(4), 677. https://doi.org/10.3390/f14040677

[24] Choi, Y. (2023). Applications of unmanned aerial vehicle and artificial intelligence technologies in mining from exploration to reclamation. *Minerals, 13*(3), 382. https://doi.org/10.3390/min13030382

[25] Mutovina, N., Nurtay, M., Kalinin, A., Tomilov, A., & Tomilova, N. (2025). Application of artificial intelligence and machine learning in expert systems for the mining industry: Modern methods and technologies. *International Journal of Electrical and Computer Engineering, 15*(3), 3291-3308. https://doi.org/10.11591/ijece.v15i3.pp3291-3308

[26] Giordan, D., Adams, M.S., Aicardi, I., Alicandro, M., Allasia, P., Baldo, M., De Berardinis, P., Dominici, D., Godone, D., Hobbs, P., Lechner, V., Niedzielski, T., Piras, M., Rotilio, M., Salvini, R., Segor, V., Sotier, B., & Troilo, F. (2020). The use of unmanned aerial vehicles (UAVs) for engineering geology applications. *Bulletin of Engineering Geology and the Environment, 79*(7), 3437-3481. https://doi.org/10.1007/s10064-020-01766-2

[27] Ren, H., Zhao, Y., Xiao, W., & Hu, Z. (2019). A review of UAV monitoring in mining areas: Current status and future perspectives. *International Journal of Coal Science & Technology, 6*(3), 320-333. https://doi.org/10.1007/s40789-019-00264-5

[28] Gupta, S., & Nair, S. (2023). A review of the emerging role of UAVs in construction site safety monitoring. *Materials Today: Proceedings*. Advance online publication. https://doi.org/10.1016/j.matpr.2023.03.135

[29] Bamford, T., Esmaeili, K., & Schoellig, A.P. (2021). A deep learning approach for rock fragmentation analysis. *International Journal of Rock Mechanics and Mining Sciences, 145*, 104839. https://doi.org/10.1016/j.ijrmms.2021.104839

[30] Ikeda, H., Sato, T., Yoshino, K., Toriya, H., Jang, H., Adachi, T., Kitahara, I., & Kawamura, Y. (2023). Deep learning-based estimation of muckpile fragmentation using simulated 3D point cloud data. *Applied Sciences, 13*(19), 10985. https://doi.org/10.3390/app131910985

[31] Pan, C., Tao, Q., Pei, H., Wang, B., & Liu, W. (2025). Belt conveyor idler fault detection algorithm based on improved YOLOv5. *Scientific Reports, 15*, 1926. https://doi.org/10.1038/s41598-024-81244-x32.

[32] Ćwiąkała, P., Gruszczyński, W., Stoch, T., Puniach, E., Mrocheń, D., Matwij, W., Matwij, K., Nędzka, M., Sopata, P., & Wójcik, A. (2020). UAV applications for determination of land deformations caused by underground mining. *Remote Sensing, 12*(11), 1733. https://doi.org/10.3390/rs12111733

[33] Hartley, R.J.A.L., Henderson, I.L., & Jackson, C.L. (2022). BVLOS unmanned aircraft operations in forest environments. *Drones, 6*(7), 167. https://doi.org/10.3390/drones6070167

[34] Politi, E., Panagiotopoulos, I., Varlamis, I., & Dimitrakopoulos, G. (2021). A survey of UAS technologies to enable beyond visual line of sight (BVLOS) operations. *Proceedings of the 7th International Conference on Vehicle Technology and Intelligent Transport Systems (VEHITS 2021), 1*, 505-512. https://doi.org/10.5220/0010446905050512

[35] Qasim, N.H., & Jawad, A.M. (2024). 5G-enabled UAVs for energy-efficient opportunistic networking. *Heliyon, 10*(12), e32660. https://doi.org/10.1016/j.heliyon.2024.e32660

[36] Vishweshwaran, M., & Sujatha, E.R. (2025). A review on applications of drones in geotechnical engineering. *Indian Geotechnical Journal, 55*(3), 2091-2105. https://doi.org/10.1007/s40098-024-01071-9

[37] Jackisch, R. (2020). Drone-based surveys of mineral deposits. *Nature Reviews Earth & Environment, 1*(4), 187. https://doi.org/10.1038/s43017-020-0042-1

[38] Shahmoradi, J., Talebi, E., Roghanchi, P., & Hassanalian, M. (2020). A comprehensive review of applications of drone technology in the mining industry. *Drones, 4*(3), 34. https://doi.org/10.3390/drones4030034

[39] Andresen, C.G., & Schultz-Fellenz, E.S. (2023). Change detection applications in the Earth sciences using UAS-based sensing: A review and future opportunities. *Drones, 7*(4), 258. https://doi.org/10.3390/drones7040258

[40] Perikleous, D., Margariti, K., Velanas, P., Sáez Blázquez, C., & González-Aguilera, D. (2025). Aerial drones for geophysical prospection in mining: A review. *Drones, 9*(5), 383. https://doi.org/10.3390/drones9050383

[41] Hussain, Y., Schlögel, R., Innocenti, A., Hamza, O., Iannucci, R., Martino, S., & Havenith, H.B. (2022). Review on the geophysical and UAV-based methods applied to landslides. *Remote Sensing, 14*(18), 4564. https://doi.org/10.3390/rs14184564

[42] Chen, B., Maurer, J., & Gong, W. (2025). Applications of UAV in landslide research: A review. *Landslides, 22*(9), 3029-3048. https://doi.org/10.1007/s10346-025-02547-2

[43] Arif, A., Zhang, C., Feng, M., Sajib, M.H., Habibullah, M., Hasan, S., Rana, M.S., Mohammadamini, K., Alip, M., & Zhang, Y. (2025). Mining-induced subsidence predicting and monitoring: A comprehensive review of methods and technologies. *Geotechnical and Geological Engineering, 43*(7), 314. https://doi.org/10.1007/s10706-025-03271-3

[44] Takasu, T., & Yasuda, A. (2009). Development of the low-cost RTK-GPS receiver with an open source program package RTKLIB. *Proceedings of the International Symposium on GPS/GNSS* (1-6). https://gpspp.sakura.ne.jp/paper2005/isgps_2009_rklib.pdf

[45] Eling, C., Wieland, M., Hess, C., Klingbeil, L., & Kuhlmann, H. (2015). Development and evaluation of a UAV based mapping system for remote sensing and surveying applications. *The International Archives of the Photogrammetry, Remote Sensing and Spatial Information Sciences, XL-1/W4*, 233-239. https://doi.org/10.5194/isprsarchives-XL-1-W4-233-2015

[46] Teunissen, P.J.G. (1995). The least-squares ambiguity decorrelation adjustment: A method for fast GPS integer ambiguity estimation. *Journal of Geodesy, 70*(1-2), 65-82. https://doi.org/10.1007/BF00863419

[47] Lowe, D.G. (2004). Distinctive image features from scale-invariant keypoints. *International Journal of Computer Vision, 60*(2), 91-110. https://doi.org/10.1023/B:VISI.0000029664.99615.94

[48] Triggs, B., McLauchlan, P.F., Hartley, R.I., & Fitzgibbon, A.W. (2000). Bundle adjustment - A modern synthesis. *Vision algorithms: Theory and practice*, 298-372. https://doi.org/10.1007/3-540-44480-7_21

[49] Furukawa, Y., & Ponce, J. (2010). Accurate, dense, and robust multiview stereopsis. *IEEE Transactions on Pattern Analysis and Machine Intelligence, 32*(8), 1362-1376. https://doi.org/10.1109/TPAMI.2009.161

[50] James, M.R., Robson, S., & Smith, M.W. (2017). 3-D uncertainty-based topographic change detection with structure-from-

motion photogrammetry: Precision maps for ground control and directly georeferenced surveys. *Earth Surface Processes and Landforms*, *42*(12), 1769-1788. https://doi.org/10.1002/esp.4125

[51] Glennie, C. (2007). Rigorous 3D error analysis of kinematic scanning LIDAR systems. *Journal of Applied Geodesy*, *1*(3), 147-157. https://doi.org/10.1515/jag.2007.017

[52] Habib, A.F., Kersting, A.P., Shaker, A., & Yan, W.-Y. (2011). Geometric calibration and radiometric correction of LiDAR data and their impact on the quality of derived products. *Sensors*, *11*(9), 9069-9097. https://doi.org/10.3390/s110909069

[53] Besl, P.J., & McKay, N.D. (1992). A method for registration of 3-D shapes. *IEEE Transactions on Pattern Analysis and Machine Intelligence*, *14*(2), 239-256. https://doi.org/10.1109/34.121791

[54] Biber, P., & Straßer, W. (2003). The normal distributions transform: A new approach to laser scan matching. *Proceedings 2003 IEEE/RSJ International Conference on Intelligent Robots and Systems (IROS 2003)*, *3*, 2743-2748. https://doi.org/10.1109/IROS.2003.1249285

[55] Zhang, J., & Singh, S. (2014). LOAM: Lidar odometry and mapping in real-time. *Robotics: Science and Systems X*. Robotics: Science and Systems Foundation. https://doi.org/10.15607/RSS.2014.X.007

[56] Groves, P.D. (2013). *Principles of GNSS, inertial, and multisensor integrated navigation systems* (2nd ed.). Artech House.

[57] Coveney, S., & Roberts, K. (2017). Lightweight UAV digital elevation models and orthoimagery for environmental applications: Data accuracy evaluation and potential for river flood risk modelling. *International Journal of Remote Sensing*, *38*(8-10), 3159-3180. https://doi.org/10.1080/01431161.2017.1292074

[58] Rehak, M., & Skaloud, J. (2015). Fixed-wing micro aerial vehicle for accurate corridor mapping. *ISPRS Annals of the Photogrammetry, Remote Sensing and Spatial Information Sciences*, *II-1/W1*, 23-31. https://doi.org/10.5194/isprsannals-II-1-W1-23-2015

[59] Chung, S.-J., Paranjape, A.A., Dames, P., Shen, S., & Kumar, V. (2018). A survey on aerial swarm robotics. *IEEE Transactions on Robotics*, *34*(4), 837-855. https://doi.org/10.1109/TRO.2018.2857475

[60] Wang, W., Zhang, Q., Hu, Y., Gallay, M., Zheng, W., & Guo, J. (2025). Recent advances in SLAM for degraded environments: A review. *IEEE Sensors Journal*, *25*(15), 27898-27921. https://doi.org/10.1109/JSEN.2025.3584218

[61] Sarkar, M., & Sahoo, P.K. (2024). Leveraging edge computing for video data streaming in UAV-based emergency response systems. *Sensors*, *24*(15), 5076. https://doi.org/10.3390/s24155076

[62] Liu, S., Jiang, S., Liu, Y., Xue, W., & Guo, B. (2022). Efficient SfM for large-scale UAV images based on graph-indexed BoW and parallel-constructed BA optimization. *Remote Sensing*, *14*(21), 5619. https://doi.org/10.3390/rs14215619

[63] Zhang, X., & Xie, Z. (2018). Reconstructing 3D scenes from UAV images using a structure-from-motion pipeline. *2018 26th International Conference on Geoinformatics*, 1-6. https://doi.org/10.1109/GEOINFORMATICS.2018.8557153

[64] Bergado, J.R., & Nex, F. (2025). UnDER: Unsupervised dense point cloud extraction routine for UAV imagery using deep learning. *Remote Sensing*, *17*(1), 24. https://doi.org/10.3390/rs17010024

[65] Jannati, H., Valadan Zoej, M.J., Ghaderpour, E., & Mazzanti, P. (2025). Dense matching with low computational complexity for disparity estimation in the radargrammetric approach of SAR intensity images. *Remote Sensing*, *17*(15), 2693. https://doi.org/10.3390/rs17152693

[66] Yin, S., Xie, D., Fu, Y., Wang, Z., & Zhong, R. (2023). Uncontrolled two-step iterative calibration algorithm for Lidar-IMU system. *Sensors*, *23*(6), 3119. https://doi.org/10.3390/s23063119

[67] Elamin, A., Abdelaziz, N., & El-Rabbany, A. (2022). A GNSS/INS/LiDAR integration scheme for UAV-based navigation in GNSS-challenging environments. *Sensors*, *22*(24), 9908. https://doi.org/10.3390/s22249908

[68] Abdelaziz, N., & El-Rabbany, A. (2023). INS/LIDAR/Stereo SLAM integration for precision navigation in GNSS-denied environments. *Sensors*, *23*(17), 7424. https://doi.org/10.3390/s23177424

[69] Page, M.J., et al.. (2021). The PRISMA 2020 statement: An updated guideline for reporting systematic reviews. *BMJ*, *372*, n71. https://doi.org/10.1136/bmj.n71

[70] van Eck, N.J., & Waltman, L. (2020). *VOSviewer manual: Manual for VOSviewer version 1.6.15*. Centre for Science and Technology Studies, Leiden University. https://www.vosviewer.com/documentation/Manual_VOSviewer_1.6.15.pdf

[71] Chrzanowski, A. (1993). Modern surveying techniques for mining and civil engineering. *Comprehensive rock engineering: Principles, practice and projects: Vol. 3. Rock testing and site characterization*, 773-809. https://doi.org/10.1016/B978-0-08-042066-0.50039-2

[72] Alias, M.F., Udin, W.S., & Piramli, M.K. (2022). High-resolution mapping using digital imagery of unmanned aerial vehicle (UAV) at quarry area, Machang, Kelantan. *IOP Conference Series: Earth and Environmental Science*, *1102*(1), 012019. https://doi.org/10.1088/1755-1315/1102/1/012019

[73] Battulwar, R., Winkelmaier, G., Valencia, J., Zare Naghadehi, M., Peik, B., Abbasi, B., Parvin, B., & Sattarvand, J. (2020). A practical methodology for generating high-resolution 3D models of open-pit slopes using UAVs: Flight path planning and optimization. *Remote Sensing*, *12*(14), 2283. https://doi.org/10.3390/rs12142283

[74] Bhatawdekar, R.M., Choudhury, S., & Modmad, E.T. (2018). UAV applications on projects monitoring in mining and civil engineering. *Journal of Mines, Metals and Fuels*, *66*(12), 867-872.

[75] Cui, W., Xie, E., Zhang, G., & Li, H. (2021). Identification of isolated dangerous rock mass in high and steep slope using unmanned aerial vehicle. *Geomatics and Information Science of Wuhan University*, *46*(6), 836-843. https://doi.org/10.13203/j.whugis20190186

[76] Askarzadeh, T., & Bridgelall, R. (2025). Cost efficiency and effectiveness of drone applications in bridge condition monitoring. *Infrastructures*, *10*(3), 63. https://doi.org/10.3390/infrastructures10030063

[77] Vishwanatha, H.S., Sreekeshava, K.S., Gopal, M., & Sunitha, S.O. (2025). Applications of drone surveying in civil engineering: A technological advancement towards efficient infrastructure development. *Journal of Civil and Construction Engineering*, *11*(2), 42-50. https://doi.org/10.46610/JOCCE.2025.v011i02.004

[78] Molnár, A., & Domozi, Z. (2017). Tracking production volumes of open-pit mines with photogrammetry. *2017 European Modelling Symposium (EMS)*, 100-106. https://doi.org/10.1109/EMS.2017.28

[79] Kujawa, P., Wajs, J., & Pleśniak, K. (2025). The approach to UAV image acquisition and processing for very shallow water mapping. *International Journal of Applied Earth Observation and Geoinformation*, *141*, 104604. https://doi.org/10.1016/j.jag.2025.104604

[80] Remondino, F., Barazzetti, L., Nex, F., Scaioni, M., & Sarazzi, D. (2011). UAV photogrammetry for mapping and 3D modeling: Current status and future perspectives. *The International Archives of the Photogrammetry, Remote Sensing and Spatial Information Sciences*, *XXXVIII-1/C22*, 25-31. https://doi.org/10.5194/isprsarchives-XXXVIII-1-C22-25-2011

[81] Maier, K., Nascetti, A., van Pelt, W., & Rosqvist, G. (2022). Direct photogrammetry with multispectral imagery for UAV-based snow depth estimation. *ISPRS Journal of Photogrammetry and Remote Sensing*, *186*, 1-18. https://doi.org/10.1016/j.isprsjprs.2022.01.020

[82] Wu, J., Wang, W., & Ni, X. (2023). Study on the application of real-time drone monitoring in Ordos open-pit coal mine. *Open Journal of Applied Sciences*, *13*(4), 483-495. https://doi.org/10.4236/ojapps.2023.134039

[83] Salgado-Almeida, B., Falquez-Torres, D.A., Romero-Crespo, P.L., Valverde-Armas, P.E., Guzmán-Martínez, F., & Jiménez-Oyola, S. (2022). Risk assessment of mining environmental liabilities for their categorization and prioritization in gold-mining areas of Ecuador. *Sustainability*, *14*(10), 6089. https://doi.org/10.3390/su14106089

[84] Quamar, M.M., Al-Ramadan, B., Khan, K., Shafiullah, M., & El Ferik, S. (2023). Advancements and applications of drone-

integrated geographic information system technology: A review. *Remote Sensing, 15*(20), 5039. https://doi.org/10.3390/rs15205039

[85] Zheng, J., Yao, W., Lin, X., Ma, B., & Bai, L. (2022). An accurate digital subsidence model for deformation detection of coal mining areas using a UAV-based LiDAR. *Remote Sensing, 14*(2), 421. https://doi.org/10.3390/rs14020421

[86] Li, Y., Lu, G., Cao, B., Zhu, X., & Yang, Z. (2025). Application of unmanned aerial vehicle 3D reconstruction for quantitative measurements of the tailing pond dry beach. *Applied Sciences, 15*(4), 2014. https://doi.org/10.3390/app15042014

[87] Atik, M.E., Arkali, M., & Atik, S.O. (2025). Impact of UAV-derived RTK/PPK products on geometric correction of VHR satellite imagery. *Drones, 9*(4), 291. https://doi.org/10.3390/drones9040291

[88] Zhong, H., Duan, Y., Tao, P., & Zhang, Z. (2025). Influence of ground control point reliability and distribution on UAV photogrammetric 3D mapping accuracy. *Geo-spatial Information Science, 28*(5), 1998-2018. https://doi.org/10.1080/10095020.2025.2451204

[89] Martínez-Carricondo, P., Agüera-Vega, F., & Carvajal-Ramírez, F. (2023). Accuracy assessment of RTK/PPK UAV-photogrammetry projects using differential corrections from multiple GNSS fixed base stations. *Geocarto International, 38*(1), 2197507. https://doi.org/10.1080/10106049.2023.2197507

[90] Medeiros, B.M., Cândido, B., Jimenez, P.A.J., Avanzi, J.C., & Silva, M.L.N. (2025). UAV-based soil water erosion monitoring: Current status and trends. *Drones, 9*(4), 305. https://doi.org/10.3390/drones9040305

[91] Ishak, M.F., Zolkepli, M.F., & Muhammad, N. (2020). The effectiveness of unmanned aerial vehicle (UAV) for digital slope mapping. *International Journal of Engineering Technology and Sciences, 7*(2), 119-136. https://doi.org/10.15282/ijets.7.2.2020.1010

[92] Gül, Y. (2019). Applications of unmanned aerial vehicle (UAV) in open-pit mines. *Türkiye Jeoloji Bülteni, 62*(1), 99-112. https://doi.org/10.25288/tjb.519506

[93] Bartlett, B., Santos, M., Dorian, T., Moreno, M., Trslić, P., & Dooly, G. (2025). Real-time UAV surveys with the modular detection and targeting system: Balancing wide-area coverage and high-resolution precision in wildlife monitoring. *Remote Sensing, 17*(5), 879. https://doi.org/10.3390/rs17050879

[94] Panigati, T., Zini, M., Striccoli, D., Giordano, P.F., Tonelli, D., Limongelli, M.P., & Zonta, D. (2025). Drone-based bridge inspections: Current practices and future directions. *Automation in Construction, 173*, 106101. https://doi.org/10.1016/j.autcon.2025.106101

[95] Mohammadloo, T.H., Jones, M., van de Kerkhof, B., Dawson, K., Smith, B.J., Conley, S., Corbett, A., & IJzermans, R. (2025). Quantitative estimate of several sources of uncertainty in drone-based methane emission measurements. *Atmospheric Measurement Techniques, 18*(5), 1301-1324. https://doi.org/10.5194/amt-18-1301-2025

[96] Davis, K.L., Silverman, E.D., Sussman, A.L., Wilson, R.R., & Zipkin, E.F. (2022). Errors in aerial survey count data: Identifying pitfalls and solutions. *Ecology and Evolution, 12*(3), e8733. https://doi.org/10.1002/ece3.8733

[97] Henharen, J., & Helmholz, P. (2024). Investigation into camera calibration flight paths for UAV-based corridor surveys. *The International Archives of the Photogrammetry, Remote Sensing and Spatial Information Sciences, XLVIII-2-2024*, 129-135. https://doi.org/10.5194/isprs-archives-XLVIII-2-2024-129-2024

[98] Zandler, H., Sulzer, W., & Kaufmann, V. (2025). Delineation of debris-covered glaciers with multi-temporal UAV images (Gössnitzkees, Schober Group/Austria). *Advances in Geodesy and Geoinformation, 74*(1), e66. https://doi.org/10.24425/agg.2025.154150

[99] Seo, D.-M., Woo, H.-J., Hong, W.-H., Seo, H., & Na, W.-J. (2024). Optimization of number of GCPs and placement strategy for UAV-based orthophoto production. *Applied Sciences, 14*(8), 3163. https://doi.org/10.3390/app14083163

[100] Sestras, P., Badea, G., Badea, A.C., Salagean, T., Roșca, S., Kader, S., & Remondino, F. (2025). Land surveying with UAV photogrammetry and LiDAR for optimal building planning. *Automation in Construction, 173*, 106092. https://doi.org/10.1016/j.autcon.2025.106092

[101] Jiménez-Jiménez, S.I., Ojeda-Bustamante, W., Marcial-Pablo, M.d.J., & Enciso, J. (2021). Digital terrain models generated with low-cost UAV photogrammetry: Methodology and accuracy. *ISPRS International Journal of Geo-Information, 10*(5), 285. https://doi.org/10.3390/ijgi10050285

[102] Burdziakowski, P., & Bobkowska, K. (2021). UAV photogrammetry under poor lighting conditions: Accuracy considerations. *Sensors, 21*(10), 3531. https://doi.org/10.3390/s21103531

[103] Maes, W.H. (2025). Practical guidelines for performing UAV mapping flights with snapshot sensors. *Remote Sensing, 17*(4), 606. https://doi.org/10.3390/rs17040606

[104] Ma, Z., & Chen, J. (2022). Adaptive path planning method for UAVs in complex environments. *International Journal of Applied Earth Observation and Geoinformation, 115*, 103133. https://doi.org/10.1016/j.jag.2022.103133

[105] Gaspari, F., Ioli, F., Barbieri, F., Belcore, E., & Pinto, L. (2022). Integration of UAV-LiDAR and UAV-photogrammetry for infrastructure monitoring and bridge assessment. *The International Archives of the Photogrammetry, Remote Sensing and Spatial Information Sciences, XLIII-B2-2022*, 995-1002. https://doi.org/10.5194/isprs-archives-XLIII-B2-2022-995-2022

[106] Man, Q., Yang, X., Liu, H., Zhang, B., Dong, P., Wu, J., Liu, C., Han, C., Zhou, C., Tan, Z., & Yu, Q. (2025). Comparison of UAV-based LiDAR and photogrammetric point cloud for individual tree species classification of urban areas. *Remote Sensing, 17*(7), 1212. https://doi.org/10.3390/rs17071212

[107] Lu, H., Liang, P., Yao, X., & Zhang, L. (2023). Extraction of elemental information of slope steps in open pit mine based on UAV. *Journal of Physics: Conference Series, 2651*(1), 012119. https://doi.org/10.1088/1742-6596/2651/1/012119

[108] Dong, Y., Wang, D., Liu, F., & Wang, J. (2022). A new data processing method for high-precision mining subsidence measurement using airborne LiDAR. *Frontiers in Earth Science, 10*, 858050. https://doi.org/10.3389/feart.2022.858050

[109] Gül, Y., Hastaoğlu, K.Ö., & Poyraz, F. (2020). Using the GNSS method assisted with UAV photogrammetry to monitor and determine deformations of a dump site of three open-pit marble mines in Eliktekke region, Amasya province, Turkey. *Environmental Earth Sciences, 79*(11), 248. https://doi.org/10.1007/s12665-020-08959-8

[110] Zhao, J., Niu, Y., Zhou, Z., Lu, Z., Wang, Z., Zhang, Z., Li, Y., & Ju, Z. (2024). Construction of mining subsidence basin and inversion of predicted subsidence parameters based on UAV photogrammetry products considering horizontal displacement. *Remote Sensing, 16*(22), 4283. https://doi.org/10.3390/rs16224283

[111] Liu, X., Zhu, W., Lian, X., & Xu, X. (2023). Monitoring mining surface subsidence with multi-temporal three-dimensional unmanned aerial vehicle point cloud. *Remote Sensing, 15*(2), 374. https://doi.org/10.3390/rs15020374

[112] gnjatović Stupar, D., Rošer, J., & Vulić, M. (2020). Investigation of unmanned aerial vehicles-based photogrammetry for large mine subsidence monitoring. *Minerals, 10*(2), 196. https://doi.org/10.3390/min10020196

[113] Jin, A.B., Chen, S.J., Zhao, A.Y., Sun, H., & Zhang, Y.S. (2021). Numerical simulation of open-pit mine slope based on unmanned aerial vehicle photogrammetry. *Rock and Soil Mechanics, 42*(1), 255-264. https://doi.org/10.16285/j.rsm.2020.0697

[114] Zhou, D., Wang, L., An, S., Wang, X., & An, Y. (2022). Integration of unmanned aerial vehicle (UAV)-based photogrammetry and InSAR for mining subsidence and parameters inversion: A case study of the Wangjiata Mine, China. *Bulletin of Engineering Geology and the Environment, 81*(8), 343. https://doi.org/10.1007/s10064-022-02845-2

[115] Nam-Bui, X., Quoc Long, N., Thi Thu Ha, L., Ngoc Quy, B., Goyal, R., Trong Hung, V., Van Chung, P., Xuan Cuong, C., Van Canh, L., & Hong Viet, L. (2020). Flight height of UAV and its influence on the precise digital elevation model of complex terrain. *Inżynieria Mineralna, 1*(1), 179-186. https://doi.org/10.29227/IM-2020-01-27

[116] Liu, J., Liu, X., Lv, X., Wang, B., & Lian, X. (2022). Novel method for monitoring mining subsidence featuring co-

registration of UAV LiDAR data and photogrammetry. *Applied Sciences*, *12*(18), 9374. https://doi.org/10.3390/app12189374

[117] Zhou, D., Qi, L., Zhang, D., Zhou, B., & Guo, L. (2020). Unmanned aerial vehicle (UAV) photogrammetry technology for dynamic mining subsidence monitoring and parameter inversion: A case study in China. *IEEE Access*, *8*, 16372-16386. https://doi.org/10.1109/ACCESS.2020.2967410

[118] Kršák, B., Blišťan, P., Pauliková, A., Puškárová, P., Kovanič, Ľ., Palková, J., & Zelizňaková, V. (2016). Use of low-cost UAV photogrammetry to analyze the accuracy of a digital elevation model in a case study. *Measurement*, *91*, 276-287. https://doi.org/10.1016/j.measurement.2016.05.028

[119] Cryderman, C., Mah, S.B., & Shufletoski, A. (2014). Evaluation of UAV photogrammetric accuracy for mapping and earthworks computations. *Geomatica*, *68*(4), 309-317. https://doi.org/10.5623/cig2014-405

[120] Du, W., Sheng, Q., Fu, X., Chen, J., Kang, J., Pang, X., Wan, D., & Yuan, W. (2025). Application of unmanned aerial vehicle remote sensing on dangerous rock mass identification and deformation analysis: Case study of a high-steep slope in an open pit mine. *Journal of Earth Science*, *36*(2), 750-763. https://doi.org/10.1007/s12583-023-1813-7

[121] Zhan, X., Zhang, X., Wang, X., Diao, X., & Qi, L. (2024). Comparative analysis of surface deformation monitoring in a mining area based on UAV-LiDAR and UAV photogrammetry. *The Photogrammetric Record*, *39*(186), 373-391. https://doi.org/10.1111/phor.12490

[122] An, S., Yuan, L., Xu, Y., Wang, X., & Zhou, D. (2024). Ground subsidence monitoring in based on UAV-LiDAR technology: A case study of a mine in the Ordos, China. *Geomechanics and Geophysics for Geo-Energy and Geo-Resources*, *10*, 57. https://doi.org/10.1007/s40948-024-00762-0

[123] Yang, B., Du, W., Zou, Y., Zhang, H., Chai, H., Wang, W., Song, X., & Zhang, W. (2024). Reconstruction of coal mining subsidence field by fusion of SAR and UAV LiDAR deformation data. *Remote Sensing*, *16*(18), 3383. https://doi.org/10.3390/rs16183383

[124] Matsimbe, J.M.J., Mdolo, W., Kapachika, C., Musonda, I., & Dinka, M. (2022). Comparative utilization of drone technology vs. traditional methods in open pit stockpile volumetric computation: A case of Njuli Quarry, Malawi. *Frontiers in Built Environment*, *8*, 1037487. https://doi.org/10.3389/fbuil.2022.1037487

[125] Crawford, B., Swanson, E., Schultz-Fellenz, E., Collins, A., Dann, J., Lathrop, E., & Milazzo, D. (2021). A new method for high resolution surface change detection: Data collection and validation of measurements from UAS at the Nevada National Security Site, Nevada, USA. *Drones*, *5*(2), 25. https://doi.org/10.3390/drones5020025

[126] Lu, J., Zhao, Y., Zhou, L., Wei, K., Ma, J., & Li, X. (2021). Accuracy analysis of 3D model of open-pit mine based on tilt photogrammetry. *IOP Conference Series: Earth and Environmental Science*, *865*(1), 012023. https://doi.org/10.1088/1755-1315/865/1/012023

[127] Pang, X., Yuan, M., Lu, Y., Du, W., Wan, D., Li, D., Ding, H., & Fu, X. (2023). Rapid identification method for the dangerous rock mass of a high-steep slope based on UAV LiDAR and ground imitation flight. *Bulletin of Geological Science and Technology*, *42*(6), 21-30. https://doi.org/10.19509/j.cnki.dzkq.tb20220427

[128] Ćwiąkała, P., Gruszczyński, W., Stoch, T., Puniach, E., Mrocheń, D., Matwij, W., Matwij, K., Nędzka, M., Sopata, P., & Wójcik, A. (2020). UAV applications for determination of land deformations caused by underground mining. *Remote Sensing*, *12*(11), 1733. https://doi.org/10.3390/rs12111733

[129] Gruszczyński, W., Puniach, E., Ćwiąkała, P., & Matwij, W. (2025). Determining vertical displacement of agricultural areas using UAV-photogrammetry and a heteroscedastic deep learning model. *Remote Sensing*, *17*(18), 3259. https://doi.org/10.3390/rs17183259

[130] Yin, Y., Jiang, C., Lv, J., Wang, J., Ju, X., Wang, H., Xing, Y., & Zhang, L. (2020). Mining ground surface information extraction and topographic analysis using UAV video data. *E3S Web of Conferences*, *194*, 05030. https://doi.org/10.1051/e3sconf/202019405030

[131] Zhou, D., An, S., Wu, K., Hu, Z., & Diao, X. (2022). Key technology and application of InSAR/UAV fusion monitoring for coal mining damages. *Coal Science and Technology*, *50*(10), 121-134. https://doi.org/10.13199/j.cnki.cst.2022-0980

[132] Wang, B., Zhang, Y., & Zhang, W. (2022). Integrated path planning and trajectory tracking control for quadrotor UAVs with obstacle avoidance in the presence of environmental and systematic uncertainties: Theory and experiment. *Aerospace Science and Technology*, *120*, 107277. https://doi.org/10.1016/j.ast.2021.107277

[133] Kuo, C.-F.J., Chen, S.-H., & Huang, C.-Y. (2023). Automatic detection, classification and localization of defects in large photovoltaic plants using unmanned aerial vehicles (UAV) based infrared (IR) and RGB imaging. *Energy Conversion and Management*, *276*, 116495. https://doi.org/10.1016/j.enconman.2022.116495

[134] Siebert, S., & Teizer, J. (2014). Mobile 3D mapping for surveying earthwork projects using an unmanned aerial vehicle (UAV) system. *Automation in Construction*, *41*, 1-14. https://doi.org/10.1016/j.autcon.2014.01.004

[135] Hussain, A., Li, S., Hussain, T., Lin, X., Ali, F., & AlZubi, A.A. (2024). Computing challenges of UAV networks: A comprehensive survey. *Computers, Materials & Continua*, *81*(2), 1999-2051. https://doi.org/10.32604/cmc.2024.056183

[136] Zhang, S. (2025). Development and challenges of UAV technology in civil engineering surveying and mapping. *Applied and Computational Engineering*, *122*, 50-54. https://doi.org/10.54254/2755-2721/2025.19599

[137] Taimoor, S., Naeem, M., Zeadally, S., & Ejaz, W. (2025). Resource optimization for minimizing latency and cost in UAV-assisted mobile edge computing (MEC) networks. *Computer Networks*, *271*, 111587. https://doi.org/10.1016/j.comnet.2025.111587

[138] Tomaštík, J., Mokroš, M., Surový, P., Grznárová, A., & Merganič, J. (2019). UAV RTK/PPK method: An optimal solution for mapping inaccessible forested areas? *Remote Sensing*, *11*(6), 721. https://doi.org/10.3390/rs11060721

[139] Narzari, R., Choudhury, B.U., Singhal, G., & Choudhary, K.K. (2025). A critical review of how UAVs can transform precision agriculture in the realm of agroecology. *Discover Soil*, *2*, 28. https://doi.org/10.1007/s44378-025-00055-2

[140] Karahan, A., Demircan, N., Özgeriş, M., Gökçe, O., & Karahan, F. (2025). Integration of drones in landscape research: Technological approaches and applications. *Drones*, *9*(9), 603. https://doi.org/10.3390/drones9090603

[141] Han, J.Y., Hsu, C.R., & Huang, C.J. (2024). Automated progress monitoring of land development projects using unmanned aerial vehicles and machine learning. *Automation in Construction*, *168*, 105827. https://doi.org/10.1016/j.autcon.2024.105827

[142] Lyu, C., Lin, S., Lynch, A., Zou, Y., & Liarokapis, M. (2025). UAV-based deep learning applications for automated inspection of civil infrastructure. *Automation in Construction*, *177*, 106285. https://doi.org/10.1016/j.autcon.2025.106285

[143] Elmokadem, T., & Savkin, A.V. (2022). A method for autonomous collision-free navigation of a quadrotor UAV in unknown tunnel-like environments. *Robotica*, *40*(4), 835-861. https://doi.org/10.1017/S0263574721000849

[144] McTegg, S.J., Tarsha Kurdi, F., Simmons, S., & Gharineiat, Z. (2022). Comparative approach of unmanned aerial vehicle restrictions in controlled airspaces. *Remote Sensing*, *14*(4), 822. https://doi.org/10.3390/rs14040822

[145] Mishra, L., & Kaabouch, N. (2025). Impact of weather factors on unmanned aerial vehicles' wireless communications. *Future Internet*, *17*(1), 27. https://doi.org/10.3390/fi17010027

[146] Román, A., Tovar-Sánchez, A., Larrad, M., Rubiano-Sánchez, F.J., Zafra, J.M., Piñeiro, R., Castillo, Á., López, F.A., Vela, A.L., Allende, A., Sánchez, G., Martínez-Alonso, A., Samper, D., García-Davalillo, J.C., Galindo, I., & Navarro, G. (2025). UAV imagery in natural disasters: Real-time damage assessment of flash flooding events. *Ecological Informatics*, *91*, 103433. https://doi.org/10.1016/j.ecoinf.2025.103433

Тау-кен ісі мен геотехникалық инженерияда ұшқышсыз технологияларды қолдануға арналған мета-талдау және жүйелі шолу

М.З. Емад*

Король Фахд атындағы мұнай және пайдалы қазбалар университеті, Дахран, Сауд Арабиясы

**Корреспонденция үшін автор: muhammadzaka.emad@kfupm.edu.sa*

Аңдатпа. Беспилоттық ұшу аппараттары (БПҰА) геотехникалық және тау-кен жұмыстарын орындау тәсілдерін айтарлықтай өзгертті, кеңістіктік деректерді жедел, жоғары дәлдікпен және экономикалық тұрғыдан тиімді алуға, жер бедерін модельдеуге және нысандарды мониторингтеуге мүмкіндік берді. Жүйелі шолу мен мета-талдауда фотограмметрия және LiDAR технологияларын қоса алғанда, БПҰА қолдану арқылы жүргізілетін түсірілім дәлдігін тахеометриялық түсірілім және жерүсті лазерлік сканерлеу сияқты дәстүрлі әдістермен салыстыру мақсатында 133-тен астам рецензияланған жарияланымның нәтижелері жинақталып талданды. Зерттеуде БПҰА-ның тау-кен массасы қоймаларының көлемін анықтауда, жер бетінің шөгуін мониторингтеуде, қалдық қоймалары мен тау жыныстары үйінділерін зерттеуде, сондай-ақ тау жыныстары массивтерін сәйкестендіруде қолданылуы қарастырылды. Мета-талдау нәтижелері ұшу параметрлерін оңтайландыру, RTK/PPK-позициялау технологияларын және жерүсті тірек нүктелерін пайдалану жағдайында БПҰА тұрақты түрде қолайлы дәлдікті қамтамасыз ете алатынын көрсетеді. Беспилоттық LiDAR түсірілім дәлдігін арттыруға мүмкіндік берсе, UAV-фотограмметрия нәтижелер сапасы мен жұмыстар құны арасындағы ұтымды тепе-теңдікті қамтамасыз етеді. Алайда қателік шамасы жер бедерінің күрделілігіне, ұшуды жоспарлауға және метеорологиялық жағдайларға байланысты болады. Библиометриялық талдау 2017 жылдан бастап жарияланымдар санының экспоненциалды өскенін көрсетті, бұл ретте Қытай қаржыландыру, авторлық үлес және зерттеулер саны бойынша жетекші орын алады. Кілт сөздер мен бірлескен авторлық желілерді талдау машиналық оқытуға, үшөлшемді реконструкцияға және цифрлық егіздерге деген қызығушылықтың артып келе жатқанын көрсетеді. SWOT-талдау БПҰА-ның негізгі артықшылықтары ретінде операциялық тиімділікті, қауіпсіздікті арттыруды және нәтижелердің көрнекілігін айқындады. Кемшіліктеріне деректерді өңдеудің үлкен көлемі, дәлдіктің біркелкі болмауы, қолайсыз жер бедері жағдайында пайдалану қиындықтары және білікті мамандардың жеткіліксіздігі жатады. Нәтижелер салалық сауалнама арқылы расталды: респонденттердің 100%-ы жұмыстар тиімділігінің артқанын атап өтсе, 71%-ы шығындардың едәуір төмендегенін көрсетті. БПҰА эксперименттік жабдық санатынан геотехникалық негізгі құралдар санатына өтіп, мониторинг, жұмыстарды жоспарлау және қауіпті факторларды талдау үшін жедел ақпарат ұсынуда. Сенсорларды интеграциялау, жасанды интеллектіні қолдану және жұмыс процестерін стандарттау БПҰА-ны тау-кен өнеркәсібін цифрландырудың негізгі факторларының біріне айналдыруы мүмкін. Болашақ зерттеулер жерасты картографиялауға, автоматтандыруға және нормативтік талаптарды біріздендіруге бағытталуы тиіс.

Негізгі сөздер: *дрондар, ұшқышсыз ұшу аппараттары (ҰҰА), ұшқышсыз авиациялық жүйелер (UAS), фотограмметрия, тау-кен қалдықтары, көлемдік өлшеулер, дәлдік, жер бетінің шөгуі, көшкін, картографиялау.*

Метаанализ и систематический обзор применения беспилотных технологий в горном деле и геотехнической инженерии

М.З. Емад*

Университет нефти и полезных ископаемых имени короля Фахда, Дахран, Саудовская Аравия

**Автор для корреспонденции: muhammadzaka.emad@kfupm.edu.sa*

Аннотация. Беспилотные летательные аппараты (БПЛА) существенно изменили подходы к выполнению геотехнических и горных работ, обеспечив быстрое, высокоточное и экономически эффективное получение пространственных данных, моделирование рельефа и мониторинг объектов. В систематическом обзоре и метаанализе обобщены результаты более 133 рецензируемых публикаций для сравнения точности съемки с применением БПЛА, включая фотограмметрию и LiDAR, с традиционными методами, такими как тахеометрическая съемка и наземное лазерное сканирование. Рассмотрено применение БПЛА для определения объемов складов горной массы, мониторинга проседания земной поверхности, исследования хвостохранилищ и породных отвалов, а также идентификации массивов горных пород. Результаты метаанализа показывают, что при оптимизации параметров полета, использовании RTK/PPK-позиционирования и наземных опорных точек БПЛА способны стабильно обеспечивать приемлемую точность. Беспилотный LiDAR позволяет повысить точность съемки, тогда как UAV-фотограмметрия обеспечивает рациональный баланс между качеством результатов и стоимостью работ. Однако величина погрешности зависит от сложности рельефа, планирования полета и метеорологических условий. Библиометрический анализ свидетельствует об экспоненциальном росте числа публикаций с 2017 года, при этом Китай занимает ведущие позиции по финансированию, авторству и количеству исследований. Анализ ключевых слов и сетей соавторства показывает усиление интереса к машинному обучению, трехмерной реконструкции и цифровым двойникам. SWOT-анализ определил операционную эффективность, повышение безопасности и наглядность результатов как основные преимущества БПЛА. К недостаткам относятся значительный объем обработки данных, неоднородность точности, сложности эксплуатации в условиях неблагоприятного рельефа и недостаток квалифицированных специалистов. Результаты подтверждены отраслевым опросом: 100% респондентов отметили повышение эффективности работ, а 71% указали на существенное снижение затрат. БПЛА переходят из категории экспериментального оборудования в категорию основных геотехнических инструментов, обеспечивающих оперативную информацию для мониторинга, планирования работ и анализа опасных факторов. Интеграция сенсоров, применение искусственного интеллекта и стандартизация рабочих процессов могут сделать БПЛА одним из ключевых факторов цифровизации горнодобывающей промышленности. Перспективные исследования должны быть направлены на подземное картографирование, автоматизацию и унификацию нормативных требований.

Ключевые слова: *дроны, беспилотные летательные аппараты (БПЛА), беспилотные авиационные системы (БАС), фотограмметрия, горные отходы, объемные измерения, точность, проседание земной поверхности, оползень, картографирование.*

Publisher's note

SATBAYEV UNIVERSITY

Engineering Journal of Satbayev University

Volume 148 (2026), Issue 3, 53-61

https://doi.org/10.51301/ejsu.2026.i3.06

Modern aspects of reclamation of coal mines

K.B. Rysbekov, N.O. Sarybayev*, B. Kakim, Y. Metelev, K. Tileubekov

Satbayev University, Almaty, Kazakhstan

**Corresponding author: n.sarybayev@satbayev.university*

Abstract. The study aims to identify and systematize the main technical, environmental, and biological factors determining the effectiveness of reclamation of lands disturbed by open-pit coal mining. The research was conducted using documentary analysis and a comparative review of domestic and international practices. Technical and biological reclamation projects for the Severnyi and Vostochnyi coal mines in the Ekibastuz coal basin were analyzed together with published data on the restoration of coal-mining areas in the United States, Mongolia, and Indonesia. The comparison covered engineering preparation of the territory, surface runoff management, erosion prevention, soil and vegetation restoration, environmental monitoring, and the economic feasibility of reclamation solutions. It was established that the two technical reclamation options proposed for the Vostochnyi coal mine differ in the scope and total cost of the planned works. The study showed that flattening the slopes of the Festivalnyi, Konveyernyi, and Prybortovoy external dumps is constrained by the risk of spontaneous combustion of carbonaceous rocks, the location of engineering infrastructure, and the possible expansion of disturbed areas into productive land. Comparison with international experience confirmed the need for long-term monitoring of water quality, backfill stability, vegetation development, and soil-forming processes. It was also found that domestic biological reclamation projects mainly rely on natural revegetation, whereas direct planting and fertilizer application may accelerate the formation of a stable vegetation cover. The main constraints and effectiveness factors associated with the reclamation of large coal mines in Kazakhstan were systematized, and directions for adapting international approaches to the conditions of the Ekibastuz coal basin were identified. The results can be used in the development and revision of reclamation projects that incorporate long-term monitoring, surface runoff control, assessment of soil formation, and active vegetation restoration.

Keywords: *coal mining, reclamation, disturbed lands, reclamation phases, monitoring*.

Received: 28 March 2026
Received in revised form: 29 May 2026
Accepted: 18 June 2026
Available online: 30 June 2026

1. Introduction

Coal has been one of the most used raw materials in the world. The global consumption of coal still remains quite high. Among the leaders are China, India and USA with 5313 million, 1200 million and 476 million tons respectively [1]. Both China and India mostly use the coal for power generation purposes. Our country used about 85 million tons of coal in 2025, which ranks 13th worldwide and mainly for the purposes of electric power generation [1, 2]. However, it should be noted that both China and India saw a drop in the consumption volume for the first time in 52 years [3]. Such a trend could be explained by the shift of both countries towards the cleaner energy sources. Air pollution and climate change are main reasons why countries are turning their attention to cleaner energy sources. Gradual decline in coal demand could mean that operation of coal mines could stop.

At the same time, a reduction in coal production does not eliminate the environmental consequences accumulated during decades of mining. Mine closure creates a need to stabilize disturbed areas, prevent further degradation and return the land to a condition suitable for environmental, agricultural, industrial or recreational use. Therefore, reclamation should be considered not only as a final stage of mine closure, but also as an integral part of the entire life cycle of a mining enterprise [4]. Progressive reclamation, in which disturbed areas are restored while mining operations are still continuing, may reduce the final closure workload and limit long-term environmental risks [5, 6].

Open pit mining of coal has damaging effect on the environment. Those mines usually occupy large areas of land. For example, Ekibastuz coal basin located in the north part of our country has an area of 155 square kilometers. North Antelope Rochelle Coal Mine, located in USA, has a mine permit area of 65805 acres or 266 square kilometers and 3,682 acres of that land were already reclaimed [7]. Reclamation of land at Ekibastuz coal basin has not fully started, because all the mines in the area are fully operational.

The environmental impact of open-pit coal mining is not limited to the direct occupation of land. Mining operations substantially modify the original relief, soil profile, surface runoff and groundwater regime. Waste dumps and exposed slopes may become sources of dust, water erosion, slope instability and contamination of surface and groundwater [8-

10]. Waste dumps and exposed slopes may become sources of dust, water erosion, slope instability and contamination of surface and groundwater. Therefore, assessment of the rock mass condition and management of slope stability should be considered during both mining and reclamation planning [11].

The removal and mixing of soil horizons also reduce soil fertility and complicate the restoration of vegetation. The removal and mixing of soil horizons also reduce soil fertility and complicate the restoration of vegetation, while the migration of contaminants may adversely affect nearby surface-water bodies and underground aquifers [12]. Consequently, successful reclamation requires coordinated geotechnical, hydrological, soil-management and biological measures rather than only surface leveling [13].

The fact that coal is a combustible rock makes the task of reclamation of coal deposits challenging, since special measures should be carried out while reclaiming such deposits [14, 15]. The coal dumps should contain screens with inert materials or non-flammable rocks, compaction level of soil in dumps should be high to avoid seepage of water. All these measures are necessary to prevent oxygen access to coal containing layers of soil [16-19].

The presence of carbonaceous material in overburden and waste dumps creates an additional risk of oxidation and spontaneous combustion. Water infiltration and oxygen penetration may intensify these processes and lead to heat generation, gas emissions and deterioration of dump stability. For this reason, the design of reclamation measures should consider the composition of waste rocks, the distribution of coal-bearing layers, the degree of compaction, drainage conditions and the long-term thermal stability of reclaimed dumps [20, 21].

Reclamation is generally divided into technical and biological phases [22]. The technical phase includes reshaping and stabilization of landforms, backfilling, slope flattening, construction of drainage systems, covering of potentially hazardous materials and preparation of the surface for further use. The biological phase is aimed at restoring soil functions and vegetation through the application of fertile soil, fertilization, seeding, planting or controlled natural succession. The effectiveness of both phases depends on local climatic conditions, soil properties, water availability and the intended post-mining land use [23-25].

Long-term monitoring is also essential because the visible completion of reclamation works does not necessarily mean that the reclaimed ecosystem has reached a stable condition [26]. Vegetation survival, soil development, erosion, surface and groundwater quality, slope stability and signs of residual contamination should be assessed during and after reclamation [27-30]. International practice shows that systematic monitoring supported by GIS, remote sensing and other geospatial technologies makes it possible to identify hazardous changes at an early stage and implement appropriate corrective measures [31].

Domestic reclamation projects already include measures for surface stabilization, drainage, isolation of disturbed areas and subsequent vegetation recovery [32, 33]. However, comparison with international experience indicates that greater attention should be paid to long-term pedogenesis, measurable monitoring criteria, active biological reclamation and the selection of plant species and fertilizers suitable for specific site conditions [34, 35]. These aspects are particularly important for the large coal-mining areas of Kazakhstan, where natural recovery may proceed slowly because of the continental and relatively dry climate.

Therefore, the information given above shows that the problem of reclamation (recultivation) of coal mines is and would be topical.

2. Materials and methods

This study employed a documentary review and comparative case-study approach to identify the main technical, environmental, and biological factors affecting the reclamation of open-pit coal mines. The analysis was based on two groups of information sources: reclamation and mine-closure documentation for coal mines in Kazakhstan, and published studies describing reclamation practices at coal-mining sites in other countries.

The domestic part of the analysis included the Severnyi and Vostochnyi coal mines located within the Ekibastuz coal basin. These sites were selected because they represent large operating open-pit coal mines and have available project documentation describing the planned technical and biological phases of reclamation. The reclamation project for the Severnyi coal mine [32] was examined with respect to landform reconstruction, formation and compaction of the leveling backfill, drainage arrangement, erosion control, use of overburden materials, and the proposed method of vegetation recovery. The mine-closure and reclamation plan for the Vostochnyi coal mine [33] was analyzed to compare alternative technical reclamation options, their estimated costs, monitoring requirements, treatment of external waste dumps, water-management measures, and potential post-mining use of infrastructure.

The international cases were selected to represent reclamation practices related to the principal issues identified in the domestic documentation. The North Antelope Rochelle Coal Mine in the United States was considered as an example of long-term regulatory monitoring and the use of GPS/GIS technologies for assessing reclaimed land [27]. Research on reclaimed coal-mining areas was used to examine the long-term development of soil profiles and pedogenesis [29]. The reclamation of coal-mine waste dumps in Mongolia was considered to assess drainage design and the prevention of water erosion and dump instability [34]. The Indonesian case was included to evaluate the effectiveness of direct planting and fertilizer application during biological reclamation [35].

The information collected was organized according to four groups of assessment criteria:

1). Technical reclamation, including landform reshaping, backfilling, compaction, slope stabilization, isolation of carbonaceous materials, drainage construction, and prevention of spontaneous combustion;

2). Biological reclamation, including soil preparation, natural revegetation, direct planting, selection of plant species, and fertilizer application;

3). Environmental protection and monitoring, including control of soil contamination, dust emissions, wind and water erosion, surface-water and groundwater quality, vegetation development, and residual contamination;

4). Economic and post-mining considerations, including the estimated cost of reclamation alternatives, the possibility of reusing infrastructure, and the intended future use of reclaimed land.

A qualitative comparative analysis was then performed. First, the reclamation measures planned for the Severnyi and Vostochnyi coal mines were compared to identify similarities and differences in technical design, biological restoration, monitoring, and cost. Second, the domestic practices were compared with the selected international cases. Particular attention was paid to measures that were absent, insufficiently developed, or only partly considered in the domestic projects.

The comparison did not aim to rank the examined mines because the sites differ in climatic conditions, mining scale, waste-rock properties, regulatory requirements, and intended post-mining land use. Instead, the analysis was used to identify transferable reclamation principles and practices that could improve the long-term environmental stability of coal-mining areas in Kazakhstan. On this basis, the key factors affecting reclamation effectiveness were identified, including systematic monitoring, long-term soil development, erosion and drainage control, active vegetation establishment, and the allocation of sufficient resources for biological reclamation.

3. Results and discussion

Reclamation of coal-mining areas in Kazakhstan is generally implemented in two successive phases: technical and biological reclamation. Technical reclamation may begin before the complete cessation of mining operations, as the required machinery and infrastructure are still available at the site. Biological reclamation is usually carried out after the completion of the principal earthworks and stabilization of the reclaimed surface. The present study considers the Severnyi and Vostochnyi coal mines of the Ekibastuz coal basin, the largest coal-producing region in Kazakhstan, located in the northern part of the country.

The first case concerns the reclamation plan developed for the Severnyi coal mine. According to the project documentation [32], the disturbed area is proposed to be reclaimed for sanitary and environmental purposes through the construction of a leveling backfill. The proposed measures take into account the sequence and duration of reclamation works, as well as their economic feasibility.

The technical reclamation phase includes the following operations:

– construction of a leveling backfill using overburden materials;

– layer-by-layer placement and compaction of the backfill;

– construction of a protective embankment;

– excavation of a drainage ditch for stormwater diversion;

– subsequent natural revegetation of the reclaimed area.

The reclamation project covers 25.3958 ha of disturbed land. The use of potentially fertile overburden materials is expected to improve the local relief, stabilize the reclaimed surface, and reduce the adverse effects associated with the withdrawal of agricultural land from use. The spatial layout of the reclamation site is shown in Figure 1.

During the technical reclamation stage, it is planned to construct a protective embankment along the upper edge of the leveling fill and to excavate a drainage ditch for the collection and diversion of stormwater from the technological road used to inspect and monitor the condition of the reclaimed area. These measures are intended to prevent uncontrolled surface runoff, reduce water infiltration into the backfill, and maintain the long-term stability of the reconstructed landform.

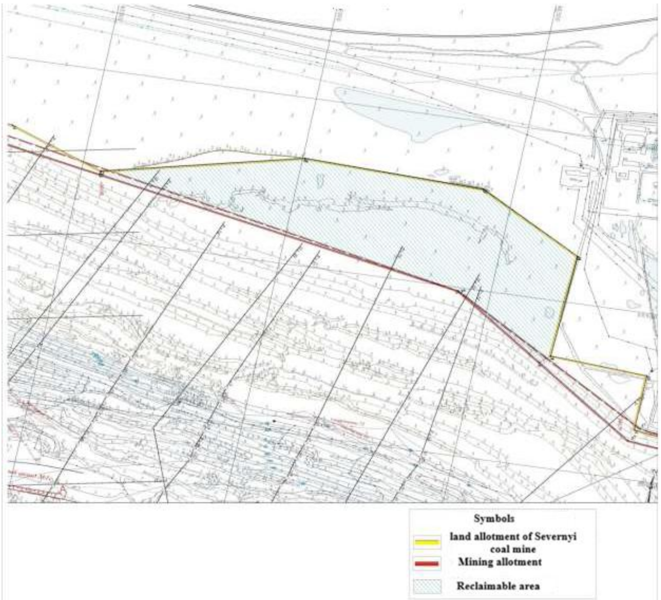

Figure 1. Situational scheme of the reclaimable land in Severnyi coal mine

The technical measures designed to improve the hydrological regime and provide erosion protection for the disturbed territory should include a system of protective and water-diversion embankments delimiting the leveling fill area. The arrangement of these structures is intended to regulate surface runoff, prevent the inflow of water from adjacent areas, and reduce the risk of erosion along the perimeter and slopes of the reclaimed site.

The reclamation project also provides for the construction of interceptor and drainage ditches along the technological road. These structures are required to collect and safely divert stormwater and thereby protect the surface of the leveling fill from water erosion. In combination with surface stabilization measures, they also contribute to reducing wind erosion by limiting the development of eroded and loose surface zones.

Water-diversion and protective structures are constructed from overburden materials using excavators or other earthmoving equipment with equivalent technical capabilities. The use of locally available overburden reduces the need to transport additional construction materials and allows the engineering structures to be integrated into the general configuration of the reclaimed landform. At the same time, the drainage ditch intended to collect and discharge runoff from the technological road is designed with a minimum longitudinal gradient of 5‰, in accordance with the requirements specified in Clause 7.3 of SP 3.03-122-2013. Compliance with this gradient is necessary to maintain the required flow velocity, prevent water stagnation, and ensure the effective operation of the drainage system.

Part of the reclamation site is already occupied by overburden materials previously placed from the pit-side area of the Severnyi coal mine. The existing deposits of overburden are therefore incorporated into the planned configuration of the leveling fill and taken into account when determining the final surface geometry and the required volume of additional material. The estimated volume of overburden materials classified as potentially fertile rocks and required for the formation of the leveling fill within the disturbed land area is 2.197 million m^3, based on the calculated volume of earth materials.

The planned position and spatial configuration of the leveling fill after completion of the reclamation works are shown in Figure 2.

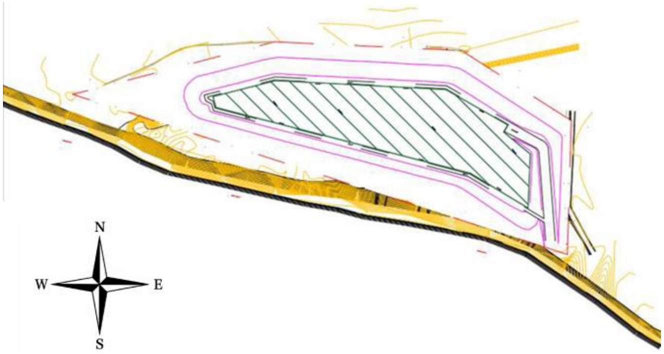

Figure 2. Position of leveling backfill on disturbed lands of Severnyi coal mine

The main part of the biological phase of reclamation in Severnyi coal mine is the natural overgrowth of natural xerophytic vegetation characteristic of this natural and climatic zone based on the soil and climatic conditions of the area and the accepted direction of reclamation.

Overgrowing with perennial grasses will allow:

– stop the process of further pollution of the environment by overburden components;

– improve and streamline the landscape of disturbed lands;

– increase the biological productivity of disturbed lands by increasing the area of green spaces and reducing environmental pollution.

For the period of reclamation, the sources of environmental pollution are parking lots for special equipment and vehicles, where fuel and lubricants may spill, and soil contamination.

When performing reclamation work, the negative impact on the environment is caused by economic activity in the form of emissions of harmful substances into the atmospheric air. The impact of emissions does not exceed the limits of a sanitary protection zone of at least 500 m in size [5].

Overburden rocks meet the radiation safety requirements for building materials and are not radioactive.

Environmental protection measures implemented during reclamation activities at the Severnyi coal mine are aimed at minimizing soil contamination, dust emissions, and erosion processes. Soil pollution is prevented through the organized collection, segregation, and temporary storage of industrial and municipal waste in designated containers, followed by its transfer to authorized disposal or recycling facilities. The adverse effects of wind erosion are reduced by limiting the duration of excavation and earth-moving operations, particularly during periods of dry and windy weather. Dust generation from disturbed surfaces, haul roads, and material handling operations is controlled through the use of water-spraying systems. In addition, engineering measures, including surface grading, soil compaction, drainage channels, and protective embankments, are applied to reduce both wind and water erosion and to ensure the long-term stability of reclaimed landforms.

The second case concerns the reclamation plan developed for the Vostochnyi coal mine in the Ekibastuz coal basin. Vostochnyi is one of the largest open-pit coal mines in the world and is known for the successful implementation of cyclic-and-continuous mining technology. Two alternative options for technical reclamation have been proposed on the basis of the current condition of the disturbed land surface, the natural and climatic characteristics of the area, technical feasibility, economic and socio-economic conditions, and the specific location of the Vostochnyi coal mine [33].

Option 1 includes the following measures:

– clearing the territory of construction waste, coarse-grained materials, and scattered rock accumulations;

– dismantling equipment, buildings, and surface structures designated for removal;

– backfilling ravines, gullies, and erosion channels, as well as leveling local surface irregularities using waste rock;

– constructing a protective embankment around the perimeter of the open-pit mine;

– leaving the reclaimed territory for subsequent natural revegetation;

Option 2 includes the following measures:

– clearing the territory of construction waste, coarse-grained materials, and scattered rock accumulations;

– dismantling equipment, buildings, and surface structures designated for removal;

– backfilling ravines, gullies, and erosion channels and leveling uneven areas using waste rock;

– retaining facilities that remain suitable for further operation during the final stage of mining after the expiration of the current contract or during the development of adjacent and nearby deposits;

– conserving the remaining coal reserves and waste dumps of the Vostochnyi coal mine.

The principal difference between the two alternatives lies in the intended post-mining use of the site and the scope of the reclamation works. Option 1 provides for more extensive isolation and stabilization of the open-pit area, including the construction of a perimeter protective embankment and the subsequent natural revegetation of the disturbed territory. Option 2 places greater emphasis on retaining technically serviceable facilities for possible future use during the development of adjacent or nearby deposits. Consequently, Option 1 requires a larger volume of reclamation works and is more expensive than Option 2, as shown by the comparative cost assessment presented in Table 1.

Table 1. Comparative cost assessment of the technical reclamation options for the Vostochnyi coal mine

Reclamation option	Costs, thousand USD		
	Direct	Indirect	Total
Option 1	34681.30	13211.04	47892.34
Option 2	24565.10	9357.51	33922.61

The biological reclamation criteria established for the Vostochnyi coal mine are intended to ensure that the restored land develops toward a stable target ecosystem. The vegetation established within the reclaimed area should correspond to the composition of the local plant community, and the species used during reclamation should be characteristic of the surrounding natural vegetation. The restored ecosystem should also be capable of retaining water and nutrients, while the physical, chemical, and biological properties of the reconstructed soils should be consistent with those of the target landscape. In addition, the quality of surface water and groundwater affected by acidic or metalliferous drainage should remain within the applicable baseline and regulatory water-quality limits.

The reclamation criteria are formulated in a measurable form so that the condition of the restored area can be objectively compared with reference sites or with land affected by similar mining activities. Their achievement is assessed using quantitative vegetation surveys conducted according to recognized methodological approaches, field measurements, and laboratory analyses of soil samples performed by an accredited laboratory. The evaluation also includes detailed topographic plans and technical specifications of the reconstructed landforms. Particular attention is given to the characteristics of surface drainage, wastewater, and receiving waters, including pH, salinity, and heavy-metal concentrations, which should comply with the established environmental criteria.

Continuous monitoring of the reclaimed area is planned after completion of the biological reclamation works at the Vostochnyi coal mine. The monitoring programme is intended to assess the long-term stability of the reclaimed land, identify signs of residual contamination, evaluate vegetation development, and control the quality of surface water. The proposed monitoring activities, their implementation periods, and recommended frequencies are presented in Table 2.

Table 2. Tentative monitoring schedule for reclaimed areas of the Vostochnyi coal mine

Monitoring activity	Implementation period	Frequency
Inspection of the site for signs of residual contamination	Before and after completion of the reclamation and mine-closure works	Once every six months
Vegetation monitoring to determine the achievement of eradication objectives	After completion of the reclamation and mine-closure works	Once a year
Surface-water sampling for quality control	After completion of the reclamation and mine-closure works	Once a year during the spring flood period
Maintenance and care of established vegetation	After completion of the reclamation and mine-closure works	Once a year

It should also be noted that no rare or endangered food and medicinal plant species subject to special protection have been identified within the area affected by the planned reclamation works at the Vostochnyi coal mine. Therefore, no additional measures specifically aimed at the protection or transplantation of such plant species are required during the biological reclamation phase.

Overburden generated at the Vostochnyi coal mine is stored in three external dumps: Prybortovoy, Konveyernyi, and Festivalnyi. According to the project documentation, the reclamation potential of these dumps is constrained by their structural characteristics, spatial location, and the properties of the stored materials [33].

At the Festivalnyi external dump, internal overburden is removed and placed within the first dump tier. Conventional surface flattening is considered unsuitable because disturbance and redistribution of the stored material may increase oxygen access to carbonaceous rocks and internal overburden, thereby creating conditions for oxidation and spontaneous combustion.

The Konveyernyi external dump is located between other waste dumps and existing engineering infrastructure. Owing to these spatial constraints and the considerable height of its slopes, transferring large volumes of material and flattening the slopes over the surrounding ground surface are considered technically impracticable. Such operations could also interfere with nearby engineering communications and require substantial additional land.

The Prybortovoy external dump is surrounded by undisturbed and biologically productive land. Consequently, flattening its slopes using a top-down approach would extend the dump footprint beyond its current boundaries and result in the additional occupation and disturbance of productive land. This option would therefore contradict the objective of minimizing the total area affected by mining and reclamation activities.

Therefore, flattening the slopes of the external dumps is considered economically unjustified and, in some cases, technically impracticable.

The external dumps are planned to be preserved for further use in accordance with their intended purpose or left for natural revegetation with xerophytic plant species characteristic of the local climatic zone.

The mined-out area is planned to be enclosed by a protective rock embankment with a height of at least 2.5 m, located at a minimum distance of 15.0 m from the edge of the upper bench. The area occupied by each external dump is presented in Table 3.

Table 3. Area occupied by dumps of Vostochnyi coal mine

Title	Area, hectares
Prybortovoy	343.2
Festivalnyi	741.2
Konveyernyi	185.7
Total by all dumps	1270.1

Protective earth embankments were constructed on the upland side of the dumps to prevent flooding by surface runoff. The embankments have a minimum height of 0.6 m, a crest width of at least 0.6 m, and a slope ratio of 1:1.5. Their cross-section is trapezoidal [33]. Buildings and surface structures located at the mine's industrial site, following the dismantling of technological equipment, as well as roads and engineering communications, may be transferred to local authorities on a contractual basis. These facilities can subsequently be used to support the development of small and medium-sized businesses and to expand the infrastructure of nearby farms.

Reclamation is the responsibility of the subsoil user. However, ensuring that the required reclamation outcomes are achieved is also the responsibility of the relevant state authorities. According to Krzyszowska Waitkus, a GPS/GIS-based system was developed to assist the Wyoming authorities in monitoring reclamation at the North Antelope Rochelle Coal Mine. This approach to sustainable reclamation management contributed to the successful restoration of the mined land within approximately 10 years. The subsoil user submitted annual reports in accordance with Wyoming regulations, after which the responsible state agency verified the reported data, paying particular attention to water quality, backfill condition, and vegetation development [27]. It should also be noted that mining operations at the North Antelope Rochelle Coal Mine have continued, demonstrating that mining and progressive reclamation can be implemented simultaneously when properly organized.

Domestic subsoil users also pay considerable attention to reclamation monitoring, as it is required not only during reclamation works but also after their completion. The example of the Vostochnyi coal mine shows that reclaimed areas should be regularly inspected to confirm that all reclamation measures have been implemented in accordance with applicable national regulations and that the restored land remains environmentally stable.

Full-scale reclamation activities in the Ekibastuz coal basin are not expected to begin in the near future because, according to the Minister of Energy of Kazakhstan, the country's coal reserves could last for approximately 300 years at the current production rate [28]. Nevertheless, the preparation of detailed reclamation and long-term monitoring plans remains an essential requirement of responsible mining.

One aspect of reclamation that is often neglected is soil formation, or pedogenesis. Spasić et al. suggest that attention is generally focused on the upper soil layer, which usually develops during the first 20-40 years after reclamation. However, the lower soil horizons may require up to 100 years to reach a relatively stable condition and may differ considerably from the upper layer. The loss of soil-profile homogeneity results from several interacting factors; according to the authors, particular attention should be paid to the influence of vegetation, especially trees, on the development of reclaimed soils [29]. The disturbance of natural soil homogeneity during mining may adversely affect endemic plant species because there is no guarantee that these species will successfully establish in the newly formed soil profile. Therefore, long-term investigation of soil-forming processes would be useful for domestic mining enterprises. State authorities should also consider pedogenesis as an important component of reclamation assessment and post-reclamation monitoring.

Frauenstein et al. demonstrated that erosion is an important factor that should be considered during the reclamation of coal mines. Their study examined coal-mining areas in Mongolia. According to the authors, a drainage system should be installed around a dump to prevent water erosion and reduce the risk of dump instability. Groundwater inflow into the dump and water accumulation at the toe are two major problems that may arise when the drainage system is inadequately designed. The authors emphasize that the required capacity of the drainage system should be determined by considering the catchment area upslope of the drain, the presence of springs and agricultural drainage systems, and natural surface-water flows that may be affected by the dump [34].

The appropriate design and construction of drainage facilities are also common in domestic reclamation practice. For example, wastewater storage facilities have been created in Lakes Aktygai and Akbidaik to collect water discharged from the Bogatyr and Vostochnyi coal mines [33].

Direct planting combined with fertilizer application may also provide effective biological reclamation results, as demonstrated by Nutayla et al. According to the authors, direct planting of *Pterocarpus indicus* seedlings with the application of bokashi and coal-based fertilizers resulted in a 100% seedling survival rate at a coal mine in Indonesia. The study used bokashi and coal fertilizers and showed that different fertilizer types should be tested and selected according to the specific soil conditions of the reclaimed site. The research was conducted at Pit 3 Barat, IUP Banko Barat, South Sumatra, Indonesia [35].

Unfortunately, active biological reclamation measures are often insufficiently represented in domestic coal-mining practice. For example, the reclamation plans for both the Severnyi and Vostochnyi coal mines, including Option 1 for Vostochnyi, provide for leaving the reclaimed territories to natural revegetation. This approach may be intended to reduce reclamation costs; however, relying exclusively on spontaneous vegetation recovery may prolong ecosystem restoration and may not ensure the establishment of a stable plant community.

4. Conclusions

In an era when decarbonization is a global priority, coal remains an important commodity that cannot yet be completely abandoned, and each country has its own reasons for continuing its use. A significant proportion of coal is extracted by open-pit mining, which occupies large areas of land. Improper reclamation of such territories may lead to serious environmental consequences. Therefore, proper planning, implementation, and long-term monitoring should be key components of any reclamation project. Additional funding for biological reclamation may be necessary and should not be neglected. Reclamation is as important as the mining process itself, since restored lands may subsequently be used for agriculture, industry, infrastructure development, or recreation. International experience shows that systematic monitoring, long-term pedogenesis assessment, effective drainage systems, and direct planting with fertilizer application play an important role in the successful reclamation of coal-mining areas.

It can be concluded that domestic coal-mine reclamation practices are generally promising; however, comparison with international experience indicates that there is still considerable potential for further improvement.

Author contributions

Conceptualization: KBR, NOS; Data curation: BK, KT; Formal analysis: NOS, BK, YM, KT; Formal analysis: BK, YM, KT; Investigation: BK, YM; Methodology: KBR, NOS; Project administration: KBR, NOS; Resources: BK, YM; Supervision: KBR, NOS; Validation: BK, KT; Visualization: YM, KT; Writing – original draft: KBR, NOS; Writing – review & editing: KBR, NOS. All authors have read and agreed to the published version of the manuscript.

Funding

This research received no external funding.

Acknowledgements

The authors acknowledge the institutional and technical support provided during the preparation of this study. They also appreciate the assistance of colleagues who contributed to the analysis, and interpretation of the research materials.

Conflicts of interests

The authors declare no conflict of interest.

Data availability statement

The original contributions presented in this study are included in the article. Further inquiries can be directed to the corresponding author.

References

[1] Database. (2026). Coal Consumption by Country. *Retrieved from:* https://www.globalfirepower.com/coal-consumption-by-country.php

[2] Panchenko, T. (2025). Coal is essential: will Kazakhstan be able to reduce emissions by 2060? *Retrieved from*: https://forbes.kz/articles/ugol-nasushnyy-uspeet-li-kazahstan-sokratit-vybrosy-k-2060-godu

[3] Myllyvirta, L. (2026). Analysis: Coal power drops in China and India for first time in 52 years after clean-energy records. *Retrieved from*: https://www.carbonbrief.org/analysis-coal-power-drops-in-china-and-india-for-first-time-in-52-years-after-clean-energy-records/

[4] Nizamova, A.T., Rasulov, A.Kh., & Maxmadiyev, D.R. (2025). Assessment of industrial waste disposal practices in the mining sector of Uzbekistan. *Engineering Journal of Satbayev University*, *147*(4), 23-29. https://doi.org/10.51301/ejsu.2025.i4.04

[5] Salieiev, I. (2024). Organization of processes for complex mining and processing of mineral raw materials from coal mines in the context of the concept of sustainable development. *Mining of Mineral Deposits*, *18*(1), 54-66. https://doi.org/10.33271/mining18.01.054

[6] Kalybekov, T., Rysbekov, K., Sandibekov, M., Bi, Y.L., & Toktarov, A. (2020). Substantiation of the intensified dump reclamation in the process of field development. *Mining of Mineral Deposits*, *14*(2), 59-65. https://doi.org/10.33271/mining14.02.059

[7] Mazza, K. (2024). DEQ awards annual coal reclamation award to North Antelope Rochelle Mine. *Retrieved from:* https://deq.wyoming.gov/2024/05/deq-awards-annual-coal-reclamation-award-to-north-antelope-rochelle-mine/

[8] Aluwong, K.C., Hashim, M.H.M., Ismail, S., & Shehu, S.A. (2024). Physico-chemical assessment of surface water from mining activities in Maiganga coal mine, Gombe state, Nigeria. *Mining of Mineral Deposits*, *18*(1), 9-17. https://doi.org/10.33271/mining18.01.009

[9] Begentayev, M., Kuldeev, Y., Nurpeissova, M., Nurpeisova, T., & Kirgizbaeva, D. (2025). The role of environmental and industrial safety during subsoil development. *Engineering Journal of Satbayev University*, *147*(5), 42-48. https://doi.org/10.51301/ejsu.2025.i5.06

[10] Pukish, A., Mandryk, O., Arkhypova, L., Syrovets, S., & Hryniuk, D. (2024). Mathematical modeling of pollution of underground aquifers due to mining of minerals. *Mining of Mineral Deposits*, *18*(3), 94-103. https://doi.org/10.33271/mining18.03.094

[11] Saik, P., Rysbekov, K., Kassymkanova, K.K., Lozynskyi, V., Kyrgizbayeva, G., Moldabayev, S., Babets, D., & Salkynov, A. (2024). Investigation of the rock mass state in the near-wall part of the quarry and its stability management. *Frontiers in Earth Science*, *12*, 1395418. https://doi.org/10.3389/feart.2024.1395418

[12] Popovych, V., Skrobala, V., Tyndyk, O., & Kaspruk, O. (2024). Hydro-ecological monitoring of heavy metal pollution of water bodies in the Western Bug River basin within the mining-industrial region. *Mining of Mineral Deposits*, *18*(4), 139-152. https://doi.org/10.33271/mining18.04.139

[13] Kalybekov, T., Rysbekov, K., & Zhakypbek, Y. (2015). Efficient land use in open-cut mining. New Developments in Mining Engineering 2015: *Theoretical and Practical Solutions of Mineral Resources Mining*, 287-291. https://doi.org/10.1201/b19901-51

[14] Nurpeisova, M.B., Yestemesov, Z.A., Lozinsky, V.G., Ashimova, A.A., & Urazova, S.S. (2023). Industrial waste recycling – one of the key directions of business development. *News of the National Academy of Sciences of the Republic of Kazakhstan, Series of Geology and Technical Sciences*, 459(3), 193-205. https://doi.org/10.32014/2023.2518-170X.309

[15] Gorova, A., Pavlychenko, A., & Borysovs'Ka, O. (2013). The study of ecological state of waste disposal areas of energy and mining companies. *Annual Scientific-Technical Colletion - Mining of Mineral Deposits*, 169-172. https://doi.org/10.1201/b16354-29

[16] Popovych, V., Bosak, P., Petlovanyi, M., Telak, O., Karabyn, V., & Pinder, V. (2021). Environmental safety of phytogenic fields formation on coal mines tailings. *News of the National Academy of Sciences of the Republic of Kazakhstan, Series of Geology and Technical Sciences*, *2*(446), 129-136. https://doi.org/10.32014/2021.2518-170x.44

[17] Querol, X., Zhuang, X., Font, O., Izquierdo, M., Alastuey, A., Castro, I., van Drooge, B.L., Moreno, T., Grimalt, J.O., Elvira, J., Cabañas, M., Bartroli, R., Hower, J.C., Ayora, C., Plana, F., & López-Soler, A. (2011). Influence of soil cover on reducing the environmental impact of spontaneous coal combustion in coal waste gobs: A review and new experimental data. *International Journal of Coal Geology*, *85*(1), 2-22. https://doi.org/10.1016/j.coal.2010.09.002

[18] Onifade, M., & Genc, B. (2019). Spontaneous combustion liability of coal and coal-shale: A review of prediction methods. *International Journal of Coal Science & Technology*, *6*, 151-168. https://doi.org/10.1007/s40789-019-0242-9

[19] Ren, H., Zhao, Y., Xiao, W., Zhang, J., Chen, C., Ding, B., & Yang, X. (2022). Vegetation growth status as an early warning indicator for the spontaneous combustion disaster of coal waste dump after reclamation: An unmanned aerial vehicle remote sensing approach. *Journal of Environmental Management*, *317*, 115502. https://doi.org/10.1016/j.jenvman.2022.115502

[20] Onifade, M., & Genc, B. (2020). A review of research on spontaneous combustion of coal. *International Journal of Mining Science and Technology*, *30*(3), 303-311. https://doi.org/10.1016/j.ijmst.2020.03.001

[21] Onifade, M., & Genc, B. (2018). Modelling spontaneous combustion liability of carbonaceous materials. *International Journal of Coal Science & Technology*, *5*, 191-212. https://doi.org/10.1007/s40789-018-0209-2

[22] Strzałkowski, P., & Kaźmierczak, U. (2019). The scope of reclamation works for areas after the exploitation of rock raw materials. *Applied Sciences*, *9*(6), 1181. https://doi.org/10.3390/app9061181

[23] Konysbayeva, A., Yessimsiitova, Z., Toktar, M., Mutushev, A., Zhakypbek, Y., Tursbekov, S., Tursbekova, G., Kozhayev, Z., Kozhamzharova, A., Mombekov, S., & Raheem, S. (2025). Result of reclamation of man-made dumps from phosphorite deposits in the semi-desert zone of Kazakhstan. *PloS ONE*, *20*(2), e0317500. https://doi.org/10.1371/journal.pone.0317500

[24] Xu, D., Li, X., Chen, J., & Li, J. (2023). Research progress of soil and vegetation restoration technology in open-pit coal mine: A review. *Agriculture*, *13*(2), 226. https://doi.org/10.3390/agriculture13020226

[25] Li, X., Lei, S., Liu, F., & Wang, W. (2020). Analysis of plant and soil restoration process and degree of refuse dumps in open-pit coal mining areas. *International Journal of Environmental Research and Public Health*, *17*(6), 1975. https://doi.org/10.3390/ijerph17061975

[26] Zhakypbek, Y., Rysbekov, K., Lozynskyi, V., Mikhalovsky, S., Salmurzauly, R., Begimzhanova, Y., Kezembayeva, G., Yelikbayev, B., & Sankabayeva, A. (2025). Geospatial and Correlation Analysis of Heavy Metal Distribution on the Territory of Integrated Steel and Mining Company Qarmet JSC. *Sustainability*, *17*(15), 7148. https://doi.org/10.3390/su17157148

[27] Krzyszowska Waitkus, A. (2022). Sustainable reclamation practices for a large surface coal mine in shortgrass prairie, semiarid environment (Wyoming, USA): case study. *International Journal of Coal Science and Technology*, *9*, 32. https://doi.org/10.1007/s40789-022-00502-3

[28] Database. (2026). Enough for 300 years – Kazakhstan's Ministry of Energy reports on coal reserves. *Retrieved from:* https://www.zakon.kz/ekonomika-biznes/6513603-khvatit-na-300-let--o-zapasakh-uglya-kazakhstana-rasskazali-v-minenergo.html

[29] Spasić, M., Borůvka, L., Vacek, O., Drábek, O., & Tejnecký, V. (2021). Pedogenesis problems on reclaimed coal mining

sites. *Soil and Water Research, 16(3),* 137-150. https://doi.org/10.17221/163/2020-SWR

[30] Rysbekov, K.B., Kyrgizbayeva, D.M., Miletenko, N.A., & Kuandykov, T.A. (2024). Integrated monitoring of the area of Zhilandy deposits. *Eurasian Mining, 41*(1), 3-6. https://doi.org/10.17580/em.2024.01.01

[31] Pham, K.C., & Nguyen, H.V. (2025). Real-time deformation monitoring of open-pit mine dump sites using self-developed GNSS receivers: A case study of the Dong Cao Son dump site, Vietnam. *Mining of Mineral Deposits, 19*(3), 120-131. https://doi.org/10.33271/mining19.03.120

[32] *Reclamation of disturbed lands of the Severnyi coal mine of Bogatyr Komir LLP*. (2022). Ekibastuz, Pavlodar region. Explanatory note. Volume I. Book 1. Kyzylorda.

[33] *A plan to eliminate the consequences of coal mining operations at the Ekibastuz coal deposit within the boundaries of the Vostochnyi coal mine*. Volume I. Explanatory note. Book 1. General explanatory note. P7646-I-1PZ. Karaganda.

[34] Frauenstein, J, Wollmann, R, Schlenstedt, J, Konrad, C & Mendjargal, T. (2021). *Sustainable re-cultivation of coal mines in Mongolia'*. Mine Closure 2021, Proceedings of the 14th International Conference on Mine Closure, QMC Group, Ulaanbaatar. https://doi.org/10.36487/ACG_repo/2152_98

[35] Nutayla, N., Rejo, A. & Adhiguna, R. T. (2023). Coal Post-Mining Reclamation Using Pterocarpus Indicus. *Journal of Ecological Engineering, 24(12),* 366-376. https://doi.org/10.12911/22998993/174091

Көмір разрездерін рекультивациялаудың қазіргі таңдағы аспектілері

Қ.Б. Рысбеков, Н.О. Сарыбаев*, Б. Кәкім, Е. Метелев, Қ. Тілеубеков

Satbayev University, Алматы, Қазақстан

**Корреспонденция үшін автор: n.sarybayev@satbayev.university*

Аңдатпа. Зерттеудің мақсаты - көмір кен орындарын ашық әдіспен игеру нәтижесінде бұзылған жерлерді рекультивациялау тиімділігін айқындайтын негізгі техникалық, экологиялық және биологиялық факторларды анықтау және жүйелеу. Зерттеу құжаттық талдау және отандық әрі шетелдік тәжірибелерді салыстырмалы қарастыру әдістерін қолдану арқылы орындалды. Екібастұз көмір бассейніндегі «Северный» және «Восточный» көмір разрездерінің техникалық және биологиялық рекультивация жобалары, сондай-ақ АҚШ, Моңғолия және Индонезиядағы көмір өндіру аумақтарын қалпына келтіру бойынша жарияланған деректер талданды. Салыстыру аумақты инженерлік дайындау, жерүсті ағынын реттеу, эрозияның алдын алу, топырақ пен өсімдік жамылғысын қалпына келтіру, экологиялық мониторинг және жобалық шешімдердің экономикалық негізділігі бағыттары бойынша жүргізілді. «Восточный» разрезінің техникалық рекультивациясының екі нұсқасы орындалатын жұмыстар көлемі мен жалпы құны бойынша ерекшеленетіні анықталды. «Фестивальный», «Конвейерный» және «Прибортовой» үйінділерінің еңістерін жайпақтау көмірлі жыныстардың өздігінен жану қаупімен, инженерлік коммуникациялардың орналасуымен және бұзылған өнімді жерлер аумағының ықтимал ұлғаюымен шектелетіні көрсетілді. Шетелдік тәжірибемен салыстыру су сапасын, үйінді жағдайын, өсімдік жамылғысының дамуын және топырақ түзілу процестерін ұзақ мерзімді бақылау қажеттілігін растады. Отандық жобаларда биологиялық рекультивация негізінен табиғи жолмен өсімдік басуын көздейтіні, ал өсімдіктерді тікелей отырғызу және тыңайтқыштарды қолдану тұрақты өсімдік жамылғысының қалыптасуын жеделдете алатыны анықталды. Қазақстанның ірі көмір разрездерін рекультивациялаудың негізгі шектеулері мен нәтижелілік факторлары жүйеленді, сондай-ақ халықаралық тәсілдерді Екібастұз бассейнінің жағдайларына бейімдеу бағыттары айқындалды. Алынған нәтижелер ұзақ мерзімді мониторингті, жерүсті ағынын реттеуді, топырақ түзілуін бақылауды және өсімдіктерді белсенді қалпына келтіруді көздейтін рекультивация жобаларын әзірлеу және түзету кезінде пайдаланылуы мүмкін.

Негізгі сөздер: *көмір өндіру, рекультивация, жердің бұзылуы, рекультивация кезеңдері,мониторинг.*

Современные аспекты рекультивации угольных разрезов

К.Б. Рысбеков, Н.О. Сарыбаев*, Б. Каким, Е. Метелев, К. Тилеубеков

Satbayev University, Алматы, Казахстан

**Автор для корреспонденции: n.sarybayev@satbayev.university*

Аннотация. Целью исследования является выявление и систематизация основных технических, экологических и биологических факторов, определяющих эффективность рекультивации земель, нарушенных открытой разработкой угольных месторождений. Исследование выполнено с использованием документального анализа и сравнительного рассмотрения отечественных и зарубежных практик. Проанализированы проекты технической и биологической рекультивации угольных разрезов «Северный» и «Восточный» Экибастузского угольного бассейна, а также опубликованные данные по восстановлению угледобывающих территорий в США, Монголии и Индонезии. Сравнение проводилось по направлениям инженерной подготовки территории, регулирования поверхностного стока, предотвращения эрозии, восстановления почв и растительности, экологического мониторинга и экономической обоснованности проектных решений. Установлено, что два варианта технической рекультивации разреза «Восточный» различаются объемом работ и общей стоимостью. Показано, что выполаживание откосов отвалов «Фестивальный», «Конвейерный» и «Прибортовой» ограничивается риском самовозгорания углесодержащих пород, расположением инженерных коммуникаций и возможным увеличением площади нарушенных продуктивных земель. Сравнение с зарубежным опытом подтвердило необходимость длительного контроля качества вод, состояния отсыпки, развития растительности и процессов почвообразования. Установлено, что в отечественных проектах биологическая рекультивация преимущественно предусматривает естественное зарастание, тогда как прямая посадка растений и применение удобрений могут ускорить формирование устойчивого растительного покрова. Систематизированы основные ограничения и факторы результативности рекультивации крупных угольных разрезов Казахстана, а также определены направления адаптации международных подходов к условиям Экибастузского бассейна. Полученные результаты могут быть использованы при разработке и корректировании проектов рекультивации, предусматривающих долгосрочный мониторинг, регулирование поверхностного стока, контроль почвообразования и активное восстановление растительности.

Ключевые слова: *добыча угля, рекультивация, нарушенные земли, этапы рекультивации, мониторинг.*

Publisher's note

All claims expressed in this manuscript are solely those of the authors and do not necessarily represent those of their affiliated organizations, or those of the publisher, the editors and the reviewers.

CONTENTS

МАЗМҰНЫ

СОДЕРЖАНИЕ

Publisher: Satbayev University

Registration:
Ministry of Information and Social Development of the Republic of Kazakhstan
No. KZ19VPY00056529 dated 30 September 2022 (re-registration)

Official website: https://vestnik.satbayev.university/index.php/journal/

Established in August 1994. Published bimonthly

Editorial Office Address:
Satpayev St., 22, Almaty, Kazakhstan
Tel.: +7(727) 292-63-46